Supersymmetric Precision Calculations of Bottom Yukawa Couplings

Dissertation
zur
Erlangung der naturwissenschaftlichen Doktorwürde
(Dr. sc. nat.)
vorgelegt der
Mathematisch-naturwissenschaftlichen Fakultät
der
Universität Zürich
von
David Noth
aus
Deutschland

Promotionskomitee
Prof. Dr. Daniel Wyler (Vorsitz)
PD Dr. Michael Spira (Leitung der Dissertation)

Zürich 2008

Zusammenfassung

Wir haben die Zwei-Schleifen SUSY-QCD Korrekturen zu effektiven Bottom Yukawa Kopplungen in der minimalen, supersymmetrischen Erweiterung des Standardmodells berechnet. Diese effektiven Kopplungen beinhalten die Resummation der nicht entkoppelnden Korrekturen Δm_b für große Werte von $\mathrm{tg}\beta$. Wir haben die Zwei-Schleifen SUSY-QCD Korrekturen zu den führenden SUSY-QCD und top-induzierten SUSY-elektroschwachen Beiträgen zu Δm_b berechnet. Die Skalenabhängigkeit der resummierten Yukawa Kopplungen wurde von $\mathcal{O}(10\%)$ auf den Prozentbereich reduziert. Folglich reduzieren unsere Resultate die theoretische Unsicherheit der MSSM Verzweigungsverhältnisse erheblich. Darüber hinaus profitieren alle Prozesse, die von den Bottom Yukawa Kopplungen vermittelt werden, von der nun erreichten, hohen Präzision, wie z.B. Higgs Boson Strahlung von Bottom Quarks, einem wichtigen Produktionskanal an allen Kollidern. Die neuen NNLO Korrekturen für die Bottom Yukawa Kopplungen können daher als Basis für experimentelle Analysen am Tevatron und am LHC, sowie am zukünftigen, linearen e^+e^- Kollider genutzt werden.

Abstract

We present the two-loop SUSY-QCD corrections to the effective bottom Yukawa couplings within the minimal supersymmetric extension of the Standard Model. These effective Yukawa couplings include the resummation of the non-decoupling corrections Δm_b for large values of $\mathrm{tg}\beta$. We have derived the two-loop SUSY-QCD corrections to the leading SUSY-QCD and top-induced SUSY-electroweak contributions to Δm_b. The scale dependence of the resummed Yukawa couplings is reduced from $\mathcal{O}\,(10\%)$ to the percent level. Consequently, our results reduce the theoretical uncertainties of the MSSM Higgs branching ratios to a high accuracy. Moreover, all processes which are mediated by the bottom Yukawa couplings are directly affect by the now reached high precision, as e.g. Higgs boson radiation off bottom quarks which is a very important production process at all colliders. The improved NNLO predictions for the bottom Yukawa couplings can thus be taken as a base for experimental analysis at the Tevatron and the LHC as well as a future linear e^+e^- collider.

Contents

Chapter 1

Introduction

The Standard Model (SM) of particle physics provides a very successful description of all experimental measurements. It comprises two kinds of matter particles (quarks and leptons) and three fundamental forces (the electromagnetic, weak and strong interactions), whereas its unification with the fourth existing force, the gravitational interaction described by Einstein's theory of general relativity, is still an active research topic [1–17]. The Standard Model predicts the existence of one scalar Higgs boson which constitutes the remainder of electroweak symmetry breaking by means of the Higgs mechanism [18–20]. In all experiments this particle has escaped detection so far. Its discovery will be of vital importance for the mathematical consistency of the SM and the success of the predictions for the precision electroweak observables which turned out be in the striking agreement with measurements at LEP (Large Electron Positron collider) and SLC (Stanford Linear Collider), if the Higgs boson mass is smaller than about 200 GeV [21]. The Higgs sector allows the theory of electroweak interactions to remain weakly interacting up to very high-energy scales. One of the major directions towards a model beyond the Standard Model of strong and electroweak interactions is the formulation of a grand unified theory (GUT) which is broken down to the low-energy SM at an energy scale of the order of 10^{16} GeV. This requires the Standard Model to be weakly interacting up to these high energy scales which is only possible, if the Higgs mass ranges between about 130 GeV and 190 GeV [22].
However, even if the Higgs mass is in this range, quantum fluctuations tend to raise the Higgs mass to the order of the GUT scale due to quadratic divergences in higher-order corrections. In order to stabilize the Higgs mass at the electroweak scale an extreme fine tuning of the corresponding mass counter terms is necessary. This hierarchy problem can be avoided by the introduction of supersymmetry (SUSY) [23–25], a novel symmetry between the bosonic and the fermionic degrees of freedom of the model, provided the new superpartners of all SM particles acquire masses below about 1 TeV [26]. Supersymmetric GUTs predict the value of the Weinberg angle in striking agreement with the precision measurements at LEP and SLC. The minimal supersymmetric extension of the SM (MSSM) requires the existence of five elementary Higgs bosons. They can be searched for at the Tevatron and the LHC (Large Hadron Collider) colliders as well as a future linear e^+e^- collider.
The big success of the SM (and MSSM) to describe the experimental data is significantly based on involved calculations of quantum corrections to experimentally measured pro-

cesses, which are mandatory in order to reach the expected experimental accuracies at present and future collider experiments. The dominant Higgs decay modes in a large range of the MSSM are the decays into bottom-antibottom quark and τ-lepton pairs. The genuine SUSY-QCD and SUSY-electroweak corrections to the decay widths are known at next-to-leading order (NLO) and turn out to be large for large values of tgβ, the ratio of the two vacuum expectation values of the two scalar MSSM Higgs fields [27]. The residual theoretical uncertainty is larger than the achievable experimental accuracy at future colliders [28], thus requiring the extension to the next perturbative order. The leading parts of the NLO corrections can be universally factorized as an effective Yukawa coupling, while the non-leading parts are under proper theoretical control.

The topic of this thesis is the calculation of the NNLO SUSY-QCD and top-induced SUSY-electroweak corrections to the effective bottom Yukawa coupling. These results will affect all processes to which the bottom Yukawa couplings contribute, i.e. in particular the Higgs decay widths and Higgs radiation off bottom quarks at hadron colliders which constitutes the dominant Higgs boson production channel for large tgβ at the Tevatron and the LHC [29–31].

This thesis is organised as follows. Chapter 1 is a short reminder of some basic theoretical principles. The Standard Model and its minimal supersymmetric extension (MSSM) are introduced. Chapter 2 deals with Higgs phenomenology at future colliders. Chapter 3 contains the technical details of our calculation. Chapter 4 reviews the status of corrections to Bottom Yukawa couplings and describes the extension to NNLO. Chapter 5 presents numerical results of our calculation. A summary is given in chapter 6. In Appendix A the one-loop and two-loop integrals are listed that were required for the calculation, Appendix B specifies necessary Feynman rules of the SM and the MSSM and Appendix C shows all calculated Feynman-diagrams. Analytic results are given in Appendix D.

1.1 Theoretical Basics

Quantum field theory is the application of quantum mechanics to dynamical systems of fields, in the same sense that quantum mechanics is concerned with the quantization of dynamical systems of particles. Given that we wish to understand processes that occur at very small (quantum-mechanical) scales and very large (relativistic) energies, one might still ask why we must study the quantization of fields. Why can't we just quantize relativistic particles the way we quantized nonrelativistic particles? Perhaps the most obvious answer is that we have no right to assume that any relativistic process can be explained in terms of a single particle, since the Einstein relation $E = mc^2$ allows for the creation of particle-antiparticle pairs. One can think of these states as existing only for a very short time, according to the uncertainty principle $\Delta E \Delta t = \hbar$. Quantum field theory provides a natural way to handle not only multiparticle states, but also transitions between states of different particle number. It provides the tools necessary to calculate innumerable scattering cross sections, particle lifetimes, and other observable quantities.

The kinematics and the interactions of fundamental point-like particles can theoreti-

cally be formulated as a gauge field theory. A gauge field theory is described by the Lagrangian density $\mathcal{L}$, which depends on all elementary fields $\phi(x)$ and their derivatives $\partial_\mu\phi(x)$. The two basic principles which restrict the allowed terms in the Lagrangian are local gauge invariance and renormalisability. From the requirement of local gauge invariance particle interactions arise naturally via the introduction of gauge fields. The invariance of the Lagrangian under global space-time transformations, generated by the Poincaré group, requires that fields belong to representations of the Lorentz group. The possible representations of the Lorentz group are characterised by their spin. Only fields with spin 0, 1/2 and 1 generate renormalisable gauge field theories [32, 33].

1.1.1 Gauge Field Theories

The Lagrangian $\mathcal{L}$ of a gauge field theory is invariant under gauge transformations of the fermion fields: $\psi \to U\psi$. U is either a phase factor for Abelian groups or a unitary matrix for non-Abelian groups acting on multiplets of fermion fields ψ. For local gauge transformations, U will depend on the space-time point x. To guarantee the invariance under local transformations, the space-time derivatives ∂_μ must be extended to covariant derivatives D_μ which include a new vector field A_μ:

$$i\partial_\mu \to iD_\mu = i\partial_\mu - gA_\mu \tag{1.1}$$

where g defines the universal gauge coupling of the system. Through the requirement of local gauge invariance a gauge boson A is naturally introduced into the Lagrangian. The gauge field A_μ is transformed by a rotation plus a shift under local gauge transformations: $A_\mu \to UA_\mu U^{-1} + \frac{i}{g}[\partial_\mu U]U^{-1}$. The field strength tensor $F_{\mu\nu} = \partial_\mu A_\nu - \partial_\nu A_\mu + ig[A_\mu, A_\nu]$, is just rotated under gauge transformations: $F_{\mu\nu} \to UF_{\mu\nu}U^{-1}$. The Lagrangian which describes the system of spin-1/2 fermions and vectorial gauge bosons for massless particles, can be cast into the compact form:

$$\mathcal{L} \;=\; \bar{\psi}\, i\not{D}\, \psi \;-\; \frac{1}{2}\,\mathrm{Tr}[F_{\mu\nu}F^{\mu\nu}] \tag{1.2}$$

From this Lagrangian, the following interaction terms can be read off

$$-g\,\bar{\psi}\not{A}\,\psi \quad , \quad ig\,\mathrm{Tr}\Big[(\partial_\nu A_\mu - \partial_\mu A_\nu)[A_\mu, A_\nu]\Big] \quad , \quad \frac{1}{2}g^2\,\mathrm{Tr}[A_\mu, A_\nu]^2 \tag{1.3}$$

which correspond to fermion-gauge boson, three-boson and four-boson couplings respectively.

1.1.2 Perturbation Theory

The Lagrangian $\mathcal{L}$ describes all fundamental tree-level interactions between the elementary particles of the model. The calculation of observable scattering probabilities requires the solution of the associated time evolution equations for physical particle states produced and detected at high-energy colliders. This leads to the concept of the **S-matrix**, which is the central quantity in most high energy calculations. The S-matrix is essentially a time evolution operator and can be expressed as the time ordered exponential of an action.

$$S = T\left\{\exp\big(-i\int_{-\infty}^{\infty} d^4x\,\mathcal{L}(x)\big)\right\} \tag{1.4}$$

Except for free particles or exceptional models, the time evolution is too complicated and cannot be calculated exactly. If the couplings between the particles in the Lagrangian $\mathcal{L}$ are small enough, it makes sense to apply perturbation theory, i.e. to expand the exponential function in these couplings. By going from time ordering to normal ordering, the terms in the expansion can be replaced by vertices and propagators and visualized by their corresponding Feynman diagrams [3]. Since the nth order of the expansion also involves n integrations (see equation (1.4)), perturbation theory gets quickly at its limits. Nevertheless it yields good approximations for calculations involving the couplings of the weak and the electromagnetic interactions. However the coupling constant of the strong interaction (QCD) is too large at small energy scales, and perturbation theory breaks down. In this regime, non-perturbative methods like e.g. Lattice QCD are required to study the theory (a consequence of the strong interaction is colour confinement which implies, that coloured particles can never be observed as isolated particles, but only inside colour neutral objects as mesons and baryons). Fortunately the non-abelian gauge structure of QCD has the property that the strong coupling constant becomes small at large momentum transfer [13]. Additionally the non-perturbative low-energy physics inside the hadrons and the high energy scattering process of the partons (quarks and gluons are called partons) can be separated rather accurately without any considerable quantum interferences. This recognition is the content of the parton model. Without the discovery of the parton model and the asymptotic freedom of the quarks and gluons, perturbative QCD calculations would not be possible.

1.1.3 Renormalisation

The Lagrangian of a quantum field theory involves a certain number of free parameters which have to be determined experimentally. These are chosen such that they have an intuitive physical meaning at tree level (physical masses, couplings), i.e. they are directly related to experimental quantities. For example in QED, the tree level electron propagator has a pole at the parameter that is called mass or the coupling is the strength of a photon scattering off an electron. This direct relation is destroyed by higher order corrections. To stick with our electron propagator example, at higher orders the electron self-energy has to be taken into account. This additional term shifts the pole of the propagator away from the mass parameter. Moreover, but not necessarily, this higher order corrections (e.g. the electron self-energy) can be UV-divergent. However, in renormalisable theories (such as the SM or the MSSM) these divergencies cancel in relations between physical quantities, thus allowing meaningful predictions. In any case, one has to connect the **bare parameters** in the Lagrangian to physical measurements. Most generally speaking, to obtain predictions from a renormalizable model one follows the following steps:

1. Calculate physical quantities in terms of the bare parameters.
2. Use as many of the resulting relations as bare parameters exist to express these in terms of physical observables.
3. Insert the resulting expressions into the remaining relations.

Thus one arrives at predictions for physical observables in terms of other physical quantities, which have to be determined from experiment. In these predictions, all UV-

divergencies (if present) cancel in any order of perturbation theory. But also at tree level, one would need to follow these steps to give physical values to the parameters of the theory. The idea is to absorb all UV-divergencies as well as any convenient finite quantity into the bare parameters, which gives new renormalised parameters. There is no reason, why this should not be valid, since the bare parameters of the Lagrangian can be defined freely. In fact, in renormalisable theories, this will always work to render the theory finite up to the calculated order. We use the counterterm approach. Here the bare parameters in the Lagrangian are redefined/renormalised in terms of physical parameter plus or times a **counterterm**. Then we define the counterterms in such a way, that all UV-divergencies cancel in physical predictions. As mentioned above, one needs as many physical quantities as there exist bare parameters to fix all counterterms. Since in renormalisable theories the counterterms are universal up to the order given, one can use the easiest physical objects possible to fix them. For example the 2-point Green's function to fix the renormalised mass. In this framework, the renormalisation procedure can be summarised as follows:

1. Choose a set of independent parameters.

2. Separate the bare parameters into renormalised parameters and counterterms.

3. Choose renormalisation conditions to fix the counterterms.

4. Express the renormalised parameters in terms of physical quantities.

5. Use measurements of these physical quantities to determine the physical value of the renormalised parameters.

6. Now evaluate any quantity that is expressed in terms of these renormalised parameters.

In the case of the electron propagator, any fraction of the self-energy can be absorbed into the bare mass parameter, which defines a new mass parameter, the renormalised mass. If the higher order corrections contain divergencies, they should be absorbed into the bare parameters to render the theory finite. But whatever fraction of the finite part of the corrections is absorbed is ambiguous. The explicit choice that is made leads to different renormalised parameters. One speaks of different **renormalisation schemes**. We can choose the counterterms such that the finite renormalised parameters are equal to physical parameters (as at tree-level) in all orders of perturbation theory. This is the on-shell renormalisation scheme. The advantage of the on-shell scheme is, that all parameters have a clear physical meaning and can be measured directly in suitable experiments (e.g. the mass is defined through the pole of the propagator). Another scheme is the minimal subtraction scheme where only divergencies are absorbed. Physical predictions are independent of the choice of the scheme, since whatever finite quantity is absorbed into the bare parameters changes also the value of the renormalised parameters, leaving the value of the physical object untouched. The choice can be made such that the calculation becomes easier. Renormalisation of masses and couplings is sufficient to obtain finite S-matrix elements, but it leaves Green's functions divergent. In order to get finite propagators and vertex functions, the fields have to be renormalised too [34, 35].

1.1.4 The Higgs mechanism

Explicit mass terms for gauge bosons in the Lagrangian violate the gauge invariance of the theory ($M^2\, A_\mu A^\mu$ is not invariant if $A_\mu \rightarrow A_\mu - \partial_\mu \chi$ where χ is a function in space-time, so M^2 must be zero). Nevertheless it is possible to introduce mass terms into the theory by the technique of **spontaneous symmetry breaking**. Here a scalar field takes on a nonzero global value. This global field has directional character and thus violates a symmetry of the Lagrangian. In such a case, the field theory contains a hidden or spontaneously broken symmetry. The common means of introducing spontaneous symmetry breaking in a gauge theory is the Higgs mechanism [18–20]. Here a Higgs field plays the role of the scalar field. Spontaneous symmetry breaking leaves the Lagrangian invariant under transformations of the gauge group but chooses an explicit vacuum expectation value for the Higgs field. Therefore the ground state is not symmetric anymore. If the original gauge group had n generators, and the ground state is still invariant under m generators, $n-m$ (would-be) Goldstone bosons appear in the theory [36]. These Goldstone bosons are unphysical fields and can be removed by a gauge transformation (unitary gauge). Each gauge boson associated with a broken generator acquires a mass. Thus the solution of the problem of massive gauge bosons is achieved at the expense of new fundamental degrees of freedom, $h-(n-m)$ massive, physical Higgs fields (h is the number of degrees of freedom of the initial scalar field). Technically this is implemented by the introduction of a self-interaction potential V in the Lagrangian. Scalar fields φ can interact with each other so that the ground state of the system, corresponding to the minimum of the scalar potential (with the Higgs self-interaction coupling λ)

$$V(\bar{\varphi}) = \frac{\lambda}{2}\left[|\bar{\varphi}|^2 - v^2\right]^2 \tag{1.5}$$

is realized for all non-zero values of the Higgs field $\bar{\varphi} \rightarrow \exp(i\theta^a T^a)\bar{v}$, parametrised by the gauge parameters θ^a, with the generators of the gauge group T^a, a multiplet of the group representation $\bar{v}$ and $|\bar{v}| = v$. The choice of an explicit vacuum expectation value, e.g. $\langle 0|\bar{\varphi}|0\rangle = \bar{v}$, breaks the symmetry of the ground state. For each spontaneously broken symmetry $T^a\bar{v} \neq 0$ a Goldstone boson appears in the theory. The physical Higgs fields are fluctuations around the ground state. The interaction energies of massless gauge bosons and fermions with the Higgs field φ in the ground state can be re-interpreted as the gauge-boson and fermion masses. The vector bosons are coupled to the ground-state Higgs field by means of the covariant derivative whereas Yukawa type terms are introduced into the Lagrangian to create fermion masses.

$$\mathcal{L}_H + \mathcal{L}_Y = |D_\mu \varphi|^2 - V(\varphi) + g_f \bar{f} f \varphi \tag{1.6}$$

Replacing the Higgs field by its ground state value, $\varphi \rightarrow \bar{v}$, one obtains the masses $M_A^2 = g^2 v^2$ and $m_f = g_f v$ for gauge bosons and fermions respectively. The Higgs mechanism leads to a renormalizable gauge field theory including non-zero gauge-boson and fermion masses [37–39].

1.1.5 Supersymmetry

Supersymmetry is a new symmetry relating fermions and bosons. A supersymmetry transformation turns a bosonic state into a fermionic state and vice versa. The operator

Q that generates such transformations must be an anticommuting spinor, with

$$Q|\text{Boson}\rangle = |\text{Fermion}\rangle \quad , \quad Q|\text{Fermion}\rangle = |\text{Boson}\rangle \tag{1.7}$$

Spinors are intrinsically complex objects, so $Q^\dagger$ (the hermitian conjugate of Q) is also a symmetry generator. Because Q and $Q^\dagger$ are fermionic operators, they carry spin 1/2, so it is clear that supersymmetry must be a space-time symmetry. The possible forms for such symmetries in an interacting quantum field theory are highly restricted by the Haag-Lopuszanski-Sohnius extension of the Coleman-Mandula theorem, which states that the symmetry group of a consistent four-dimensional quantum field theory is the direct product of the space-time symmetry group and the internal symmetry group [40, 41]. For realistic theories that, like the Standard Model, have chiral fermions (i.e. fermions whose left- and right-handed pieces transform differently under the gauge group) and thus the possibility of parity-violating interactions, this theorem implies that the generators Q and $Q^\dagger$ must satisfy an algebra of anticommuting and commuting relations a graded Lie algebra [42]

$$\{Q, \bar{Q}\} = P^\mu \quad , \quad \{Q, Q\} = \{\bar{Q}, \bar{Q}\} = 0 \quad , \quad [P^\mu, Q] = [P^\mu, \bar{Q}] = 0 \tag{1.8}$$

where P^μ is the four-momentum generator of space-time translations. Since the anticommutator of two SUSY transformations generates a space-time translation, the internal symmetries between fermions and bosons are intrinsically entangled with the space-time symmetries.
The single-particle states of a supersymmetric theory fall into irreducible representations of the supersymmetric algebra, the supermultiplets. Each supermultiplet contains both fermion and boson states, which are commonly known as superpartners of each other. The squared-mass operator $-P^2$ commutes with the operators $Q, Q^\dagger$, and with all space-time rotations and translation operators, so it follows that particles inhabiting the same irreducible supermultiplet must have equal eigenvalues of $-P^2$, and therefore equal masses. The supersymmetry generators $Q, Q^\dagger$ also commute with the generators of gauge transformations. Therefore particles in the same supermultiplet must also be in the same representation of the gauge group, and so must have the same quantum numbers. From the spin-statistic theorem follows, that each supermultiplet contains an equal number of fermionic and bosonic degrees of freedom.
Mathematically most appealing is the **superfield formalism**, which combines all fields of a supermultiplet in a single object, a superfield (which is always denoted by a "hat"). The superfields live in superspace which is spanned by the usual space-time dimensions plus additional fermionic coordinates θ_α and $\bar{\theta}^{\dot{\alpha}}$ ($\alpha = 1, 2$). The most general superfield can be expanded as

$$\hat{\mathcal{F}} = f + \theta\,\phi + \bar{\theta}\,\bar{\chi} + \theta\theta\,M + \bar{\theta}\bar{\theta}\,N + \theta\sigma^\mu\bar{\theta}\,A_\mu + \theta\theta\bar{\theta}\,\bar{\lambda} + \bar{\theta}\bar{\theta}\theta\,\alpha + \theta\theta\bar{\theta}\bar{\theta}\,d \tag{1.9}$$

with four complex scalar fields $f(x)$, $M(x)$, $N(x)$, $d(x)$, two left-handed Weyl spinor fields $\phi(x)$, $\alpha(x)$, two right-handed Weyl spinor fields $\bar{\chi}(x)$, $\bar{\lambda}(x)$ and a complex vector field $A_\mu(x)$, which is fixed by the requirement that $\hat{\mathcal{F}}$ is a Lorentz scalar. Linear combinations of superfields are again superfields. Therefore superfields yield a linear representation of the SUSY-algebra. However this representation is reducible. Through the demand of certain attributes one obtains irreducible representations.

- $\bar{D}_{\dot{\alpha}}\hat{\Phi} = 0$: The **chiral superfield** $\hat{\Phi}(y,\theta) = \tilde{q}(y) + \sqrt{2}\theta q(y) + \theta\theta F(y)$ contains one complex scalar field $\tilde{q}$, one left-handed 2-component Weyl spinor field q and one complex auxiliary field F. Here $\bar{D}_{\dot{\alpha}} = -\bar{\partial}_{\dot{\alpha}} + i(\tilde{\sigma}^{\mu}\theta)_{\dot{\alpha}}\,\partial_{\mu}$ is the covariant derivative and $y^{\mu} = x^{\mu} + i\theta\sigma^{\mu}\bar{\theta}$ are complex coordinates.

- $\bar{D}_{\alpha}\hat{\Phi}^{\dagger} = 0$: The **antichiral superfield** $\hat{\Phi}^{\dagger}(\bar{y},\theta) = \tilde{q}^{*}(\bar{y}) + \sqrt{2}\bar{\theta}\bar{q}(\bar{y}) + \bar{\theta}\bar{\theta}F^{*}(\bar{y})$ contains one complex scalar field $\tilde{q}^{*}$, one right-handed 2-component Weyl spinor field $\bar{q}$ and one complex auxiliary field F^{*}. Here $\bar{D}_{\alpha} = \partial_{\alpha} + i(\sigma^{\mu}\bar{\theta})_{\alpha}\,\partial_{\mu}$ is the covariant derivative and $\bar{y}^{\mu} = x^{\mu} - i\theta\sigma^{\mu}\bar{\theta}$ are complex coordinates.

- $\hat{V} = \hat{V}^{\dagger}$: The **vector superfield** $\hat{V}(x,\theta,\bar{\theta}) = (\theta\sigma^{\mu}\bar{\theta})V_{\mu}(x) + i\theta\theta\bar{\theta}\bar{\tilde{v}}(x) - \bar{\theta}\bar{\theta}\theta\tilde{v}(x) + \theta\theta\bar{\theta}\bar{\theta}D(x)$ contains one real massless vector field $V_{\mu}(x)$, one complex Weyl spinor field $\tilde{v}(x)$ and one real auxiliary field $D(x)$. In the Wess-Zumino gauge the remaining 7 degrees of freedom are removed by a supersymmetric gauge transformation. The associated supersymmetric field strength tensor of a vector superfield is denoted by $\hat{F}$.

The goal is to find a supersymmetric Lagrangian, which leaves the action $S = \int d^4x\mathcal{L}$ invariant under SUSY transformations. Therefore all terms that transform under SUSY maximally as a total-divergence (these terms vanish after the d^4x integration in S), are possible candidates for the Lagrangian. This is true for the $\theta\theta$ component of a chiral superfield, and the $\theta\theta\bar{\theta}\bar{\theta}$ component of a vector superfield. Products of chiral superfields again yield chiral superfields (e.g. Φ^2), whereas each real superfield is per definition a vector superfield. Therefore the product of a chiral superfield and an antichiral superfield $\Phi\Phi^{\dagger}$ is a vector superfield. A simple Lagrangian with chiral superfields would be

$$\mathcal{L} = \Phi^{\dagger}(x,\theta,\bar{\theta})\Phi(x,\theta,\bar{\theta})\Big|_{\theta\theta\bar{\theta}\bar{\theta}} - m\,\Phi^2(x,\theta,\bar{\theta})\Big|_{\theta\theta} - g\,\Phi^3(x,\theta,\bar{\theta})\Big|_{\theta\theta} + h.c. \tag{1.10}$$

This corresponds to a kinetic term, a mass term and an interaction term respectively. Introductions to Supersymmetry can be found in [43–45].

1.2 The Standard Model

The ambition of particle physics is to describe the kinematics and the interactions of the most elementary building blocks of the world. The laws of nature which can be probed by present high-energy colliders are in good agreement with the Standard Model of particle physics (SM). In several cases it has been tested to a precision better than one part in a million. The Standard Model describes the electromagnetic, the weak and the strong force and is formulated as a local gauge field theory as described in 1.1.1 and is based on the gauge group G_{SM} of unitary gauge transformations.

$$G_{\mathrm{SM}} = SU(3)_c \times SU(2)_L \times U(1)_Y \tag{1.11}$$

1.2.1 The Particles of the SM

The basic constituents of the **matter** sector are the fermionic spin-1/2 leptons and quarks which are shown in Table 1.1. Both appear in three generations of identical structure. Each lepton family consists of a charge $Q = -1$ particle namely electron e^{-},

Field	$SU(3)_c$	$SU(2)_L$	$U(1)_Y$	Particle Content		
f_L	1	2	-1	$(\nu_e, e^-)_L$	$(\nu_\mu, \mu^-)_L$	$(\nu_\tau, \tau^-)_L$
	3	2	$\frac{1}{3}$	$(u, d)_L$	$(c, s)_L$	$(t, b)_L$
f_R	1	1	-2	e^-_R	μ^-_R	τ^-_R
	3	1	$\frac{4}{3}$	u_R	c_R	t_R
	3	1	$-\frac{2}{3}$	d_R	s_R	b_R

Table 1.1: Fermionic particle content of the SM.

Field	$SU(3)_c$	$SU(2)_L$	$U(1)_Y$	Particle Content
G^a_μ	8	1	0	g^a $a = 1 \dots 8$
W^i_μ	1	3	0	W^i $i = 1, 2, 3$
B_μ	1	1	0	B

Table 1.2: Gauge bosons of the SM.

muon μ^- and tau τ^-, and an electrically neutral associated neutrino ν_e, ν_μ and ν_τ. The quark families comprise the up (u), charm (c) and top (t) quarks with electromagnetic charge $Q = 2/3$ and the associated down(d), strange (s) and bottom (b) quarks with charge $Q = -1/3$. Each generation consists of a left-handed $SU(2)$ doublet f_L with weak isospin $I = 1/2$ and a right-handed $SU(2)$ singlet f_R with $I = 0$. Every quark appears in three different colour states, therefore belongs to a $SU(3)$ triplet, while the leptons are colourless $SU(3)$ singlets. The hypercharge Y relates to the electric charge Q and the isospin I_3 by the Gell-Mann-Nishijima relation $Q = I_3 + Y/2$. These fermions as well as their antiparticles (for each particle exists an associated antiparticle with the same mass but opposite quantum numbers) have all been experimentally identified. The different isospin assignments to left-handed and right-handed fields allows for maximal parity violation in the weak interactions. At least three generations must be realized in Nature to incorporate CP violation in the Standard Model [46]. The bosonic particle content of the SM constitutes the **gauge sector** of the theory. The SM Lagrangian is invariant under local $SU(3)_c$, $SU(2)_L$ and $U(1)_Y$ transformations. $SU(3)_c$ is the non-Abelian symmetry group of the strong interactions. The eight gluonic gauge fields G^a are coupled to the color charges as formalized in Quantum Chromodynamics (QCD). $SU(2)_L$ is the non-Abelian electroweak-isospin group, to which three gauge fields W^i are associated. $U(1)_Y$ is the Abelian hypercharge group with gauge field B. The gauge theory of the electroweak interactions based on the symmetry group $SU(2)_L \times U(1)_Y$ is known as the Glashow-Salam-Weinberg theory [5, 9, 10]. The spin-1 gauge fields are shown in Table 1.2. The B field and the third component of the W triplet field mix to form the photon field A and the electroweak field Z. The other two components W^1 and W^2 of the triplet constitute the two charged fields $W^\pm$.

$$\begin{pmatrix} A_\mu \\ Z_\mu \end{pmatrix} = \begin{pmatrix} \cos\theta_W & \sin\theta_W \\ -\sin\theta_W & \cos\theta_W \end{pmatrix} \begin{pmatrix} B_\mu \\ W^3_\mu \end{pmatrix} \quad , \quad W^\pm_\mu = \frac{1}{\sqrt{2}} \left(W^1_\mu \mp i W^2_\mu \right) \tag{1.12}$$

θ_W is the Weinberg or weak mixing angle. These fields are the mass eigenstates of the massive theory, because experimental measurements require the electroweak gauge bosons $W^{\pm}$ and Z to be massive. Thus the gauge group $SU(2)_L \times U(1)_Y$ must be spontaneously broken. Since gluons and photons are massless, the $SU(3)_c \times U(1)_{elm}$ symmetry remains intact in the physical states and interactions. Spontaneous symmetry breaking occurs in the **Higgs sector**. To combine left-handed doublets and right-handed singlets in the fermion-Higgs Yukawa interaction, the Higgs field must be an isodoublet field $\varphi = (\varphi^+, \varphi^0)$ with hypercharge $Y_H = 1$. The value of the field in the ground state is determined by the minimum of the scalar potential $V(\varphi)$, cf. equation (1.5). A field component $H(x)$ which describes small oscillations around the ground state defines the physical Higgs field. Thus the scalar isodoublet field may be parametrized as:

$$\varphi(x) = U(x) \begin{pmatrix} 0 \\ v + H(x) \end{pmatrix} \tag{1.13}$$

where the matrix U incorporates the three remaining Goldstone degrees of freedom which can be removed by a gauge transformation (unitary gauge). With the choice of a vacuum expectation value $\langle 0|\varphi|0\rangle = \bar{v} = (0, v)$ the $SU(2)_L \times U(1)_Y$ symmetry is spontaneously broken. But the vacuum expectation value is still symmetric under transformations $\exp(i\alpha Q)$ of the subgroup $U(1)_{elm}$ with the charge generator

$$Q = I_3 + Y/2 = \begin{pmatrix} 1 & 0 \\ 0 & 0 \end{pmatrix} \tag{1.14}$$

In this way the $SU(2)_L \times U(1)_Y$ symmetry is broken down to $U(1)_{elm}$. The unbroken symmetry corresponds to the massless gauge boson, the photon.

1.2.2 The Interactions of the SM

The interactions of the Standard Model are summarized by three terms in the basic Standard Model Lagrangian

$$\mathcal{L}_{SM} = \mathcal{L}_{Gauge} + \mathcal{L}_{Fermions} + \mathcal{L}_{Higgs} \tag{1.15}$$

In fact this is not the whole story because for higher order calculations one would need additional terms for the gauge fixing and the ghost sector. Additional ghost fields are required to remove unphysical timelike and longitudinal polarisation states of non-Abelian gauge bosons. However, the ghost fields are only a computational tool and do not correspond to any physical particles. The terms in the SM Lagrangian have the following form

$$\mathcal{L}_{Gauge} = -\frac{1}{4} W^i_{\mu\nu} W^{i\,\mu\nu} - \frac{1}{4} B_{\mu\nu} B^{\mu\nu} - \frac{1}{4} G^a_{\mu\nu} G^{a\,\mu\nu} \quad , \quad \mathcal{L}_{Fermions} = \sum_f \bar{f}\, i\not{D}\, f$$

$$\mathcal{L}_{Higgs} = |D_\mu \varphi|^2 + g^l_f\, \bar{L}_L\, \varphi\, l_R + g^d_f\, \bar{Q}_L\, \varphi\, q^d_R + g^u_f\, \bar{Q}_L\, \tilde{\varphi}\, q^u_R + \text{h.c.} - \frac{\lambda}{2} \left[|\varphi|^2 - v^2 \right]^2 \tag{1.16}$$

The first term $\mathcal{L}_{Gauge}$ is built up by the gauge fields and their self-interactions with the field strengths

$$W^i_{\mu\nu} = \partial_\nu W^i_\mu - \partial_\mu W^i_\nu - g \epsilon^{ijk} W^j_\mu W^k_\nu \quad , \quad B_{\mu\nu} = \partial_\nu B_\mu - \partial_\mu B_\nu$$
$$G^a_{\mu\nu} = \partial_\nu G^a_\mu - \partial_\mu G^a_\nu - g_s f^{abc} G^b_\mu G^c_\nu \tag{1.17}$$

The tensors ϵ^{ijk} and f^{abc} are the $SU(2)$ and $SU(3)$ structure constants and g and g_s are the weak-isospin and the strong coupling, respectively. The second term $\mathcal{L}_{Fermions}$ summarizes the fermion-gauge boson couplings with the sum running over the left- and right-handed field components of the leptons and quarks. Depending on the fermion species, the covariant derivative takes the form

$$iD_\mu = i\partial_\mu - g\, I^i W_\mu^i - g' \frac{Y}{2} B_\mu - g_s\, T^a G_\mu^a \tag{1.18}$$

where the hypercharge coupling is denoted by g'. Finally, the Higgs Lagrangian $\mathcal{L}_{Higgs}$ contains the Higgs-gauge boson interactions generated by the covariant derivative, the Higgs-fermion Yukawa couplings and the potential of the Higgs self-interactions. The field φ generates the masses for down-type leptons and quarks f^d, while the field $\tilde{\varphi} = i\sigma_2\varphi^* = (\varphi^{0*}, -\varphi^-)$ is the charge-conjugated Higgs field which generates the masses of the up-type quarks f^u. In the SM the neutrinos are defined to be massless, although experiments show that the neutrinos carry small masses as well [47]. The Yukawa couplings g_f in (1.16) are matrices in flavour space which leads to non-diagonal mass matrices after spontaneous symmetry breaking. The diagonalisation of these matrices yields the physical mass eigenstates. The Cabibbo-Kobayashi-Maskawa (CKM) matrix is a remnant of this diagonalisation and generates couplings of the gauge bosons $W^\pm$ to quark mass eigenstates of different generations. This is the only source of flavour changing quark interactions within the Standard Model. Moreover the CKM matrix contains the Kobayashi-Maskawa phase δ_{KM} which is the single source of CP violation in the quark sector of the Standard Model [46, 48].
The Lagrangian $\mathcal{L}_{SM}$ summarizes the laws of physics for the three basic interactions, the electromagnetic, the weak and the strong interactions between the leptons and the quarks, and it predicts the form of the self-interactions between the gauge fields. Moreover, the specific form of the Higgs interactions generates the masses of the fundamental particles, the leptons and quarks, the gauge bosons and the Higgs boson itself, and it predicts the interactions of the Higgs particle [49].

1.3 The Minimal Supersymmetric Extension of the SM

Although the SM describes the experiments performed at previous and present high-energy colliders very successfully, it cannot be considered as a final theory to describe the fundamental particle interactions up to very high energy scales. At the latest at the Planck scale ($\Lambda_{Pl} \approx 10^{19} GeV$) the theory will break down because the gravitational force becomes as strong as the other three forces and a unified quantum mechanical treatment is required. But already at much lower energies there are several problems that cannot be solved without adding new physics to the SM. Prominent mysteries in the SM are the evidence for dark matter in the universe, the unnatural fine tuning in the gauge hierarchy problem, and the missing explanation for the family structure of the fermions. One of the most favourite extensions of the SM is Supersymmetry. The minimal low-energy effective theory which comprises the SM is the MSSM, the Minimal Supersymmetric Extension of the SM.

1.3.1 The Particles of the MSSM

The minimal supersymmetric extension of the Standard Model (MSSM) contains all SM particles and as few additional particles as possible to render the theory invariant under SUSY transformations, that means we need to double the entire spectrum, placing the observed SM particles in superfields with new postulated superpartners. In the superfield formalism all scalar and spinor fields of the SM are converted to chiral superfields, and the gauge fields to corresponding vector superfields. The new superpartners of quarks, leptons, gauge and Higgs bosons are called squarks, sleptons, gauginos and Higgsinos respectively (the usual notation is to denote the supersymmetric partner of a fermion or gauge field with the same letter and a tilde). The particles of the MSSM and their quantum numbers are specified in Tables 1.3 and 1.4. We follow a standard convention,

Superfield	SU(3)	$SU(2)_L$	$U(1)_Y$	Particle Content
$\hat{Q}$	3	2	$\frac{1}{3}$	(u_L, d_L), $(\tilde{u}_L, \tilde{d}_L)$
$\hat{U}^c$	$\overline{3}$	1	$-\frac{4}{3}$	$u_R^\dagger$, $\tilde{u}_R^*$
$\hat{D}^c$	$\overline{3}$	1	$\frac{2}{3}$	$d_R^\dagger$, $\tilde{d}_R^*$
$\hat{L}$	1	2	-1	(ν_L, e_L), $(\tilde{\nu}_L, \tilde{e}_L)$
$\hat{E}^c$	1	1	2	$e_R^\dagger$, $\tilde{e}_R^*$
$\hat{H}_1$	1	2	-1	(H_1^0, H_1^-), $(\tilde{H}_1^0, \tilde{H}_1^-)$
$\hat{H}_2$	1	2	1	(H_2^+, H_2^0), $(\tilde{H}_2^+, \tilde{H}_2^0)$

Table 1.3: Chiral Superfields of the MSSM

Superfield	SU(3)	$SU(2)_L$	$U(1)_Y$	Particle Content
$\hat{G}^a$	8	1	0	g, $\tilde{g}$
$\hat{W}^i$	1	3	0	W_i, $\tilde{\omega}_i$
$\hat{B}$	1	1	0	B, $\tilde{b}$

Table 1.4: Vector Superfields of the MSSM

that all chiral supermultiplets are defined in terms of left-handed Weyl spinors, so that the conjugates of the right-handed quarks and leptons (and their superpartners) appear in Table 1.3. This protocol for defining chiral supermultiplets turns out to be very useful for constructing supersymmetric Lagrangians. Later on, the left-handed and right-handed Weyl spinors will be combined to form 4-component Dirac spinors $\psi = (\psi_L, \psi_R)$. It is important to note that the left-handed and the right-handed component of the Dirac spinor represent different degrees of freedom. Only in the case of a Majorana spinor they are connected by a transformation $\psi_L = i\sigma_2\psi_R^*$. The MSSM respects the same $SU(3)_c \times SU(2)_L \times U(1)_Y$ gauge symmetry as does the Standard Model. There are quark and lepton superfields for all 3 generations but in Table 1.3 only the members of the first generation are shown. The superfield $\hat{Q}$ thus consists of an $SU(2)_L$ doublet of quarks Q and their scalar partners $\tilde{Q}$ which are also in an $SU(2)_L$ doublet. Similarly,

the antichiral superfield $\hat{U}^{c\dagger}$ ($\hat{D}^{c\dagger}$) contains the right-handed up (down) quark u_R (d_R), and its scalar partner $\tilde{u}_R$ ($\tilde{d}_R$). We see that each quark has 2 scalar partners, one corresponding to each quark chirality. The leptons are contained in the $SU(2)_L$ doublet superfield $\hat{L}$ which contains the left-handed fermions, and their scalar partners. Finally, the right-handed electron e_R is contained in the superfield $\hat{E}^{c\dagger}$ and has a scalar partner $\tilde{e}_R$. The $SU(3)_c \times SU(2)_L \times U(1)_Y$ gauge fields all obtain fermion partners in a SUSY model. The $\hat{G}^a$ superfield contains the gluons g^a and their partners the gluinos $\tilde{g}^a$, $\hat{W}_i$ contains the $SU(2)_L$ gauge bosons W_i and their fermionic partners $\tilde{\omega}_i$ (winos), and $\hat{B}$ contains the $U(1)$ gauge field B and its fermionic partner $\tilde{b}$ (bino). In order for the theory to be free of anomalies, there are two Higgs doublets in Table 1.3. The Standard Model contains a single $SU(2)_L$ Higgs doublet. In the supersymmetric extension of the Standard Model, this scalar doublet acquires a SUSY partner which is an $SU(2)_L$ doublet of fermion fields $\tilde{H}_1$ (the Higgsinos), which contribute to the triangle $SU(2)_L$ and $U(1)_Y$ gauge anomalies. Since the fermions of the Standard Model have exactly the right quantum numbers to cancel these anomalies, it follows that the contribution from the fermionic partner of the Higgs doublet remains uncancelled. Since renormalisable gauge theories cannot have anomalies, these contributions must be cancelled in a sensible SUSY theory. The simplest way is to add a second Higgs doublet with precisely the opposite $U(1)_Y$ quantum numbers from the first Higgs doublet. In a SUSY Model, this second Higgs doublet will also have fermionic partners, $\tilde{H}_2$, and the contributions of the fermionic partners of the two Higgs doublets to gauge anomalies will precisely cancel each other, leaving an anomaly free theory. Moreover two Higgs doublets are required in order to give both the up and down quarks masses in a SUSY theory.

1.3.2 The Interactions of the MSSM

After all superfields of the theory have been specified, the next step is to construct the supersymmetric Lagrangian. There is very little freedom in the allowed interactions between the ordinary particles and their supersymmetric partners. It is this feature of a SUSY model which implies its predictive power. In the superfield formalism, the SM Lagrangian (1.15) is extended to the supersymmetric Lagrangian

$$\begin{aligned} \mathcal{L}_{SUSY} &= \mathcal{L}_{Vector} + \mathcal{L}_{Chiral} + \mathcal{L}_{Superpot} \quad , \quad \mathcal{L}_{Vector} = \frac{1}{4}\sum_{\hat{V}} \hat{F}^a \hat{F}_a \Big|_{\theta\theta} + \text{h.c.} \\ \mathcal{L}_{Chiral} &= \textstyle\sum_{\hat{\Phi}} \hat{\Phi}^\dagger \exp\left(\sum_{\hat{V}} g_V \hat{V}\right) \hat{\Phi} \Big|_{\theta\theta\bar{\theta}\bar{\theta}} \quad , \quad \mathcal{L}_{Superpot} = \hat{W}\Big|_{\theta\theta} + \text{h.c.} \end{aligned} \tag{1.19}$$

The first two terms $\mathcal{L}_{Vector}$ and $\mathcal{L}_{Chiral}$ generate the kinetic energy and the gauge couplings of all vector superfields $\hat{V} = \hat{V}^a T^a \in \{\hat{G}^a T^a, \hat{W}^i T^i, \hat{B}Y/2\}$ and all chiral superfields $\hat{\Phi} \in \{\hat{Q}, \hat{U}^c, \hat{D}^c, \hat{L}, \hat{E}^c, \hat{H}_1, \hat{H}_2\}$. All gauge couplings are still fixed by the principle of gauge invariance and the gauge group $SU(3)_c \times SU(2)_L \times U(1)_Y$. The only freedom in constructing the supersymmetric Lagrangian (once the superfields and the gauge symmetries are chosen) is contained in the **superpotential** $\hat{W}$. It can be considered as the analogue to the Higgs potential $V(H)$ and the Yukawa couplings in the SM. The superpotential is a polynomial function of all chiral superfields in Table 1.3, but due to renormalisability only bilinear and trilinear terms are possible and derivative interactions are forbidden. Furthermore only products of chiral (or antichiral) fields are allowed to appear in the superpotential. Mixed products of chiral and antichiral superfields would

destroy supersymmetry. Therefore the SM mechanism to generate masses for the up- and down-type fermions through the interaction with the Higgs field H and its charge conjugated field H^c cannot be repeated in the MSSM. All supersymmetric extensions of the SM contain at least two complex $SU(2)_L$ Higgs doublets H_1 and H_2 with hypercharge -1 and $+1$. The usual approach is to write the most general $SU(3)_c \times SU(2)_L \times U(1)_Y$ invariant superpotential with arbitrary coefficients for the interactions

$$\begin{aligned}\hat{W} &= \epsilon_{ij}\mu\hat{H}_1^i\hat{H}_2^j + \epsilon_{ij}\Big[\lambda_L\hat{H}_1^i\hat{L}^j\hat{E}^c + \lambda_D\hat{H}_1^i\hat{Q}^j\hat{D}^c + \lambda_U\hat{H}_2^j\hat{Q}^i\hat{U}^c\Big] \\ &\quad +\epsilon_{ij}\Big[\lambda_1\hat{L}^i\hat{L}^j\hat{E}^c + \lambda_2\hat{L}^i\hat{Q}^j\hat{D}^c\Big] + \lambda_3\hat{U}^c\hat{D}^c\hat{D}^c \qquad (1.20)\end{aligned}$$

(where i, j are $SU(2)$ indices). We have written the superpotential in terms of the fields of the first generation. In principle, the λ_i could all be matrices which mix the interactions of the 3 generations. The terms in the second line of equation (1.20) (proportional to λ_1, λ_2 and λ_3) contribute to lepton and baryon number violating interactions and can mediate proton decay at tree level through the exchange of the scalar partner of the down quark. There are several possible solutions to the problem of the lepton and baryon number violating interactions. The usual strategy is to require that all of these undesirable lepton and baryon number violating terms are forbidden by a symmetry. A symmetry which fulfils this requirement is **R-parity**. R-parity can be defined as a multiplicative quantum number such that all particles of the Standard Model carry R parity $+1$, while their SUSY partners carry R parity -1. Such a symmetry forbids the lepton and baryon number violating terms of equation (1.20). It is worth noting that in the Standard Model, the problem of baryon and lepton number violating interactions does not arise, since these interactions are forbidden by the gauge symmetries to contribute to dimension-4 operators and first arise in dimension-6 operators which are suppressed by factors of some heavy mass scale. The assumption of R parity conservation has profound experimental consequences:

- SUSY partners can only be pair produced from Standard Model particles.
- A theory with R parity conservation exhibits a lightest SUSY particle (LSP) which is stable.

The auxiliary fields F and D in the chiral and vector superfields have no kinetic energy term in the Lagrangian. After the superfields are expanded in terms of their component fields, they can be removed by substituting the solutions of the equations of motion. After this procedure, the Lagrangian of equation (1.19) acquires the form

$$\begin{aligned}\mathcal{L}_{Vector} &= -\frac{1}{4}\sum_{V^a} F^a_{\mu\nu}F^{a\mu\nu} + \frac{1}{2}\sum_{\tilde{v^a}} \bar{\tilde{v}}^a \; i\not{D}\; \tilde{v}^a - \frac{1}{2}\sum_{V^a} g_V^2\big(\sum_{\phi}\phi^* T^a\phi\big)^2 \\ \mathcal{L}_{Chiral} &= \sum_{\psi}\bar{\psi}\; i\not{D}\; \psi + \sum_{\phi}|D_\mu\phi|^2 + \sum_{\psi,\varphi,\tilde{v}}\sqrt{2}g_V[i\bar{\psi}\tilde{v}^a T^a\phi + \text{h.c.}] \\ \mathcal{L}_{Superpot} &= -\sum_{\phi}\Big|\frac{\partial W}{\partial\phi}\Big|^2 - \frac{1}{2}\sum_{\phi,\phi'}\Big[\overline{\psi^c}\;\frac{\partial^2 W}{\partial\phi\partial\phi'}\psi' + \text{h.c.}\Big] \qquad (1.21)\end{aligned}$$

This Lagrangian is expressed in terms of 4-component Dirac fermions namely $\psi \in \{Q, u_R, d_R, L, e_R, \tilde{H}_1, \tilde{H}_2\}$ and their superpartners $\phi \in \{\tilde{Q}, \tilde{u}_R, \tilde{d}_R, \tilde{L}, \tilde{e}_R, H_1, H_2\}$. The

superpartners of the gauge fields are Majorana fermions $\tilde{v} \in \{\tilde{g}^a T^a, \tilde{w}^i I^i, \tilde{b} Y/2\}$. The superpotential W is the same as $\hat{W}$ in equation (1.20) but with all superfields replaced by their corresponding scalar field. The $\mu \hat{H}_1 \hat{H}_2$ term in the superpotential (1.20) gives mass terms for the Higgs bosons when we apply $|\partial W/\partial\phi|^2$ and μ is called the Higgsino mass parameter. The terms in the square brackets of W proportional to λ_L, λ_D, and λ_U yield the usual Yukawa interactions of the fermions with the Higgs bosons from the term $\bar{\psi^c}(\partial^2 W/\partial\phi\partial\phi')\psi'$. Hence these coefficients are determined in terms of the fermion masses and the vacuum expectation values of the neutral members of the scalar components of the Higgs doublets and are not free parameters.

Supersymmetry Breaking

As a consequence of supersymmetry, all particles in a supermultiplet must have the same masses. Since mass degenerated particles were never observed (e.g. a scalar particle with the mass of the electron) SUSY must be broken. The mechanism of supersymmetry breaking is not well understood. It is typically assumed that the SUSY breaking occurs at a high scale, say M_{pl}, and perhaps results from some complete theory including gravity. At the moment the usual approach is to assume that the MSSM, which is the theory at the electroweak scale, is an effective low energy theory. The supersymmetry breaking is implemented by including explicit "soft" mass terms for the scalar members of the chiral multiplets and for the gaugino members of the vector supermultiplets in the Lagrangian. These interactions are termed soft because they do not re-introduce the quadratic divergences whose cancellation is one of the major motivations for SUSY. The dimension of soft operators in the Lagrangian must be 3 or less, which means that the possible soft operators are mass terms, bi-linear mixing terms ("B" terms), and tri-linear scalar mixing terms ("A" terms). The philosophy is to add all of the mass and mixing terms which are allowed by the gauge symmetries. The origin of these supersymmetry breaking terms is left unspecified. The complete set of soft SUSY breaking terms (which respect R parity and the $SU(3)_c \times SU(2)_L \times U(1)_Y$ gauge symmetry) for the first generation is given by the Lagrangian:

$$\begin{aligned}
-\mathcal{L}_{Soft} \;=\; & m_1^2 \mid H_1 \mid^2 + m_2^2 \mid H_2 \mid^2 - B\mu\epsilon_{ij}(H_1^i H_2^j + \text{h.c.}) + \tilde{M}_Q^2(\tilde{u}_L^* \tilde{u}_L + \tilde{d}_L^* \tilde{d}_L) \\
& + \tilde{M}_u^2 \tilde{u}_R^* \tilde{u}_R + \tilde{M}_d^2 \tilde{d}_R^* \tilde{d}_R + \tilde{M}_L^2(\tilde{e}_L^* \tilde{e}_L + \tilde{\nu}_L^* \tilde{\nu}_L) + \tilde{M}_e^2 \tilde{e}_R^* \tilde{e}_R \\
& + \frac{1}{2}\left[M_3 \bar{\tilde{g}} \tilde{g} + M_2 \overline{\tilde{\omega}_i} \tilde{\omega}_i + M_1 \bar{\tilde{b}} \tilde{b} \right] + \frac{g}{\sqrt{2} M_W} \epsilon_{ij} \left[\frac{m_d}{\cos\beta} A_d H_1^i \tilde{Q}^j \tilde{d}_R^* \right. \\
& \left. + \frac{m_u}{\sin\beta} A_u H_2^j \tilde{Q}^i \tilde{u}_R^* + \frac{m_e}{\cos\beta} A_e H_1^i \tilde{L}^j \tilde{e}_R^* + \text{h.c.} \right]
\end{aligned} \tag{1.22}$$

This Lagrangian exhibits arbitrary masses for the scalars and gauginos and also arbitrary tri-linear and bi-linear mixing terms. The scalar and gaugino mass terms yield the desired effect of breaking the degeneracy between the particles and their SUSY partners. The tri-linear A-terms have been defined with an explicit mass factor. We have also included an angle β in the normalization of the A terms. The factor β is related to the vacuum expectation values of the neutral components of the Higgs fields and is defined in the next section. The normalization is arbitrary. If the A_i terms are non-zero, the scalar partners of the left- and right-handed fermions can mix after the Higgs bosons acquire vacuum expectation values, and are no longer mass eigenstates. The B term mixes the scalar

components of the 2 Higgs doublets. All of the mass and interaction terms of equation (1.22) may be matrices involving all three generations. $\mathcal{L}_{soft}$ breaks supersymmetry since the SUSY partners of the ordinary particles have obtained arbitrary masses. However, this comes at the expense of introducing a large number of unknown parameters. The reason for this large number of unknown parameters is the ignorance of the exact SUSY breaking mechanism. What is really needed is a theory of how the soft SUSY breaking terms arise in order to reduce the parameter space.
We have now constructed the Lagrangian describing a softly broken supersymmetric theory which is assumed to be the effective theory at the weak scale. The complete Lagrangian of the MSSM is

$$\mathcal{L}_{MSSM} = \mathcal{L}_{SUSY} + \mathcal{L}_{Soft} \quad . \tag{1.23}$$

Higgs sector

The Higgs potential $V(H_1, H_2)$ is obtained from equations (1.21) and (1.22) by extracting all terms containing only scalar Higgs fields

$$\begin{aligned} V &= \left(\mid \mu \mid^2 + m_1^2\right) \mid H_1 \mid^2 + \left(\mid \mu \mid^2 + m_2^2\right) \mid H_2 \mid^2 - \mu B \epsilon_{ij} \left(H_1^i H_2^j + \text{h.c.}\right) \\ &\quad + \frac{g^2 + g'^2}{8} \left(\mid H_1 \mid^2 - \mid H_2 \mid^2\right)^2 + \frac{g^2}{2} \mid H_1^\dagger H_2 \mid^2 \end{aligned} \tag{1.24}$$

The Higgs potential determines the physical mass eigenstates of the Higgs fields and their self-interactions. The MSSM contains a light and a heavy CP-even Higgs boson h and H, one CP-odd Higgs boson A and two charged Higgs bosons $H^\pm$. The remaining three real degrees of freedom are absorbed by the heavy gauge bosons as in the SM. The terms in the first line of equation (1.24) involve the soft SUSY breaking parameters m_1^2, m_2^2 and $B\mu$ which are not contained in the superpotential. The quartic Higgs self-couplings in the second line are completely determined by the known gauge couplings g and g'. Therefore the Higgs potential depends on three independent parameters $m_1^2+\mu^2$, $m_2^2+\mu^2$ and $B\mu$. If $B\mu = 0$ then all the terms in the potential are positiv and the minimum of the potential occurs with $V = 0$ and $\langle H_1^0 \rangle = \langle H_2^0 \rangle = 0$ leaving the electroweak symmetry unbroken. Hence all three parameters need to be non-zero in order for the electroweak symmetry to be broken. The condition that the $W^\pm/Z$ bosons acquire the correct masses determines one of the three parameters. The usual choice for the remaining two free parameters is the pseudoscalar Higgs boson mass M_A and the ratio of the vacuum expectation values of the two Higgs fields, defined by $\text{tg}\beta \equiv v_2/v_1$. The mixing terms in equation (1.24) can be diagonalised by means of the two mixing angles α and β.

$$\begin{aligned} \begin{pmatrix} H_1^0 \\ H_1^- \end{pmatrix} &= \begin{pmatrix} \frac{1}{\sqrt{2}}[v_1 + H\cos\alpha - h\sin\alpha + i\ A\sin\beta - i\ G^0\cos\beta] \\ H^-\sin\beta - G^-\cos\beta \end{pmatrix} \\ \begin{pmatrix} H_2^+ \\ H_2^0 \end{pmatrix} &= \begin{pmatrix} H^+\cos\beta + G^+\sin\beta \\ \frac{1}{\sqrt{2}}[v_2 + H\sin\alpha + h\cos\alpha + i\ A\cos\beta + i\ G^0\sin\beta] \end{pmatrix} \end{aligned} \tag{1.25}$$

Here $\sin\beta = v_2/v$ and $\cos\beta = v_1/v$ with $v = \sqrt{v_1^2 + v_2^2}$ and α is the mixing angle between the original neutral scalar Higgs fields of definite weak hypercharge $H_{1,2}^0$ and

the mass eigenstates. The diagonalisation yields 5 physical Higgs bosons: two neutral CP-even (scalar) bosons h, H, one neutral CP-odd (pseudoscalar) boson A and two charged bosons $H^{\pm}$. The Goldstone bosons G^0 and $G^{\pm}$ are absorbed by the Z and $W^{\pm}$ gauge bosons to give them masses.

Sfermion sector

The mass degeneracy of the fermions f and their superpartners $\tilde{f}$ is destroyed by the soft SUSY breaking terms and off-diagonal elements in the squark mass matrix are created by chirality changing Yukawa-interactions. Therefore the gauge eigenstates $\tilde{f}_L$ and $\tilde{f}_R$ can mix with each other. The symmetric squark mass matrix in the chirality basis is given by

$$\mathbf{M}^2_{\tilde{q}_{LR}} = \begin{pmatrix} M^2_{\tilde{q}_L} + m_q^2 + (I_q^3 - e_q sin^2\theta_W) M_Z^2 \cos 2\beta & m_q(A_q - \mu r_q) \\ m_q(A_q - \mu r_q) & M^2_{\tilde{q}_R} + m_q^2 + e_q \sin^2\theta_W M_Z^2 \cos 2\beta \end{pmatrix}$$

The electric charge is denoted by e_q, the third component of the weak isospin is $I^3_{u/d} = \pm 1/2$ and

$$r_q = \begin{cases} \cot\beta & \text{for up} - \text{type } q \\ \text{tg}\beta & \text{for down} - \text{type } q \end{cases} \tag{1.26}$$

The factor r_q increases for small tgβ the up- and for large tgβ the down-type mixing. The off-diagonal mixing terms are proportional to the quark masses, therefore mixing effects are primarily relevant for the third generation fermions. If the D-terms proportional to M_Z^2 are absorbed into the parameter $M^2_{\tilde{q}_{L/R}}$, the squark mass matrix becomes

$$\mathbf{M}^2_{\tilde{q}_{LR}} = \begin{pmatrix} M^2_{LL} & M^2_{LR} \\ M^2_{RL} & M^2_{RR} \end{pmatrix} = \begin{pmatrix} M^2_{\tilde{q}_L} + m_q^2 & m_q(A_q - \mu r_q) \\ m_q(A_q - \mu r_q) & M^2_{\tilde{q}_R} + m_q^2 \end{pmatrix} \tag{1.27}$$

The mass eigenstates are denoted by $\tilde{f}_1$ and $\tilde{f}_2$ which are usually chosen to fulfill the inequality $M_{\tilde{f}_1} < M_{\tilde{f}_2}$. The mass matrix is rotated into its mass basis by means of the angle $\widetilde{\theta}_q$.

$$\begin{pmatrix} \widetilde{q}_1 \\ \widetilde{q}_2 \end{pmatrix} = \mathbb{R}(\widetilde{\theta}_q) \begin{pmatrix} \widetilde{q}_L \\ \widetilde{q}_R \end{pmatrix} \quad , \quad \mathbb{R}(\widetilde{\theta}_q) = \begin{pmatrix} +\cos\widetilde{\theta}_q & +\sin\widetilde{\theta}_q \\ -\sin\widetilde{\theta}_q & +\cos\widetilde{\theta}_q \end{pmatrix} \tag{1.28}$$

Thus we get the mass eigenstates $\widetilde{q}_1$ and $\widetilde{q}_2$ through mixing of $\widetilde{q}_L$ and $\widetilde{q}_R$ and the diagonal squark mass matrix

$$\mathbf{M}^2_{\tilde{q}_{12}} = \begin{pmatrix} M^2_{\tilde{q}_1} & 0 \\ 0 & M^2_{\tilde{q}_2} \end{pmatrix} \ , \ M_{\tilde{q}_{1/2}} = \frac{1}{2}\left(M^2_{LL} + M^2_{RR} \mp \sqrt{(M^2_{RR} - M^2_{LL})^2 + 4M^2_{LR}M^2_{RL}} \right)$$

and the useful expressions

$$\sin 2\widetilde{\theta}_q = \frac{2M^2_{LR}}{M^2_{\tilde{q}_1} - M^2_{\tilde{q}_2}} = \frac{2m_q(A_q - \mu r_q)}{M^2_{\tilde{q}_1} - M^2_{\tilde{q}_2}} \quad , \quad \cos 2\widetilde{\theta}_q = \frac{M^2_{LL} - M^2_{RR}}{M^2_{\tilde{q}_1} - M^2_{\tilde{q}_2}} \tag{1.29}$$

We will often use the abbreviations $c_{2\widetilde{\theta}} = \cos 2\widetilde{\theta}$ and $s_{2\widetilde{\theta}} = \sin 2\widetilde{\theta}$.

Gaugino and Higgsino sector

The gaugino and Higgsino fields in the MSSM are spin 1/2 fields and can mix if they carry the same electromagnetic charge. This yields the physical mass eigenstates of the gauginos $\tilde{w}^i$, $\tilde{b}$ and the Higgsinos $\tilde{H}_1$, $\tilde{H}_2$. These mass eigenstates are called neutralinos $\tilde{\chi}^0$ and charginos $\tilde{\chi}^\pm$. The eight degrees of freedom yield four neutralinos $\tilde{\chi}_1^0$, $\tilde{\chi}_2^0$, $\tilde{\chi}_3^0$, $\tilde{\chi}_4^0$ and two charginos $\tilde{\chi}_1^\pm$, $\tilde{\chi}_2^\pm$. In general the mass eigenstates do not correspond to the photino (the fermion partner of the photon) or a zino (the fermion partner of the Z boson) but are mixtures of these states. The lightest neutralino $\tilde{\chi}_1^0$ is assumed to be the LSP, the lightest SUSY particle.

Chapter 2

MSSM Higgs Boson Phenomenology

While the Standard Model of electroweak and strong interactions is in excellent agreement with the numerous experimental measurements, the dynamics responsible for electroweak symmetry breaking are still unknown. Within the Standard Model, the Higgs mechanism is invoked to break the electroweak symmetry. A doublet of complex scalar fields is introduced of which a single neutral scalar particle, the Higgs boson, remains after symmetry breaking. Many extensions of this minimal version of the Higgs sector have been proposed, including a scenario with two complex Higgs doublets as realized in the Minimal Supersymmetric Standard Model (MSSM). Within the Standard Model, the Higgs boson is the only particle that has not been discovered so far. The direct search at the e^+e^- collider LEP remained fruitless although it helped to set a lower mass bound. At the end of this year, the world's largest particle collider will start its operation. For many years, the Large Hadron Collider (LHC) will be the most important tool to study physics beyond the Standard Model. The LHC is a proton-proton collider with a beam energy of 7 TeV each, or correspondingly a maximal center of mass collision energy of $\sqrt{s} = 14$ TeV. It is believed, that the LHC is capable to discover supersymmetric particles up to 2.5 TeV. At the LHC six different experiments detect the emerging particles and analyse their properties. Of these, ATLAS and CMS are the two biggest detectors. Their main goal is the discovery of the Higgs boson. In the following, MSSM Higgs bosons are considered only. The Minimal Supersymmetric Standard Model contains two complex Higgs doublets, leading to five physical Higgs bosons after electroweak symmetry breaking: two neutral CP-even bosons h, H, one neutral CP-odd boson A and a pair of charged Higgs bosons $H^{\pm}$.

2.1 Mass Limits

The Higgs boson masses are very important parameters and it is essential to understand their theoretical and experimental constraints. The tree level Higgs potential (1.24) is fixed by two parameters, usually the pseudoscalar Higgs boson mass M_A and the ratio of the vacuum expectation values of the two Higgs fields, defined by $\mathrm{tg}\beta \equiv v_2/v_1$. The quadratic terms compose the Higgs mass matrix, while the higher powers in the Higgs field determine the self-interactions of the Higgs fields. The Higgs mass matrix can

easily be diagonalized and yields the following values for the physical Higgs fields and the mixing angle α at **tree level**

$$\begin{aligned} M_{H^\pm}^2 &= M_A^2 + M_W^2 \quad , \quad M_H^2 = M_A^2 + M_Z^2 - M_h^2 \\ M_h^2 &= \frac{1}{2}\Big[M_A^2 + M_Z^2 - \sqrt{(M_A^2 - M_Z^2)^2 \cos^2 2\beta + (M_A^2 + M_Z^2)^2 \sin^2 2\beta}\Big] \\ \tan 2\alpha &= \tan 2\beta \; [(M_A^2 + M_Z^2)/(M_A^2 - M_Z^2)] \end{aligned} \tag{2.1}$$

From these mass formulae two important relations can be derived, which are by construction valid at tree level

$$M_h \leq M_A, M_Z \leq M_H \quad , \quad M_A, M_W \leq M_{H^\pm} \tag{2.2}$$

The existence of an upper bound for the light Higgs boson mass in the MSSM is a consequence of the gauge structure of the MSSM, in which all trilinear and quartic Higgs self-couplings are fixed by the electroweak gauge couplings g, g'. The superpotential does not contain any trilinear and quartic interaction terms with unknown parameters. This in contrast to the SM where the value of the Higgs boson mass is a free parameter proportional to the Higgs self-coupling λ. This upper bound is of great phenomenological importance. Since the tree-level prediction is in contradiction with experiments, **radiative corrections** must play an important role. The leading one-loop corrections are proportional to m_t^4, therefore the Higgs mass bounds depend strongly on the value of the top quark mass. Their origin are incomplete cancellations between virtual top and stop loops, reflecting the breaking of supersymmetry. Moreover, the mass relations are affected by the potentially large mixing between $\tilde{t}_L$ and $\tilde{t}_R$ due to the top Yukawa coupling. The dominant one-loop corrections are determined by the parameter δ [50–52].

$$\delta = \frac{3G_F}{\sqrt{2}\pi^2} \frac{m_t^4}{\sin^2\beta} \Big[\log \frac{M_S^2}{m_t^2} + \frac{X_t^2}{M_S^2}\Big(1 - \frac{X_t^2}{12\, M_S^2}\Big)\Big] \tag{2.3}$$

The supersymmetric scale M_S^2 is the square root of the arithmetical average of the light and heavy stop masses, $M_S^2 = (M_{\tilde{t}_1}^2 + M_{\tilde{t}_2}^2)/2$. The first term in the bracket is the dominant contribution and it would vanish without SUSY breaking (mass degeneracy between t and $\tilde{t}$). The second term includes the leading effect in the case of a non-vanishing mixing angle in the stop sector, which is proportional to the characteristic parameter $X_t = A_t - \mu \cot\beta$. The approximation involves the assumption that the supersymmetric particles appearing in the loop are of order M_{SUSY}. The improved Higgs boson masses including the leading one-loop corrections are given by

$$\begin{aligned} M_{H^\pm}^2 &= M_A^2 + M_W^2 \quad , \quad M_H^2 = M_A^2 + M_Z^2 - M_h^2 + \delta \\ M_h^2 &= \frac{1}{2}\Big[M_A^2 + M_Z^2 + \delta - \sqrt{[(M_A^2 - M_Z^2)\cos 2\beta + \delta]^2 + (M_A^2 + M_Z^2)^2 \sin^2 2\beta}\Big] \end{aligned} \tag{2.4}$$

The LO prediction for the charged Higgs boson mass $M_{H^\pm}$ is not altered by the leading NLO corrections but the mixing angle α receives large corrections too

$$\tan 2\alpha = [(M_A^2 + M_Z^2)\sin 2\beta]/[(M_A^2 - M_Z^2)\cos 2\beta + \delta] \tag{2.5}$$

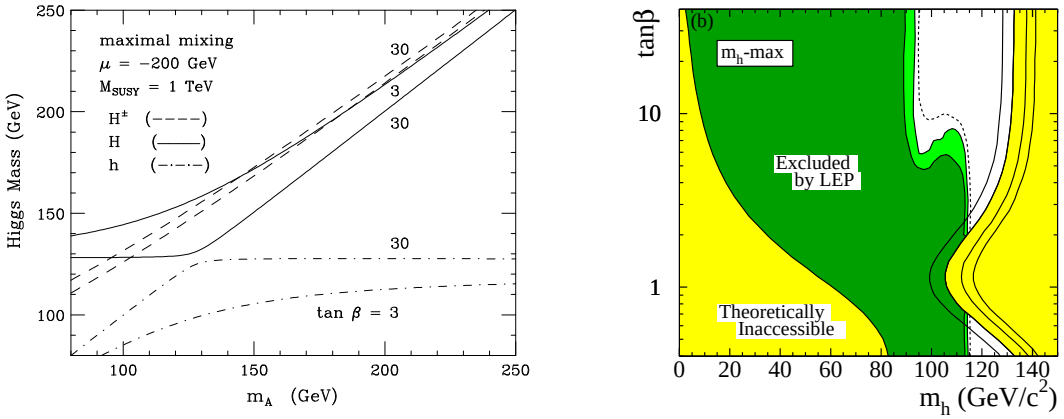

Figure 2.1: Left: The $\mathcal{CP}$-even and charged MSSM Higgs boson masses as a function of m_A for tg$\beta = 3$ and 30, including radiative corrections in the maximal mixing scenario [54]. Right: The MSSM exclusion limits at 95% CL (light-green) and 99.7% CL (dark-green), obtained by LEP for the maximal mixing scenario, with $m_t = 174.3$ GeV. The figure shows the excluded and theoretically inaccessible regions in the $(M_h, \text{tg}\beta)$ projection. The upper bound of the parameter space is sensitive to the top quark mass, it is indicated from left to right for $m_t = 169.3, 174.3, 179.3$ and 183.0 GeV [55].

therefore higher order corrections allow for the small α_{eff} scenario ($\alpha \to 0$). Equation 2.4 yields a new approximate upper bound for the light Higgs mass

$$M_h^2 \leq M_Z^2 + \delta \frac{\sin^2 \beta}{2} \tag{2.6}$$

The correction δ to the upper bound of the light Higgs mass is positive as long as $M_{\tilde{t}_1} M_{\tilde{t}_2} \geq m_t^2$ and it becomes maximal for a large stop mixing angle $\widetilde{\theta}_t \propto X_t$. The value X_t for which the upper bound is maximal is called **maximal mixing** or M_h^{max} scenario [53]. This scenario yields by definition the most conservative bound on the light Higgs mass. The other maximal mixing benchmark parameters are

$$m_t = 174.3\,\text{GeV}\ ,\ M_A \leq M_{SUSY} = 1\,\text{TeV}\ ,\ \mu = 200\,\text{GeV}\ ,\ M_{\tilde{g}} = 0.8\,M_{SUSY}\ ,\ A_t = A_b$$

The relation between the various Higgs boson masses as a function of M_A is illustrated in Figure 2.1 left for two different values of $\tan\beta = 3, 30$ in the maximal mixing scenario. The upper bound from equation (2.6) of the light Higgs boson mass is shifted to about $M_h \leq 135$ GeV if the uncertainties in the top quark mass and the higher-order corrections are included [56]. Figure 2.1 right shows the dependence of the upper mass bound on tgβ more clearly, and also the lower experimental bounds from the direct search for Higgs bosons. At LEP the MSSM Higgs bosons have been searched in the channels $e^+e^- \to Z, A + h/H$ and $e^+e^- \to H^+H^-$ [57, 58]. The obtained lower bounds are

$$M_{h,H} \geq 92.8\text{GeV}\ ,\ M_A \geq 93.4\text{GeV}\ ,\ M_{H^\pm} \geq 79.3\text{GeV} \quad \text{at 95\% CL} \tag{2.7}$$

The upper bound on M_h depends strongly on the choice of the top mass, see equation (2.6). This is illustrated by the four different m_t values for the upper M_h bound in Figure 2.1 right. For $m_t = 174.3$ GeV the tgβ region between 0.7 and 2.0 is excluded at 95%

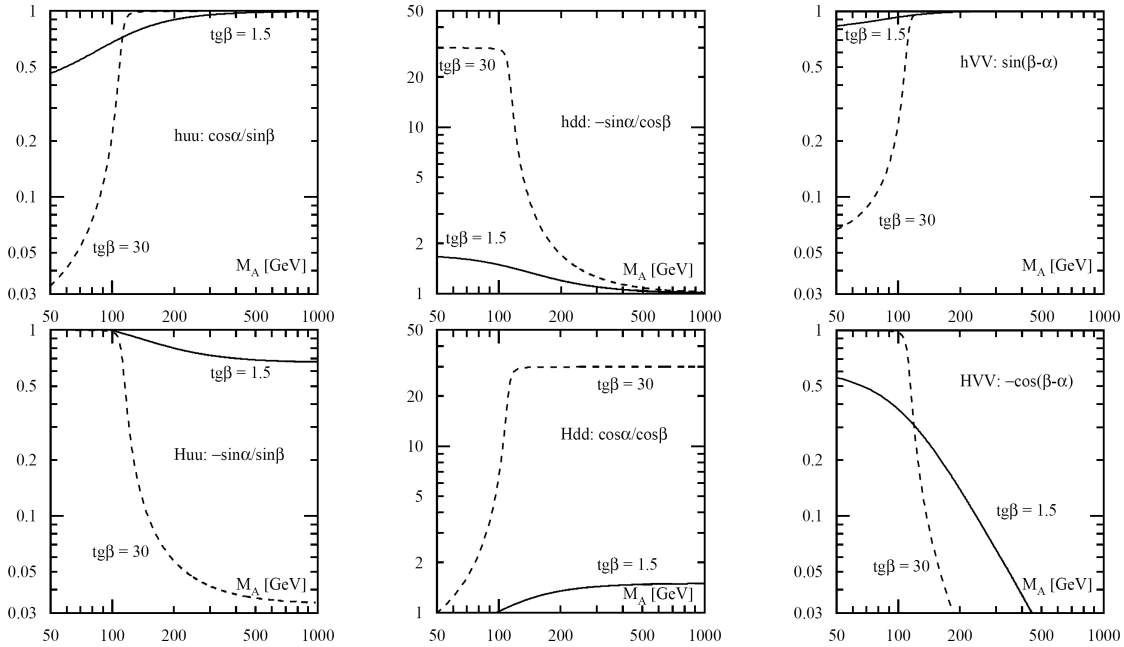

Figure 2.2: The coupling parameters of the neutral MSSM Higgs bosons as a function of the pseudoscalar mass M_A for two values of $\mathrm{tg}\beta = 1.5, 30$ and vanishing mixing. These couplings are defined in Table 2.1.

CL, but for $m_t > 181.5$ GeV no $\mathrm{tg}\beta$ values can be excluded anymore. However, the data from Tevatron exclude most of the $\mathrm{tg}\beta$ values above 50 for moderate pseudoscalar Higgs masses M_A below 200 GeV [59]. The beam energy of the LHC is more than sufficient to produce a light Higgs boson in the allowed mass range. However, the question if the LHC is able to discover a Higgs boson depends on the size of the production cross sections, and especially on the detector performance to separate the large SM background from the new signals.

2.2 Couplings to SM Particles

As in the SM, the couplings of the MSSM Higgs bosons to particles grow with the particle masses, if these are generated by the Higgs mechanism. Thus the MSSM Higgs bosons predominantly couple to heavy quarks and gauge bosons. The size of MSSM Higgs couplings to quarks, leptons and gauge bosons is similar to the Standard Model, yet modified by the mixing angles α and β. They are listed in Table 2.1, normalized to the SM values. The Higgs boson interaction with the vector bosons is always reduced with respect to the SM. For large values of $\mathrm{tg}\beta$ the couplings to down-type quarks are enhanced, therefore the coupling to bottom quarks may be much larger than to top quarks. The pseudoscalar Higgs boson A does not couple to gauge bosons at tree level, but the coupling, compatible with $\mathcal{CP}$ symmetry, can be generated by higher-order loops. The charged Higgs bosons interact with up- and down-type fermions via the left- and right-chiral couplings $g_\pm = -\left[g_u(1 \mp \gamma_5) + g_d(1 \pm \gamma_5)\right]/\sqrt{2}$ where $g_{u,d} = \sqrt{2}m_{u,d}/v_{2,1}$. The modified couplings incorporate the renormalization due to SUSY radiative corrections, to leading order in m_t, if the mixing angle α is related to β and

Φ		g_u^Φ	g_d^Φ	g_V^Φ
SM	H	1	1	1
MSSM	h	$\cos\alpha/\sin\beta$	$-\sin\alpha/\cos\beta$	$\sin(\beta-\alpha)$
	H	$\sin\alpha/\sin\beta$	$\cos\alpha/\cos\beta$	$\cos(\beta-\alpha)$
	A	$1/\tan\beta$	$\tan\beta$	0

Table 2.1: MSSM Higgs couplings to SM particles relative to SM Higgs couplings.

M_A as given in the corrected formula (2.5) for $\tan 2\alpha$. A very important region is the **decoupling limit** for $M_A \gg M_Z$ [60]. In this limit all heavy Higgs bosons are approximately mass degenerate $M_A \simeq M_H \simeq M_{H^\pm}$, and the mixing angles are related by $\beta - \alpha = \pi/2$. The relative coupling factors approach the values

$$g_{f,V}^h = 1 \ , \ g_u^H = -\cot\beta \ , \ g_d^H = \tan\beta \ , \ g_V^H = 0 \tag{2.8}$$

In the decoupling limit the light MSSM Higgs boson couples to fermions and gauge bosons like the SM Higgs boson and all couplings of heavy MSSM Higgs bosons to down-type fermions are strongly enhanced for large tgβ, and strongly suppressed for up-type fermions. For energies below M_A this model can be described by an effective low-energy theory where the light Higgs boson is decoupled from the heavy particles, and the couplings of h to fermions and gauge bosons approach their SM values. As a consequence, the experimental distinction between the SM and the MSSM becomes very difficult as long as one cannot discover any additional SUSY particles.

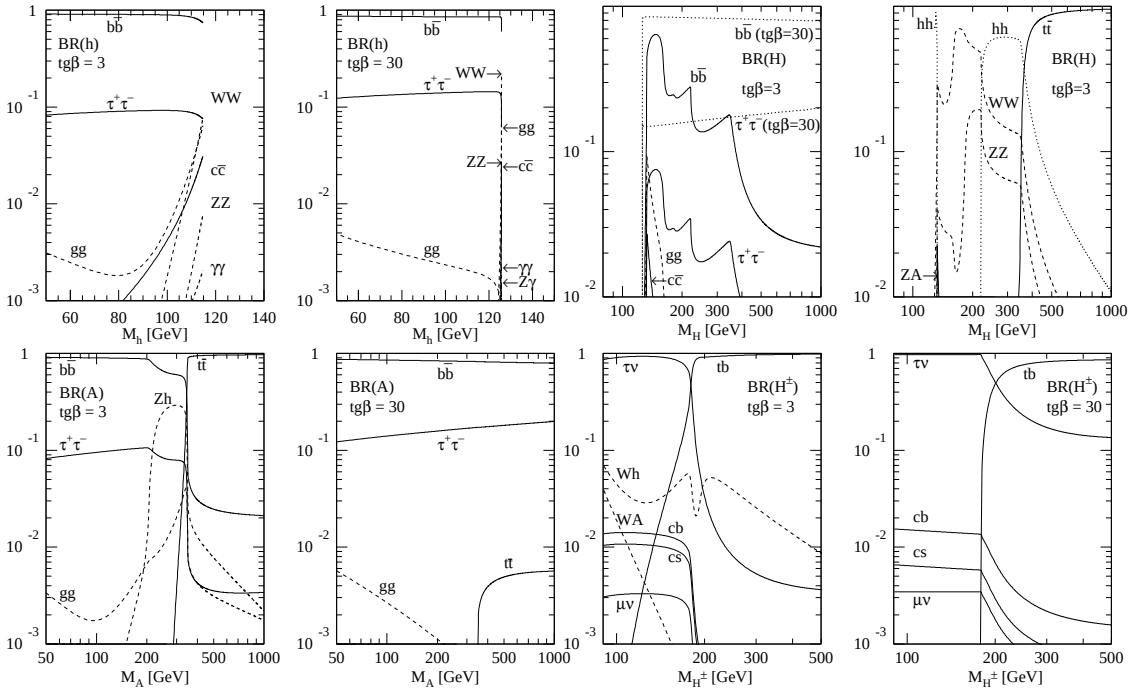

Figure 2.3: Branching ratios of the MSSM Higgs bosons $h, H, A, H^\pm$ for non-SUSY decay modes as a function of the masses for two values of tg$\beta = 3, 30$ and vanishing stop mixing. The common squark mass has been chosen as $M_S = 1$ TeV [61].

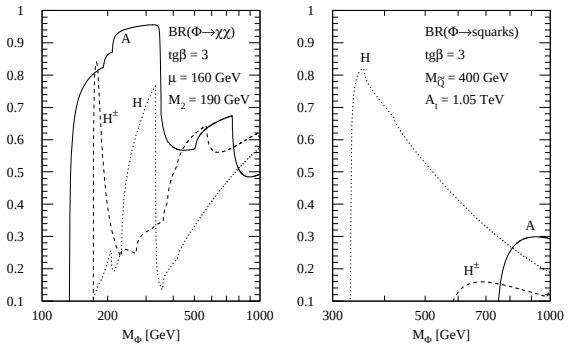

Figure 2.4: Branching ratios of the MSSM Higgs boson $H, A, H^{\pm}$ decays into charginos/neutralinos and squarks as a function of their masses for tg$\beta = 3$. The mixing parameters have been chosen as $\mu = 160$ GeV, $A_t = 1.05$ TeV, $A_b = 0$ and the squark masses of the first two generations as $M_{\widetilde{Q}} = 400$ GeV. The gaugino mass parameter has been set to $M_2 = 190$ GeV [61].

2.3 Decay Channels

The MSSM Higgs bosons $h, H, A, H^{\pm}$ will decay into different particles. The branching ratios of the Higgs bosons for non-SUSY decay modes are shown in Figure 2.3 and for decays into charginos, neutralinos and squarks in Figure 2.4. Under the assumption that all SUSY particles are heavier than the MSSM Higgs bosons, the relevant tree-level decays of neutral Higgs bosons $\Phi^0 = h, H, A$ are decays into quark pairs ($\Phi^0 \to t\bar{t}, b\bar{b}$), τ-lepton pairs ($\Phi^0 \to \tau^+\tau^-$), gauge boson pairs ($h, H \to WW, ZZ$) and Higgs boson pairs ($H \to hh$). The lightest **neutral Higgs boson** h will decay mainly into fermion pairs since the mass is smaller than ~ 135 GeV. These are, in general, also the dominant decay modes of the pseudoscalar boson A. For large values of tgβ and for masses less than ~ 140 GeV, the main decay modes of the neutral Higgs bosons are decays into $b\bar{b}$ and $\tau^+\tau^-$ pairs. The branching ratios are of order $\sim 90\%$ and 8%, respectively. The decays into $c\bar{c}$ pairs and gluons are suppressed, especially for large tgβ. For large masses, the top decay channels $H, A \to t\bar{t}$ open up. However for large tgβ this mode remains suppressed and the neutral Higgs bosons decay almost exclusively into $b\bar{b}$ and $\tau^+\tau^-$ pairs. In contrast to the pseudoscalar Higgs boson A, the heavy CP-even Higgs boson H can in principle decay into weak gauge bosons, $H \to WW, ZZ$, if the mass is large enough. However, since the partial widths are proportional to $\cos^2(\beta - \alpha)$, they are strongly suppressed in general, and the ZZ signal of the heavy Higgs boson in the Standard Model is lost in the supersymmetric extensions. As a result, the total widths of the Higgs bosons are much smaller in supersymmetric theories than in the Standard Model. In contrast to the gluon fusion $gg \to \Phi^0$, the loop induced Higgs boson decay $\Phi^0 \to gg$ into gluons does not play an important role. The photonic decays $\Phi^0 \to \gamma\gamma$, mediated by heavy quark and W-boson loops, are very rare. The heavy neutral Higgs boson H can also decay into two lighter Higgs bosons ($H \to hh, AA$). Other possible channels are Higgs cascade decays and decays into supersymmetric particles, Figure 2.4. In addition to light sfermions, Higgs boson decays into charginos and neutralinos could eventually be important. These new channels can be kinematically accessible, at least for the heavy Higgs bosons H, A and $H^{\pm}$. In fact, the branching fractions can be large and they can

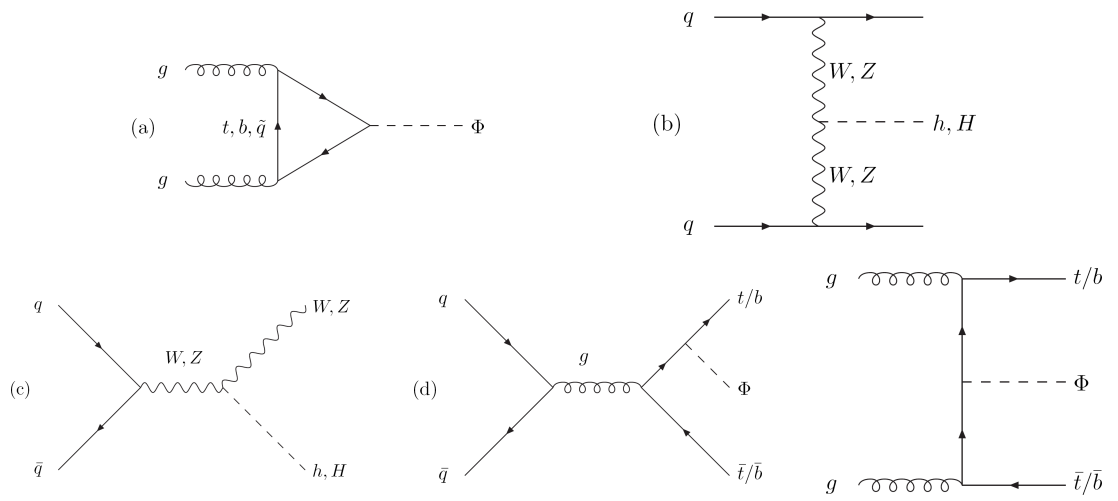

Figure 2.5: Typical diagrams for the production of a Higgs boson Φ: (a) gluon fusion $gg \to \Phi$, (b) Vector boson fusion $qq \to qqV^*V^* \to qqh/qqH$, (c) Higgs-strahlung $q\bar{q} \to V^* \to Vh/VH$ and (d) Higgs bremsstrahlung $q\bar{q}/gg \to Q\bar{Q}'\Phi$ $(Q, Q' = t, b)$.

even become dominant in some regions of the MSSM parameter space. Decays of h into the lightest neutralinos (LSP) are also important, exceeding 50% in some parts of the parameter space. These decays strongly affect experimental search techniques. The **charged Higgs particles** decay into quark-antiquark pairs ($H^+ \to t\bar{b}, c\bar{b}, c\bar{s}$), but also, if allowed kinematically, into the lightest neutral Higgs and a W boson ($H^+ \to hW^+$). Below the tb and Wh thresholds, the charged Higgs particles will decay mostly into $\tau\nu_\tau$ pairs ($H^+ \to \tau^+\nu_\tau$) and cs pairs, the former being dominant for $\mathrm{tg}\beta > 1$. For large $M_{H^\pm}$ values, the top-bottom decay mode $H^+ \to t\bar{b}$ becomes dominant. In some parts of the SUSY parameter space, decays into supersymmetric particles may exceed 50%. Adding up the various decay modes, the width of all five Higgs bosons remains very narrow, being of order 10 GeV even for large masses.

2.4 Production at the LHC

Several processes can be exploited to produce Higgs particles in hadron colliders. In this section we focus mainly on neutral Higgs bosons.

Gluon fusion	:	$gg \to \Phi$	Vector boson fusion	:	$W^+W^-, ZZ \to \Phi$
Higgs-strahlung	:	$W, Z \to W, Z + \Phi$	Bremsstrahlung	:	$q\bar{q}, gg \to Q\bar{Q}' + \Phi$

Typical diagrams for these production channels are shown in Figure 2.5. The **gluon fusion** mechanism $pp \to gg \to \Phi$ $(\Phi = h, H, A)$ is the dominant production channel for neutral Higgs bosons at the LHC for small and moderate values of $\mathrm{tg}\beta < 10$. Only for large $\mathrm{tg}\beta$ can the associated $\Phi b\bar{b}$ production channel develop a large cross section due to the enhanced Higgs couplings to bottom quarks. The gluon coupling to the Higgs boson is mediated by triangular loops of top and bottom quarks. For small $\mathrm{tg}\beta$ the contribution of the top is dominant, while for large $\mathrm{tg}\beta$ the bottom loop is strongly

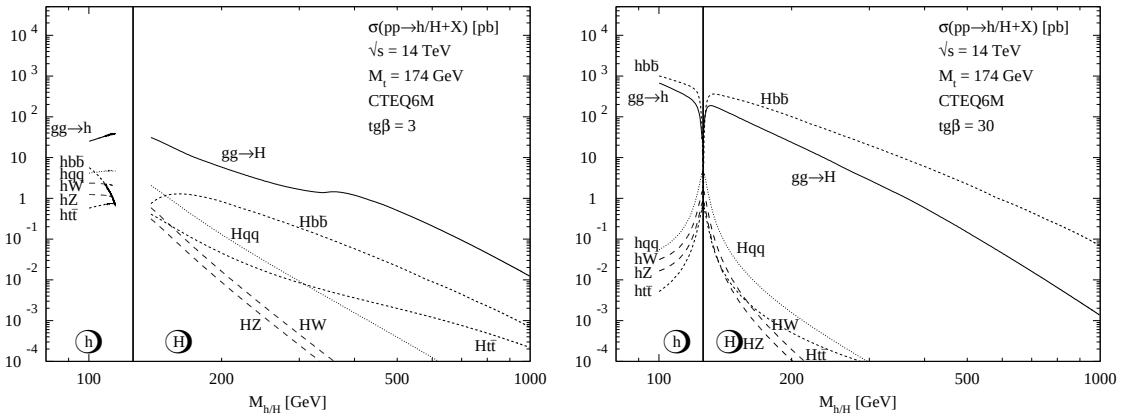

Figure 2.6: Neutral MSSM Higgs production cross sections at the LHC for gluon fusion $gg \to h/H$, vector-boson fusion $qq \to qqVV \to qqh/qqH$, Higgs-strahlung $q\bar{q} \to V^* \to hV/HV$ and the associated production $gg, q\bar{q} \to b\bar{b}\Phi/t\bar{t}\Phi$ ($\Phi = h, H$), including all known QCD corrections. Left: h, H production for $\mathrm{tg}\beta = 3$, Right: h, H production for $\mathrm{tg}\beta = 30$ [61].

enhanced. Squark loops can be significant for squark masses below ~ 400 GeV. The QCD corrections to the gluon fusion process are very important. They stabilize the theoretical predictions for the cross section when the renormalization and factorization scales are varied. Moreover, they are large and positive, thus increasing the production cross section for Higgs bosons [62–67]. The second channel for Higgs production is **Vector-boson fusion**, $pp \to qqV^*V^* \to qq\Phi$ ($\Phi = h, H$). Due to the absence of vector boson couplings to pseudoscalar Higgs particles A, only the scalar Higgs bosons h, H can be produced via this mechanism at tree level. However these processes are suppressed with respect to the SM cross section due to the MSSM couplings in Table 2.1. This channel becomes only important if the light Higgs boson h is very close to its upper mass bound, or if the heavy Higgs boson is right above this bound [68–70]. For the same reason as in the vector boson fusion case, the **Higgs-strahlung** off W, Z bosons $q\bar{q} \to V^* \to V\Phi$ ($V = W, Z\,, \Phi = h, H$) is of no great importance for the scalar MSSM Higgs particles h, H. Again the coupling to the pseudoscalar boson A is zero [71–73]. The last discussed production mechanism is **Higgs bremsstrahlung** off heavy quarks Q, $pp \to Q\bar{Q}'\Phi$ ($\Phi = h, H, A, H^{\pm}$). Because the top quark coupling to MSSM Higgs bosons is suppressed with respect to the SM for $\mathrm{tg}\beta > 1$ the Higgs bremsstrahlung off top quarks is less important. On the other hand Higgs bremsstrahlung off bottom quarks will be the dominant Higgs production channel for large $\mathrm{tg}\beta$ due to the strongly enhanced bottom quark Yukawa couplings. Here the QCD and SUSY-QCD corrections can be huge due to the $\mathrm{tg}\beta$ enhanced corrections and the radiation of soft bottom quarks with small transverse momenta. The same applies for the charged Higgs boson production with bottom quarks in the final state [74–81]. The cross sections of the various MSSM Higgs production mechanisms at the LHC are shown in Figure 2.6 for the two neutral Higgs bosons h and H and for two representative values of $\mathrm{tg}\beta = 3, 30$ as a function of the corresponding Higgs mass. The total center of mass energy has been chosen as $\sqrt{s} = 14$ TeV, which corresponds to the maximal collision energy at the LHC.

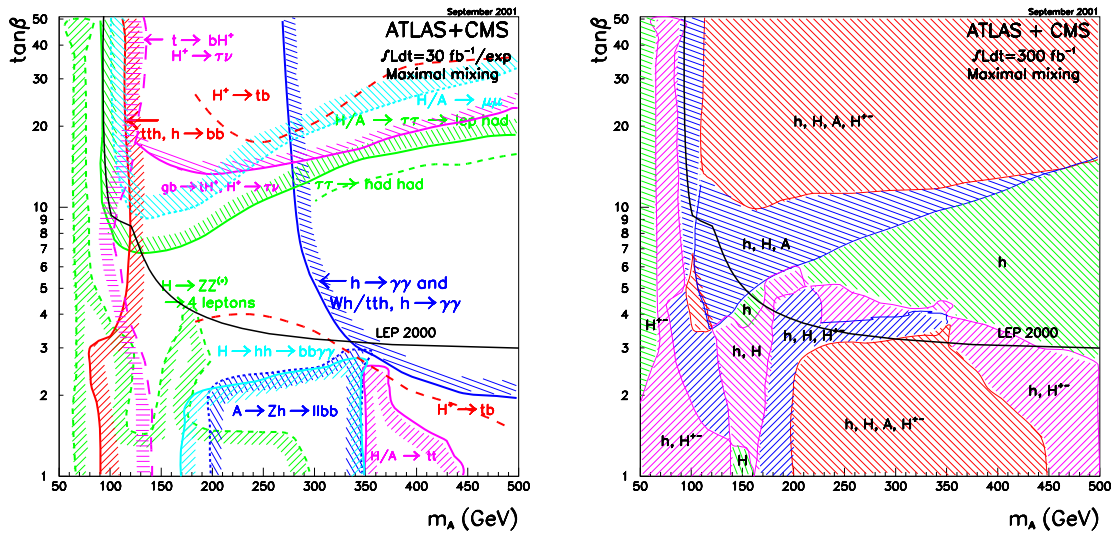

Figure 2.7: The ATLAS and CMS sensitivity for the discovery of the MSSM Higgs bosons in the case of maximal mixing. The 5σ discovery curves/regions are shown in the $(\mathrm{tg}\beta, M_A)$ plane for the individual channels and for an integrated luminosity of $30fb^{-1}/300fb^{-1}$. The region below the solid black curve is excluded by direct searches at LEP2 [82].

2.5 Discovery Potential at the LHC

The LHC experiments have a large potential in the investigation of the MSSM Higgs sector. The experimental searches carried out at LEP and presently continued at the Tevatron can be extended to much larger Higgs boson masses. The production cross sections at hadron colliders, at the LHC in particular, are sizable so that a large sample of Higgs particles can be produced in this machine. Experimental difficulties arise from the huge number of background events that come along with the Higgs signal events. In the search for the light, Standard Model-like Higgs boson h the same channels as in the search for the Standard Model Higgs boson can be used (namely $h \to \gamma\gamma$ and $h \to ZZ^* \to 4l$ and the vector boson fusion channel $qq \to qqh \to qq\tau\tau$). Since the LHC detectors have been especially optimised for this channel, the $h \to \gamma\gamma$ decay belongs to the most promising discovery channels for the light Higgs boson h. Heavier Higgs bosons can be searched for in additional decay channels which become accessible in certain regions of the MSSM parameter space ($\Phi b\bar{b} \to b\bar{b}\tau\tau$, $\Phi b\bar{b} \to b\bar{b}\mu\mu$, $H \to hh$, $A \to hZ$, $H^+ \to \tau^+\nu_\tau$ and $H^+ \to t\bar{b}$ with $\Phi = H, A$). Although in general the hadronic decay modes exhibit a higher branching ratio, the leptonic decay modes into muon and tau pairs have a better discovery reach for Higgs bosons [30, 31, 83]. They provide a cleaner signal in the detector and have higher trigger efficiencies and smaller uncertainties compared with the more complicated jet signatures from hadronic decay modes. For example, the associated Higgs production with top quarks followed by the decay into $b\bar{b}$ pairs ($t\bar{t}\Phi^0$ with $\Phi^0 \to b\bar{b}$) is not considered as a discovery channel anymore, since the efficiency to reduce the background is not good enough. But once the Higgs boson mass is known, it is still an important channel for crosschecks and to measure the Yukawa couplings in combination with the $\tau\tau$ mode. However, the process $b\bar{b}\Phi^0 \to b\bar{b}b\bar{b}$ remains an important

channel for the Higgs search. If it is assumed that the supersymmetric particle spectrum is heavy, so that decays of Higgs bosons into SUSY particles are suppressed, the essential dependences of the production and decay processes are determined by $\mathrm{tg}\beta$ and M_A, and the other MSSM parameters enter through corrections only. In this case it is possible to make a representative illustration of the LHC discovery potential in the $M_A, \mathrm{tg}\beta$-plane. Figure 2.7 shows the most important discovery channels for MSSM Higgs bosons at the LHC for both detectors ATLAS and CMS in the maximal mixing scenario. The investigation of SUSY decay modes, e.g. of Higgs boson decays into light charginos and neutralinos, can cover additional regions in the intermediate $\mathrm{tg}\beta$ parameter region. Even though the entire supersymmetric Higgs parameter space of the MSSM is expected to be finally covered by the LHC experiments, the entire ensemble of individual Higgs bosons is accessible only in part of the parameter space [61, 84].

Chapter 3

Calculation

This chapter introduces the calculational tools and conventions we required in the course of our calculation. First of all, in section 3.1 a Low-Energy theorem is explained which allows us to calculate self-energy diagrams instead of three-point functions with external Higgs bosons. Subsequently, in section 3.2 the structure of the self-energy is analysed. Section 3.3 specifies some definitions and identities concerning colour matrices. Section 3.4 describes how we computed the occurring two-loop integrals and how these integrals can be expanded and reduced to master-integrals. In section 3.5 our method of regularising the occurring ultraviolet divergencies is explained. We close this chapter with section 3.6, where the renormalisation of the ultraviolet divergencies is examined, all required counterterms are given and concepts as renormalisation schemes, running parameters and anomalous counterterms are discussed.

3.1 Low-Energy Theorem

Low-Energy Theorems (LET) as presented in [85, 86] significantly simplify our calculation. They serve to calculate loop amplitudes with external scalar or pseudoscalar Higgs bosons which are light compared to the loop particles, and provide the first term of an expansion in small external momenta, which corresponds to a heavy mass expansion in the inverse loop-particle masses. In the case of vanishing 4-momentum p_ϕ the Higgs boson acts as a constant field, since $[\mathcal{P}_\mu, \phi] = i\partial_\mu\phi = 0$, with $\mathcal{P}_\mu$ being the 4-momentum operator. As a consequence, the kinetic terms of the Higgs Lagrangian vanish in this limit. Moreover, in most of the practical cases the external Higgs particle is defined on-shell, so that $p_\phi^2 = M_\phi^2$ and the mathematical limit of vanishing Higgs momentum coincides with the limit of small Higgs masses. In the MSSM, the Lagrangian for the interaction of a particle with these constant Higgs fields can be derived by means of the replacements

$$v_1 \to \sqrt{2}H_1^0 \quad , \quad v_2 \to \sqrt{2}H_2^{0*} \tag{3.1}$$

in the corresponding mass operator $\bar{\psi}(m^0 + \Sigma(m))\psi$ of the particle. Since we calculate corrections to the bottom Yukawa coupling λ_b in an effective Lagrangian approach, we need to calculate the bottom mass operator, i.e. the bottom quark self-energy $\Sigma_b(m_b)$, up to the desired order and perform the replacements in (3.1) to obtain the effective interaction of the Higgs bosons with bottom quarks.

3.2 Self-Energy

The fermion self-energy can be decomposed into scalar, a pseudoscalar, a vector and an axial vector part according to

$$\Sigma(p) = m\,\Sigma_S(p) + m\gamma_5\,\Sigma_P(p) + \not{p}\,\Sigma_V(p) + \not{p}\gamma_5\,\Sigma_A(p) \tag{3.2}$$

where m is the mass of the fermion. These parts can be extracted by taking the trace of the complete self-energy

$$\begin{aligned} \Sigma_S(p) &= \frac{1}{4m}\mathrm{Tr}\left[\Sigma(p)\right] \quad , \quad \Sigma_P(p) = \frac{1}{4m}\mathrm{Tr}\left[\gamma_5\Sigma(p)\right] \\ \Sigma_V(p) &= \frac{1}{4p^2}\mathrm{Tr}\left[\not{p}\Sigma(p)\right] \quad , \quad \Sigma_A(p) = \frac{1}{4p^2}\mathrm{Tr}\left[\gamma_5\not{p}\Sigma(p)\right] \end{aligned} \tag{3.3}$$

When calculating the mass operator, the Dirac equation is used in $\bar{\psi}\Sigma(m)\psi$. This eliminates the axial vector part but leads to contributions from the vector part to the mass operator. The pseudo scalar part would lead to CP-violation and is absent as expected. Thus, the mass operator is given by $\bar{\psi}\,m^0(1+\Sigma_S(m)+\Sigma_V(m))\,\psi$.

3.3 Colour Sums

We list here some identities which are useful in performing the sums over initial and final colour states [87]. The summation convention is assumed throughout the discussion. The generators of the fundamental representation of the group $SU(N)$ are denoted by T^a and the generators of the adjoint representation by $[T^a_{adj}]_{bc} = -if_{abc}$ where f_{abc} are the structure constants of the group. The algebra of the group is defined by the commutation relation

$$[T^a, T^b] \;=\; i\,f_{abc}\,T^c \tag{3.4}$$

The trace over two generators of the fundamental representation determines the constant T_R, and the Casimir operator T^2 determines the constant C_F.

$$\mathrm{Tr}[T^aT^b] \;=\; [T^aT^b]_{ii} \;=\; T_R\,\delta_{ab}\;,\; T^2 \;=\; [T^a\,T^a]_{ij} \;=\; C_F\,\delta_{ij}\;,\; C_F \;=\; \Big(N - \frac{1}{N}\Big)T_R \tag{3.5}$$

A useful identity is $\{T^a, T^a\}_{ij} = 2C_F\delta_{ij}$. The trace over two generators of the adjoint representation yields the constant C_A.

$$-\mathrm{Tr}[T^a_{adj}T^b_{adj}] \;=\; -[T^a_{adj}T^b_{adj}]_{cc} \;=\; f_{acd}\,f_{bcd} \;=\; C_A\,\delta_{ab} \quad , \quad C_A \;=\; 2\,T_R\,N \tag{3.6}$$

For the $SU(3)$ colour group these constants become

$$T_R \;=\; \frac{1}{2} \qquad C_F \;=\; \frac{4}{3} \quad , \quad C_A \;=\; 3 \tag{3.7}$$

All colour structures in this work are given in terms of the matrices T^a and the constants f_{abc}, T_R, C_F and C_A.

3.4 Two-loop Integrals

Since we calculate 2-loop scalar self-energies, all integrals can be written as

$$T_{12345}(m_1, m_2, m_3, m_4, m_5) = \int \frac{d^n k}{(2\pi)^n} \frac{d^n q}{(2\pi)^n} \frac{1}{P_1\, P_2\, P_3\, P_4\, P_5} \tag{3.8}$$

We use dimensional regularisation with $n = 4 - 2\epsilon$ (see chapter 3.5). The terms in the denominator are defined as

$$\begin{aligned} &P_1 = (k^2 - m_1^2)\ ,\ P_2 = ((k+p)^2 - m_2^2)\ ,\ P_3 = ((k-q)^2 - m_3^2) \\ &P_4 = (q^2 - m_4^2)\ ,\ P_5 = ((q+p)^2 - m_5^2) \end{aligned} \tag{3.9}$$

Here p is the external momentum.

3.4.1 Symmetries

The number of occurring integrals can be reduced considerably by taking into account their symmetries with respect to permutations (ij) of P_i and P_j. All T-integrals are invariant under the permutations

$$(12)(45)\ ,\ (14)(25)\ ,\ (15)(24) \tag{3.10}$$

Application of the first permutation yields for example

$$T_{1234}(m_1, m_2, m_3, m_4) = T_{1235}(m_2, m_1, m_3, m_4) \tag{3.11}$$

The validity of the symmetries listed in (3.10) can be understood by using the invariance properties of the integrals with respect to changes of the integration momenta. Additional symmetry relations hold if an index does not occur in the integral

$$\text{(23) if 1 is absent} \quad , \quad \text{(35) if 4 is absent} \quad , \quad \text{(13) if 2,5 are absent} \tag{3.12}$$

These relations are used to map every integral onto a standard representation, i.e. all integrals which are related by symmetry transformations are brought to the same form.

3.4.2 Reduction

If the external momentum is zero, that is if the 2-loop integral contains no propagators P_2 and P_5 with external momentum, the integral can be reduced to 1-loop scalar integrals A_0 and the scalar 2-loop masterintegral T_{134}. For the reduction of two-loop integrals of the form $T_{1\ldots3\ldots4\ldots}$ the method of partial integration can be used. This method is based on the fact, that dimensionally regularised integrals are invariant under translations.

$$\int d^n k\ f(k) = \int d^n k\ f(k+p) \tag{3.13}$$

From this, identities of the form

$$0 = \int d^n k\ \frac{\partial}{\partial k_\mu} f(k) \tag{3.14}$$

can be derived. For the integrals

$$T_{\underbrace{1\ldots}_{\nu_1}\underbrace{3\ldots}_{\nu_3}\underbrace{4\ldots}_{\nu_4}}(m_1, m_3, m_4) \tag{3.15}$$

one obtains three independent identities.

$$\begin{aligned}
\int d^n k d^n q \frac{\partial}{\partial k_\mu} \left\{ \frac{k_\mu}{(k^2 - m_1^2)^{\nu_1}((k-q)^2 - m_3^2)^{\nu_3}(q^2 - m_4^2)^{\nu_4}} \right\} &= 0 \\
\int d^n k d^n q \frac{\partial}{\partial q_\mu} \left\{ \frac{q_\mu}{(k^2 - m_1^2)^{\nu_1}((k-q)^2 - m_3^2)^{\nu_3}(q^2 - m_4^2)^{\nu_4}} \right\} &= 0 \\
\int d^n k d^n q \frac{\partial}{\partial q_\mu} \left\{ \frac{k_\mu}{(k^2 - m_1^2)^{\nu_1}((k-q)^2 - m_3^2)^{\nu_3}(q^2 - m_4^2)^{\nu_4}} \right\} &= 0
\end{aligned} \tag{3.16}$$

With these equations, the results in Appendix A.3 were calculated.

3.4.3 Heavy Mass Expansion

The analytical evaluation of a 2-loop Feynman diagram which depends on two parameters, e.g. a mass squared and a momentum squared, is generally a rather complicated problem. If however the parameters involved differ in scale, it is reasonable to expand the diagram in their small ratio. It has been shown in [88, 89] that an asymptotic expansion in an arbitrary limit with two scales can be written explicitly as an infinite series of products of certain one-scale Feynman integrals, with a power-like dependence on the expansion parameters, which can be evaluated analytically much more easily than the initial 2-scale integral. The original Feynman integral can then be replaced by a sufficiently large number of terms of its expansion. Since the SUSY masses are much larger than the SM mass m_{SM}^2, integrals can be expanded in the small ratios $(m_{SM}^2, p^2)/M_{SUSY}^2$ ($p^2 = m_{SM}^2$). In the work at hand, only the first term in any expansion in these small ratios is needed. Therefore the reduction technique of section 3.4.2 can always be used. The strategy will be shown by some examples. The small-momentum expansions in equation (3.17) of a propagator with a small external momentum p^2 and a large mass M^2 is the simplest example of such an expansion.

$$\frac{1}{(k+p)^2 - M^2} = \frac{1}{k^2 - M^2} - \frac{2p \cdot k + p^2}{(k^2 - M^2)^2} + \mathcal{O}\left(\frac{p^2}{M^4}\right) \tag{3.17}$$

Note that terms with odd powers of the integration variable (like $2p{\cdot}k$) always vanish after integration, if the denominator is symmetric with respect to sign change of the integration variable. A more complicated example would be the 2-loop integral $T_{134}(m, M_1, M_2)$ with the small mass m and the heavy masses M_1 and M_2, that is $m \ll M_1, M_2$.

$$\begin{aligned}
T_{134}(m, M_1, M_2) &= \int \frac{d^n k}{(2\pi)^n} \frac{d^n q}{(2\pi)^n} \frac{1}{(k^2 - m^2)((k-q)^2 - M_1^2)(q^2 - M_2^2)} \\
&= \int \frac{d^n k}{(2\pi)^n} \underbrace{\frac{1}{(k^2 - m^2)}}_{=f_1(k)} \underbrace{\int \frac{d^n q}{(2\pi)^n} \frac{1}{((k-q)^2 - M_1^2)(q^2 - M_2^2)}}_{=f_2(k)} \equiv P
\end{aligned} \tag{3.18}$$

The expansions of $f_1(k)$ and $f_2(k)$ with respect to m and k are given by:

$$\begin{aligned} T_m^{(i)}[f_1(k)] &= \frac{1}{k^2} + \frac{m^2}{(k^2)^2} + \ldots + \frac{(m^2)^i}{(k^2)^{i+1}} \\ T_k^{(i)}[f_2(k)] &= f_2(0) + k^2 f_2'(0) + \ldots + \frac{(k^2)^i}{i!} f_2^{(i)}(0) \end{aligned} \tag{3.19}$$

We define the following rest of the expansion and estimate its order by using the $i+1$ expansion summands in (3.19), with $f_2^{(i)} = \mathcal{O}\left(M_1^2, M_1^2\right)^{-i}$:

$$R^{(i)}P = \int \frac{d^n k}{(2\pi)^n} \left(f_1(k) - T_m^{(i)}[f_1(k)]\right) \left(f_2(k) - T_k^{(i)}[f_2(k)]\right) = \mathcal{O}\left(\frac{m^2}{M_1^2, M_2^2}\right)^{i+1} \tag{3.20}$$

It can be shown, that the rest does not contain any ultraviolet (UV) or infrared (IR) divergencies which were not already present in the original integral. The expansion of (3.20) yields:

$$\begin{aligned} R^{(i)}P &= \int \frac{d^n k}{(2\pi)^n} \left(f_1(k) - T_m^{(i)}[f_1(k)]\right) \left(f_2(k) - T_k^{(i)}[f_2(k)]\right) \\ &= \underbrace{\int \frac{d^n k}{(2\pi)^n} f_1(k) f_2(k)}_{=P} + \underbrace{\int \frac{d^n k}{(2\pi)^n} \left(T_m^{(i)}[f_1(k)]\right) \left(T_k^{(i)}[f_2(k)]\right)}_{=0} \\ &\quad - \int \frac{d^n k}{(2\pi)^n} f_1(k) \left(T_k^{(i)}[f_2(k)]\right) - \int \frac{d^n k}{(2\pi)^n} \left(T_m^{(i)}[f_1(k)]\right) f_2(k) = \mathcal{O}\left(\frac{m^2}{M_1^2, M_2^2}\right)^{i+1} \end{aligned}$$

Scaleless integrals are always zero if dimensionally regularised. Therefore we get

$$\begin{aligned} T_{134}(m, M_1, M_2) &= \int \frac{d^n k}{(2\pi)^n} \left[f_1(k) \left(T_k^{(0)}[f_2(k)]\right) + \left(T_m^{(0)}[f_1(k)]\right) f_2(k) \right] + \mathcal{O}\left(\frac{m^2}{M_1^2, M_2^2}\right) \\ &= A_0(m) B_0(0; M_1, M_2) + T_{134}(0, M_1, M_2) + \mathcal{O}\left(\frac{m^2}{M_1^2, M_2^2}\right) \end{aligned} \tag{3.21}$$

A slightly more complicated integral addresses the problem, that the external momentum p^2 can occur together with a small mass m^2 in a propagator. Then equation (3.17) can not be used.

$$\begin{aligned} T_{1234}(0, m, M_1, M_2) &= \int \frac{d^n k}{(2\pi)^n} \frac{d^n q}{(2\pi)^n} \frac{1}{k^2((k+p)^2 - m^2)((k-q)^2 - M_1^2)(q^2 - M_2^2)} \\ &= \int \frac{d^n k}{(2\pi)^n} \underbrace{\frac{1}{k^2((k+p)^2 - m^2)}}_{=f_1(k)} \underbrace{\int \frac{d^n q}{(2\pi)^n} \frac{1}{((k-q)^2 - M_1^2)(q^2 - M_2^2)}}_{=f_2(k)} \equiv P \end{aligned} \tag{3.22}$$

The object that we called $f_2(k)$ is the same as in the example above,

$$T_{p,m}^{(i)}[f_1(k)] = \frac{1}{(k^2)^2} + \frac{1}{(k^2)^2} \underbrace{\left[\frac{m^2 - p^2 - 2k \cdot p}{k^2} + \frac{(2k \cdot p)^2}{(k^2)^2} \right]}_{=\mathcal{O}\left(\frac{p^2, m^2}{k^2}\right)} + \cdots + \frac{1}{(k^2)^2} \underbrace{\left[\qquad \right]}_{=\mathcal{O}\left(\frac{(p^2, m^2)^i}{(k^2)^i}\right)}$$

Here it can be shown, that the rest $R^{(0)}P$ does not contain any IR or UV divergences. Therefore all present divergencies in the original integral are reproduced by the leading order of the expansion. We get the following result:

$$\begin{aligned} &T_{1234}(0, m, M_1, M_2) \\ &\quad = \int \frac{d^n k}{(2\pi)^n} f_1(k) \left(T_k^{(i)}[f_2(k)] \right) + \int \frac{d^n k}{(2\pi)^n} \left(T_{p,m}^{(i)}[f_1(k)] \right) f_2(k) + \mathcal{O}\left(\frac{p^2, m^2}{M_1^2, M_2^2} \right)^{i+1} \\ &\quad = B_0(p; 0, m) B_0(0; M_1, M_2) + T_{1134}(0, 0, M_1, M_2) + \mathcal{O}\left(\frac{p^2, m^2}{M_1^2, M_2^2} \right) \end{aligned} \tag{3.23}$$

The integral $T_{1134}(0, 0, M_1, M_2)$ does not need to be calculated because it can be reduced. Its reduction is given in equation (A.19).

3.5 Regularisation of Divergencies

In order to deal with divergences that appear in loop corrections to Green functions we have to regularize the theory to have an explicit parametrization of the singularities. In this work, the technique of **dimensional regularisation** is employed, which was introduced by 't Hooft and Veltman [90] and which preserves gauge and Lorentz invariance. In this regularisation, integrals are evaluated in $n = 4 - 2\epsilon$ space-time dimensions, since any loop-integral will converge for sufficiently small n. The singularities are then extracted as poles for $\epsilon \to 0$. Thus the results of one-loop or two-loop calculations develop the following general structure

$$\begin{aligned} \text{One} - \text{Loop Result} &= \frac{\mathrm{a}_1}{\epsilon} + \mathrm{b}_1 \\ \text{Two} - \text{Loop Result} &= \frac{\mathrm{a}_2}{\epsilon^2} + \frac{\mathrm{b}_2}{\epsilon} + \mathrm{c}_2 \end{aligned} \tag{3.24}$$

where a_i, b_i and c_2 are finite. In supersymmetric theories however, a complication occurs. In $n \neq 4$ dimensions a mismatch between the number of gluon $(n-2)$ and gluino (2) degrees of freedom is introduced. Since this $\mathcal{O}(\epsilon)$ mismatch will result in non-zero contributions, supersymmetry is explicitly violated in higher orders. Nevertheless, this problem can be fixed by the introduction of anomalous counterterms which are discussed in section 3.6.3.

3.6 Renormalisation

In order to get rid of ultraviolet divergencies which are parametrised as poles $1/\epsilon$, we need to renormalise our results. This was already explained qualitatively in chapter 1.1.3. All bare parameters (always denoted by the superscript 0) in our final result are split into a renormalised parameter plus a counterterm, e.g. $m^0 = m + \delta m$. The only condition that the counterterms must fulfil, is that all divergences are canceled, but finite terms can be shifted between the counterterms and the renormalised parameters which define different renormalisation schemes. To perform an explicit calculation and to relate the parameters to measured observables, one must choose a renormalisation scheme that fixes all counterterms. A theoretical prediction for a physical quantity is independent

of the chosen renormalisation scheme, provided one can calculate it to any loop order. In practise, only a small number of higher-order corrections can be evaluated, and the choice of a good renormalisation scheme may be significant. The following parameters need to be renormalized in our calculation

$$\begin{aligned} &m_t^0 = m_t + \delta m_t \quad , \quad \lambda_t^0 = \lambda_t + \delta\lambda_t \quad , \quad M_{\tilde{q}_i}^{0\,2} = M_{\tilde{q}_i}^2 + \delta M_{\tilde{q}_i}^2 \quad , \quad M_{\tilde{g}}^0 = M_{\tilde{g}} + \delta M_{\tilde{g}} \\ &\widetilde{\theta}_t^0 = \widetilde{\theta}_t + \delta\widetilde{\theta}_t \quad , \quad A_t^0 = A_t + \delta A_t \quad , \quad g_s^0 = g_s\,(1+\delta g_s) \end{aligned} \tag{3.25}$$

i.e. the top mass, the top Yukawa coupling, the squark masses, the gluino mass, the top squark mixing angle, the top trilinear coupling and the strong coupling constant.

3.6.1 Renormalisation Schemes

In this work, the on-shell scheme is used for all masses m_t, $M_{\tilde{q}_i}^2$, $M_{\tilde{g}}$ and the trilinear coupling A_t. A modified version of the $\overline{MS}$ scheme, the Collins-Wilczek-Zee scheme, is used for the strong coupling constant g_s and the top Yukawa coupling λ_t.

On-shell Scheme

The on-shell scheme (OS) is the physical renormalisation scheme in the sense that the finite renormalized parameters are equal to physical parameters (as at tree-level) in all orders of perturbation theory. The advantage of the on-shell scheme is, that all parameters have a physical meaning and can be measured directly in suitable experiments. We use the on-shell scheme to renormalize the masses. The counterterms are defined by two conditions: firstly the propagator of a particle exhibits a pole at the physical mass, and secondly the residue of the propagator is one. Generically, the self-energy contributing to the propagator can be expanded around the renormalised mass

$$\Sigma(p) = \Sigma(m) + (\not{p} - m)\left.\frac{\partial\Sigma}{\partial\not{p}}\right|_{\not{p}=m} + \mathcal{O}\left(\left[\not{p} - m\right]^2\right) \tag{3.26}$$

which fixes the counterterms of all masses in terms of the corresponding self-energy.

$$\delta m^{OS} = -\mathrm{Re}\Sigma(m) \tag{3.27}$$

Here the real part of the self-energy is taken, because for unstable particles, which can decay into lighter particles, the self-energy has also a finite imaginary part (Breit-Wigner propagator). This defines the decay width Γ [33]. The mixing angle counterterm $\delta\widetilde{\theta}_q$ is defined by the off-diagonal elements Σ_{12} of the squark self-energy matrix.

$$\delta\widetilde{\theta}_q^{OS} = -\frac{\mathrm{Re}\Sigma_{12}(M_{\tilde{q}_1}^2) + \mathrm{Re}\Sigma_{12}(M_{\tilde{q}_2}^2)}{2(M_{\tilde{q}_1}^2 - M_{\tilde{q}_2}^2)} \tag{3.28}$$

Using equation (1.29), the counterterm for the trilinear coupling is completely defined by the counterterms for the quark mass δm_q, for the mixing angle $\delta\widetilde{\theta}_q$ and the squark masses $\delta M_{\tilde{q}_i}$.

$$\delta A_q^{OS} = \frac{M_{\tilde{q}_1}^2 - M_{\tilde{q}_2}^2}{2m_q}\left[\,2c_{2\widetilde{\theta}_q}\,\delta\widetilde{\theta}_q^{OS} - s_{2\widetilde{\theta}_q}\,\frac{\delta m_q^{OS}}{m_q}\,\right] + \frac{\delta M_{\tilde{q}_1}^{2\,OS} - \delta M_{\tilde{q}_2}^{2\,OS}}{2m_q}\,s_{2\widetilde{\theta}_q} \tag{3.29}$$

Collins-Wilczek-Zee Scheme

The strong coupling constant $\alpha_s = g_s^2/4\pi$ cannot be renormalised in a natural way by an on-shell renormalisation condition at zero or small momentum transfer. In this regime the strong force is that strong, that perturbation theory cannot be applied and non-perturbative effects are significant. The introduction of a large renormalisation scale μ_R allows to avoid this problem by imposing the renormalisation conditions at a scale where the strong coupling is small. The renormalisation scale is best thought of as parametrising a whole sequence of possible renormalisation conditions that are connected by renormalisation group equations. The modified minimal subtraction scheme ($\overline{MS}$) is intrinsically tied to dimensional regularisation in $n = 4 - 2\epsilon$ dimensions, i.e. fields, phase space and loop momenta are defined in n-dimensions. It is defined by the prescription that the counterterms only absorb the $1/\epsilon$ poles accompanied by a few universal constants.

$$\Gamma[1+\epsilon]\,(4\pi)^\epsilon\,\frac{1}{\epsilon} + \log\frac{\mu^2}{m^2} \to \log\frac{\mu_R^2}{m^2} \tag{3.30}$$

Here μ^2 is the 't Hooft scale which is introduced before renormalisation to render the strong coupling dimensionless and m^2 represents any mass or kinematical invariant appearing in the loop diagram. An advantage of the $\overline{MS}$ scheme is that the renormalisation constants develop an especially simple form. Therefore the β and γ-functions are simple too, and the corresponding renormalisation group equations have simpler approximate solutions, see (3.49). However in the $\overline{MS}$ scheme, due to the mass independence of the β-function, heavy particles will not decouple in the low-energy regime as it would be guaranteed by the Appelquist-Carazzone theorem [91] in momentum subtraction schemes (the decoupling theorem states that the massive particles play no role in the low-momentum dynamics). One can repair this drawback by making the renormalisation condition (3.30) dependent on the large scales M^2 in order to absorb large logarithms in the renormalisation constants.

$$2\,\Gamma[1+\epsilon]\,(4\pi)^\epsilon\,\frac{1}{\epsilon} + \log\frac{\mu^2}{m^2} + \log\frac{\mu^2}{M^2} \to \log\frac{\mu_R^2}{m^2} \tag{3.31}$$

This can be achieved by adjusting the counterterms in the right way. The $\overline{MS}$ scheme is used to cancel all divergencies and to replace the 't Hooft scale μ by the renormalisation scale μ_R and the momentum subtraction scheme at zero momentum transfer cancels the potentially large logarithms. This hybrid scheme is called **Collins-Wilczek-Zee** renormalisation scheme [92]. In this scheme the coupling counterterm looks like

$$\alpha_s^0 = \alpha_s(\mu_R^2)\left\{1 + \frac{\alpha_s(\mu_R^2)}{4\pi}\left[\Big(-\Gamma[1+\epsilon]\,(4\pi)^\epsilon\,\frac{1}{\epsilon} - \log\frac{\mu^2}{\mu_R^2}\Big)\,\beta_0 - \log\frac{\mu_R^2}{M^2}\,\beta_0^H\right]\right\} \tag{3.32}$$

where the part multiplied by β_0 is the $\overline{MS}$ counterterm and β_0^H is the contribution of the heavy particle to $\beta_0 = \beta_0^L + \beta_0^H$. In our calculation, all SUSY particles and the top quark are decoupled, i.e. the corresponding logarithms are subtracted as shown above. This can be inferred from e.g. equation (3.42). Therefore the heavy particles do not contribute to the running of $\alpha_s(\mu_R^2)$. A slightly modified version is used for the renormalisation of the top Yukawa coupling, where the $\overline{MS}$ scheme is used to renormalize the QCD corrections to the top propagator $\Sigma_{\rm QCD}$ and the on-shell scheme for the SUSY-QCD

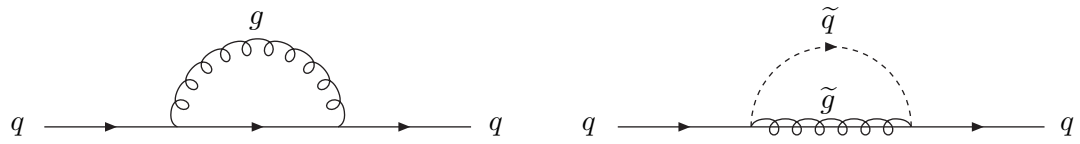

Figure 3.1: Diagrams contributing to the quark mass counterterm δm_q.

corrections Σ_{SQCD}. The on-shell scheme for the renormalisation of the SUSY-QCD part subtracts not only potentially large logarithms including SUSY masses, but also additional constants contained in the self-energy Σ_{SQCD}.

$$\begin{aligned}
\lambda_t^0 &= \lambda_t(\mu_R^2) + \delta\lambda_{t\,\text{QCD}} + \delta\lambda_{t\,\text{SQCD}} \\
\delta\lambda_{t\,\text{QCD}} &= -\lambda_t(\mu_R^2)\,\frac{\alpha_s}{\pi}\left\{\Gamma[1+\epsilon]\,(4\pi)^\epsilon\,\frac{1}{\epsilon} + \log\frac{\mu^2}{\mu_R^2}\right\} \\
\delta\lambda_{t\,\text{SQCD}} &= -\text{Re}\Sigma_{\text{SQCD}}(m_t)
\end{aligned} \tag{3.33}$$

This renormalisation prescription ensures that the gluino and stop contributions are decoupled from the running of the top Yukawa coupling. Since the pure QCD corrections to the top mass are $\overline{MS}$ subtracted, we are left with the conventional $\overline{MS}$ Yukawa coupling of QCD. The relation between this $\overline{MS}$ Yukawa coupling of QCD and the on-shell coupling is given by

$$\lambda_t(\mu_R^2) = \lambda_t\left\{1 - \frac{\alpha_s}{\pi}C_F\big(1+\frac{3}{4}\log\frac{\mu_R^2}{m_t^2}\big)\right\} \tag{3.34}$$

This translates directly to the corresponding relation between the $\overline{MS}$ quark mass $\overline{m}_q(\mu_R^2)$ and the on-shell pole mass m_q.

$$\overline{m}_q(\mu_R^2) = m_q\left\{1 - \frac{\alpha_s}{\pi}C_F\big(1+\frac{3}{4}\log\frac{\mu_R^2}{m_q^2}\big)\right\} \tag{3.35}$$

3.6.2 Counterterms

In the following all counterterms used in this work are given in terms of one loop integrals and the ultraviolet divergences are extracted. To keep the limit $m \to 0$ under control, the following terms are made explicit for masses which are potentially small, as the bottom mass.

$$C_\epsilon\,(m_q) = \left(\frac{\mu^2}{m_q^2}\right)^\epsilon \tag{3.36}$$

These terms are kept in results and counterterms until the end of the calculation. Then they are set to zero ($C_\epsilon\,(m_b) \to 0$) in case of the bottom mass and to one ($C_\epsilon\,(m_t) \to 1$) in case of the top mass. To fix the quark mass counterterm, two diagrams contribute to the self-energy in (3.27). The first is the pure QCD correction with a quark-gluon loop and the second the SUSY-QCD correction with a squark-gluino loop. The calculation of

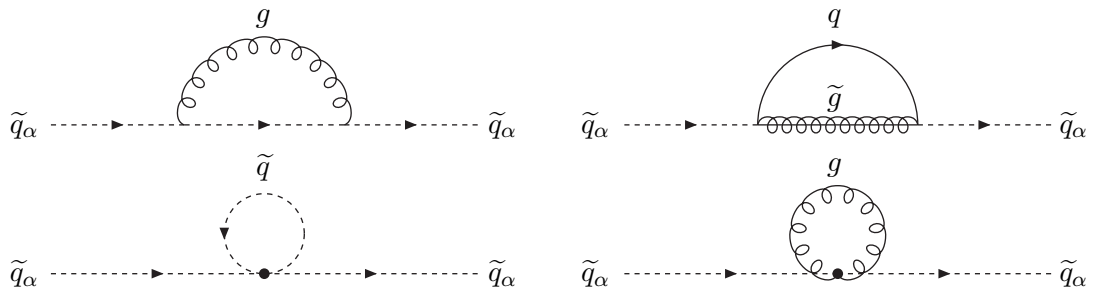

Figure 3.2: Diagrams contributing to the squark mass counterterms $\delta M^2_{\tilde{q}_{1/2}}$.

the diagrams in Figure 3.1 yields the quark mass counterterm given by the expression

$$\frac{\delta m_q}{m_q} = -i\ C_F\, g_s^2 \Bigg\{ \Bigg[\frac{(n-2)}{2m_q^2}\Big(-A_0(m_q) + 2m_q^2 B_0(m_q;0,m_q)\Big) - n\, B_0(m_q;0,m_q)\Bigg]_{\rm QCD}$$
$$+ \Bigg[\frac{1}{2m_q^2}\Big(A_0(M_{\tilde{q}_1}) + A_0(M_{\tilde{q}_2}) - 2A_0(M_{\tilde{g}}) + \sum_{i=1,2}\Big((m_q^2 + M_{\tilde{g}}^2 - M_{\tilde{q}_i}^2) B_0(m_q; M_{\tilde{q}_i}, M_{\tilde{g}})\Big)$$
$$- s_{2\tilde{\theta}}\, \frac{M_{\tilde{g}}}{m_q}\Big(B_0(m_q; M_{\tilde{q}_1}, M_{\tilde{g}}) - B_0(m_q; M_{\tilde{q}_2}, M_{\tilde{g}})\Big)\Bigg]_{\rm SQCD}\Bigg\} \tag{3.37}$$

To extract the $\frac{1}{\epsilon}$-pole, we paste the corresponding one-loop integrals from Appendix A.1.

$$\delta m_q\Big|_{UV} = \ -C_F\ \frac{\alpha_s}{4\pi}\ m_q \Big\{ \big[3\, C_\epsilon\,(m_q)\,\big]_{\rm QCD} + \big[\,-1\big]_{\rm SQCD}\Big\}\,\frac{1}{\epsilon} \tag{3.38}$$

To calculate the diagonal elements of the squark self-energy matrix, to obtain the squark counterterms, we need to consider squark propagators $\widetilde{q}_\alpha \to \widetilde{q}_\alpha$ $(\alpha = 1,2)$. Three diagrams contribute to the self-energy of the squark propagator, namely a squark-gluon loop, a quark-gluino loop (with a factor of -1 because of the fermion loop) and a squark tadpole. The gluon tadpole yields no contributions because the gluon is massless (A.5). The calculation of the diagrams in Figure 3.2 yields the following squark mass counterterms given by

$$\delta M^2_{\tilde{q}_1} = \ -i\, C_F\, g_s^2 \Big\{ A_0(M_{\tilde{q}_1}) - 4M^2_{\tilde{q}_1} B_0(M_{\tilde{q}_1}; M_{\tilde{q}_1}, 0) + A_0(M_{\tilde{q}_1}) c_{2\tilde{\theta}} + A_0(M_{\tilde{q}_2}) s^2_{2\tilde{\theta}}$$
$$- 2\Big(A_0(m_q) + A_0(M_{\tilde{g}}) + \big(m_q^2 + M_{\tilde{g}}^2 - 2m_q M_{\tilde{g}} s_{2\tilde{\theta}} - M^2_{\tilde{q}_1}\big)\, B_0(M_{\tilde{q}_1}; M_{\tilde{g}}, m_q)\Big)\Big\}$$
$$\delta M^2_{\tilde{q}_2} = \ -i\, C_F\, g_s^2 \Big\{ A_0(M_{\tilde{q}_2}) - 4M^2_{\tilde{q}_2} B_0(M_{\tilde{q}_2}; M_{\tilde{q}_2}, 0) + A_0(M_{\tilde{q}_2}) c^2_{2\tilde{\theta}} + A_0(M_{\tilde{q}_1}) s^2_{2\tilde{\theta}}$$
$$- 2\Big(A_0(m_q) + A_0(M_{\tilde{g}}) + \big(m_q^2 + M_{\tilde{g}}^2 + 2m_q M_{\tilde{g}} s_{2\tilde{\theta}} - M^2_{\tilde{q}_2}\big)\, B_0(M_{\tilde{q}_2}; M_{\tilde{g}}, m_q)\Big)\Big\}$$

To extract the $\frac{1}{\epsilon}$-pole, we paste the corresponding one-loop integrals from Appendix A.1.

$$\delta M^2_{\tilde{q}_{1/2}}\Big|_{UV} = \ -\,C_F\ \frac{\alpha_s}{4\pi}\Big\{ 2m_q^2(1 + C_\epsilon\,(m_q)) + 4\left(M_{\tilde{g}}^2 - m_q M_{\tilde{g}} s_{2\tilde{\theta}}\right) \pm \left(M^2_{\tilde{q}_1} - M^2_{\tilde{q}_2}\right) s^2_{2\tilde{\theta}}\Big\}\frac{1}{\epsilon}$$

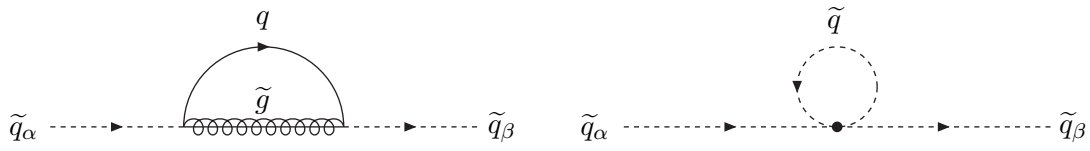

Figure 3.3: Diagrams contributing to the mixing angle counterterm $\delta\widetilde{\theta}_q$.

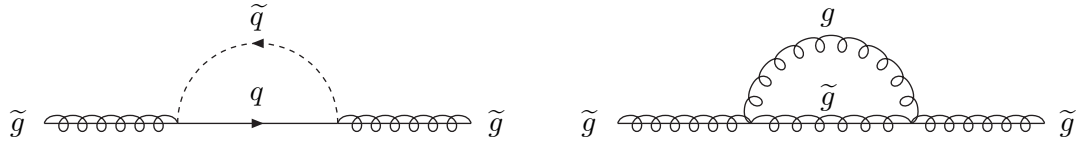

Figure 3.4: Diagrams contributing to the gluino mass counterterm $\delta M_{\tilde{g}}$.

The mixing angle counterterm is calculated via the off-diagonal elements of the squark self-energy matrix, i.e. with an incoming squark $\widetilde{q}_\alpha$ and an outgoing squark $\widetilde{q}_\beta$ ($\widetilde{q}_\alpha \to \widetilde{q}_\beta$) with $\alpha, \beta = 1, 2$ and $\alpha \neq \beta$. Two diagrams contribute to the off-diagonal elements of the self-energy, namely a quark-gluino loop and a squark tadpole. A mere gluon correction to this self-energy vanishes, because there is no mixing at a gluon vertex. The calculation of the diagrams in Figure 3.3 yields the mixing angle counterterm given by the expression

$$\delta\widetilde{\theta}_q = -i\, C_F\, g_s^2 \frac{1}{M_{\tilde{q}_1}^2 - M_{\tilde{q}_2}^2} \Big\{ 2\, m_q\, M_{\tilde{g}}\, c_{2\widetilde{\theta}} \Big(B_0(M_{\tilde{q}_1}; M_{\tilde{g}}, m_q) + B_0(M_{\tilde{q}_2}; M_{\tilde{g}}, m_q) \Big) - s_{2\widetilde{\theta}}\, c_{2\widetilde{\theta}} \left(A_0(M_{\tilde{q}_1}) - A_0(M_{\tilde{q}_2}) \right) \Big\} \tag{3.39}$$

To extract the $\frac{1}{\epsilon}$-pole, we paste the corresponding one-loop integrals from Appendix A.1.

$$\delta\widetilde{\theta}\Big|_{UV} = -\, C_F\, \frac{\alpha_s}{4\pi}\, c_{2\widetilde{\theta}} \Big\{ \frac{4 m_q M_{\tilde{g}}}{M_{\tilde{q}_1}^2 - M_{\tilde{q}_2}^2} - s_{2\widetilde{\theta}} \Big\} \frac{1}{\epsilon} \tag{3.40}$$

The gluino propagator is corrected by a quark-squark loop and and gluon-gluino loop. In the case of the quark-squark loop both flavour-flow directions need to be considered as well as all possible flavours in the loop. The calculation of the diagrams in Figure 3.4 yields the gluino mass counterterm given by the expression

$$\begin{aligned} \delta M_{\tilde{g}} = &-\, i\, T_R\, g_s^2 \sum_q \Bigg\{ \frac{1}{M_{\tilde{g}}} \Big[A_0(M_{\tilde{q}_1}) + A_0(M_{\tilde{q}_2}) - 2A_0(m_q) \\ &+ (M_{\tilde{g}}^2 + m_q^2 - M_{\tilde{q}_1}^2) B_0(M_{\tilde{g}}; M_{\tilde{q}_1}, m_q) + (M_{\tilde{g}}^2 + m_q^2 - M_{\tilde{q}_2}^2) B_0(M_{\tilde{g}}; M_{\tilde{q}_2}, m_q) \Big] \\ &- 2 s_{2\widetilde{\theta}}\, m_q \Big[B_0(M_{\tilde{g}}; M_{\tilde{q}_1}, m_q) - B_0(M_{\tilde{g}}; M_{\tilde{q}_2}, m_q) \Big] \Bigg\} \\ &- i\, C_A\, g_s^2 \Bigg\{ (2 - n) \frac{A_0(M_{\tilde{g}})}{2 M_{\tilde{g}}} - 2 M_{\tilde{g}} B_0(M_{\tilde{g}}; M_{\tilde{g}}, 0) \Bigg\} \end{aligned}$$

where the sum runs over all possible quark flavours in the loop ($q = u, d, c, s, t, b$). To extract the $\frac{1}{\epsilon}$-pole, we paste the corresponding one-loop integrals from Appendix A.1.

$$\delta M_{\tilde{g}}\Big|_{UV} = -2\,T_R\,\frac{\alpha_s}{4\pi}\,\frac{1}{M_{\tilde{g}}}\sum_q\left\{(C_\epsilon\,(m_q)-1)m_q^2 - M_{\tilde{g}}^2\right\}\frac{1}{\epsilon} - C_A\,\frac{\alpha_s}{4\pi}\left\{3M_{\tilde{g}}\right\}\frac{1}{\epsilon} \quad (3.41)$$

For the coupling renormalisation, the Collins-Wilczek-Zee scheme (a hybrid scheme) is employed, in which the $\overline{MS}$ scheme is used to renormalise the light quarks and gluons, and the momentum subtraction scheme is used to renormalise the heavy particles.

$$\begin{aligned}\delta g_s = i\,g_s^2\,\frac{1}{2}\Bigg\{&\frac{11}{3}C_A B_0(0;\mu_R,\mu_R) - \frac{4}{3}T_R N_F B_0(0;\mu_R,\mu_R) - \frac{4}{3}T_R B_0(0;m_t,m_t)\\ &- \frac{2}{3}C_A B_0(0;M_{\tilde{g}},M_{\tilde{g}}) - \frac{1}{3}T_R\sum_{\tilde{q}_i} B_0(0;M_{\tilde{q}_i},M_{\tilde{q}_i})\Bigg\}\end{aligned} \quad (3.42)$$

The divergence is given by

$$\delta g_s\Big|_{UV} = -\frac{\alpha_s}{4\pi}\left\{\frac{\beta_0}{2}\right\}\frac{1}{\epsilon} \quad (3.43)$$

The coefficient β_0 of the SUSY-QCD β-function can be decomposed into a sum of contributions from light and heavy particles:

$$\beta_0 = \left[\frac{11}{3}C_A - \frac{4}{3}T_R N_F\right] + \left[-\frac{2}{3}C_A - \frac{4}{3}T_R - \frac{2}{3}T_R(N_F+1)\right] = \beta_0^L + \beta_0^H \quad (3.44)$$

This counterterm is chosen such that only the five lightest quarks (N_F is the number of active flavours in the coupling and is chosen to be $N_F = 5$) and gluons contribute to the running of α_s with the renormalisation scale μ_R^2, while the heavy particles (top quark, squarks and gluinos) are decoupled through the subtraction of logarithms in equation (3.42)

$$\mu_R^2\frac{\partial\alpha_s(\mu_R^2)}{\partial\mu_R^2} = \beta(\alpha_s(\mu_R^2)) = -\frac{\alpha_s^2(\mu_R^2)}{4\pi}\beta_0^L \quad (3.45)$$

These counterterms suffice to render our results UV finite.

3.6.3 Anomalous Counterterms

As was already mentioned, a complication occurs in supersymmetric theories if dimensional regularisation is employed. In $n \neq 4$ dimensions a mismatch between the number of gluon $(n-2)$ and gluino (2) degrees of freedom is introduced. Since this $\mathcal{O}(\epsilon)$ mismatch will result in finite non-zero contributions at NLO, supersymmetry is explicitly violated in higher orders. This can be fixed by **anomalous counterterms** [93]. In the supersymmetric limit (a theory with unbroken supersymmetry), the new parameters of the supersymmetric theory as (super)couplings and sparticle masses, should coincide with the masses and couplings of their corresponding Standard Model partners. In particular, the Yukawa coupling $\hat{g}_s$, which is the coupling between quark, squark and gluino, should by supersymmetry coincide with the gauge coupling g_s, but deviates from it by

a finite amount at NLO. Requiring the physical amplitudes to preserve the supersymmetric relation, a shift between the bare Yukawa coupling and the bare gauge coupling must be introduced.

$$\hat{g}_s^0 = g_s^0\Big[1 + \frac{\alpha_s}{4\pi}\Big(\frac{2}{3}C_A - \frac{1}{2}C_F\Big)\Big] \tag{3.46}$$

which effectively subtracts the contributions of the false, non-supersymmetric degrees of freedom. In the supersymmetric limit of the MSSM, the quark and squark masses must coincide as well. However as with the strong coupling, at the one loop level the scalar mass $m_{\tilde{q}}$ and the fermion mass m_q deviate by a finite amount, so that a correction must be introduced as well to render the theory consistent. In fact this problem arises in the Yukawa couplings, where the following equation holds generically

$$\lambda^0_{hqq} = \lambda^0_{h\tilde{q}\tilde{q}}\Big[1 + \frac{\alpha_s}{4\pi}C_F\Big] = \lambda^0_{\tilde{h}\tilde{q}q}\Big[1 + \frac{3}{2}\frac{\alpha_s}{4\pi}C_F\Big] \tag{3.47}$$

Here the subscripts indicate which kind of vertex the coupling defines. Again as above, the goal is to express all SUSY Yukawa couplings ($\lambda_{h\tilde{q}\tilde{q}}$ and $\lambda_{\tilde{h}\tilde{q}q}$) in terms of the Standard Model coupling λ_{hqq}. But for inserting the appropriate shift, the origin of the parameter must be known. For example, our SUSY-electroweak result is proportional to λ_t^2. One coupling stems from a higgsino squark quark vertex and the other from a higgs squark squark vertex. Consequently one needs to introduce the finite shift $(-5/8\frac{\alpha_s}{\pi}C_F)$ in the counterterm to express everything in terms of λ_{hqq}. Thus the complete renormalisation is

$$\lambda_t^{0\,2} \;=\; \lambda_t^2 \;+\; 2\,\lambda_t\,\delta\lambda_t \;-\; \lambda_t^2\,\frac{5}{2}\,\frac{\alpha_s}{4\pi}\,C_F \tag{3.48}$$

The trilinear coupling A_t is renormalized as well through the counterterm of the top mass, see (3.29). The Yukawa coupling in this mass parameter is of the type $\lambda_{h\tilde{q}\tilde{q}}$ because the relation (1.29) originates from the squark mass matrix. Therefore the top mass counterterm in (3.29) obtains the finite shift $(-\frac{\alpha_s}{4\pi}C_F)$. A last shift needs to be introduced for the bottom Yukawa coupling λ_b in our calculation, which arises in SUSY-QCD calculation at the Higgs squark vertex yielding the shift $(-\frac{\alpha_s}{4\pi}C_F)$, and in the SUSY-electroweak calculation at the Higgsino vertex yielding the shift $(-3/8\frac{\alpha_s}{\pi}C_F)$. In the following we use these finite subtractions to renormalize the strong coupling and the different Yukawa couplings. In this way on the one hand supersymmetry is preserved, while on the other hand the definitions of the strong gauge coupling and the Yukawa couplings correspond to the usual Standard-Model parameters.

3.6.4 Running Coupling Constant

Because the analytical result of physical quantities depends explicitly on the renormalisation scale μ_R but the physical quantity itself must be independent of this artificial scale, the strong coupling $\alpha_s = g_s^2/4\pi$ must also depend on μ_R to compensate this dependence. The coupling varies with the scale μ_R and it is called running coupling constant $\alpha_s(\mu_R)$. The explicit form of the running is determined by a renormalisation group equation

$$\mu_R^2\frac{\partial\alpha_s(\mu_R^2)}{\partial\mu_R^2} = \beta(\alpha_s(\mu_R^2)) \tag{3.49}$$

where the β-function depends on the specific choice of the renormalisation scheme

$$\beta(\alpha_s) = -\frac{\alpha_s^2}{4\pi}\Big[\beta_0 + \beta_1\frac{\alpha_s}{4\pi} + \beta_2\left(\frac{\alpha_s}{4\pi}\right)^2 + \dots\Big] \tag{3.50}$$

Only the first two coefficients are scheme independent and are given by [14, 15]

$$\beta_0 = \frac{11C_A - 2N_F}{3} \quad , \quad \beta_1 = 2\frac{153 - 19N_F}{3} \tag{3.51}$$

if the coupling runs with N_F flavours and all SUSY particles are decoupled. Solving equation (3.49) up to β_1 yields the approximate result

$$\alpha_s(\mu_R) = \frac{4\pi}{\beta_0 \log\left(\frac{\mu_R^2}{\Lambda^2}\right)} \left(1 - \frac{\beta_1}{\beta_0^2} \frac{\log\left(\log\left(\frac{\mu_R^2}{\Lambda^2}\right)\right)}{\log\left(\frac{\mu_R^2}{\Lambda^2}\right)}\right) + \mathcal{O}\left(\frac{1}{\log^3}\left(\frac{\mu_R^2}{\Lambda^2}\right)\right) \tag{3.52}$$

where the fundamental scale $\Lambda = \Lambda_{QCD}$ needs to be determined from experiment. Looking at (3.52) the coupling decreases as the scale μ_R increases, corresponding to the property of asymptotic freedom [13, 15]. A physical quantity is only independent of μ_R if calculated to all orders in perturbation theory. If not, the remaining dependence on μ_R can be used as an estimate of the remaining theoretical uncertainties caused by unknown higher order corrections.

3.6.5 Running Quark Mass

The running of the quark masses is determined by the anomalous dimension $\gamma(\alpha_s)$ and the renormalisation group equation

$$\mu_R^2 \frac{\partial \overline{m}_q(\mu_R^2)}{\partial \mu_R^2} = \gamma(\alpha_s(\mu_R^2))\, \overline{m}_q(\mu_R^2) \tag{3.53}$$

where the γ-function depends on the specific choice of the renormalisation scheme.

$$\gamma(\alpha_s) = -\frac{\alpha_s}{\pi}\left[\gamma_0 + \gamma_1 \frac{\alpha_s}{\pi} + \gamma_2 \left(\frac{\alpha_s}{\pi}\right)^2 + \dots\right] \tag{3.54}$$

Only the first coefficient γ_0 in the expansion is scheme independent (when the coupling runs with N_F flavours and all SUSY particles are decoupled). γ_1 is given in the $\overline{MS}$ scheme [94–96].

$$\gamma_0 = \frac{3}{4}\, C_F \quad , \quad \gamma_1^{\overline{MS}} = \frac{1}{32} C_F \left[\left(3C_F + \frac{97}{3} C_A\right) - \frac{20}{3} T_R N_F\right] \tag{3.55}$$

The solution of the renormalisation group equation (3.53) can be written in the form

$$\overline{m}_q(\mu_R^2) \;=\; \overline{m}_q(m_q^2)\, \frac{c(\alpha_s(\mu_R^2)/\pi)}{c(\alpha_s(m_q^2)/\pi)} \quad , \quad \overline{m}_q(m_q^2) \;=\; \frac{m_q}{1 \,+\, C_F \frac{\alpha_s(m_q^2)}{\pi}} \tag{3.56}$$

with the coefficient function [97–99]

$$\begin{aligned}
c(x) &= \left(\frac{9}{2}\, x\right)^{\frac{4}{9}} [1 + 0.895x + 1.371\, x^2 + 1.952\, x^3] && \text{for } M_s < \mu < M_c \\
c(x) &= \left(\frac{25}{6}\, x\right)^{\frac{12}{25}} [1 + 1.014x + 1.389\, x^2 + 1.091\, x^3] && \text{for } M_c < \mu < M_b \\
c(x) &= \left(\frac{23}{6}\, x\right)^{\frac{12}{23}} [1 + 1.175x + 1.501\, x^2 + 0.1725\, x^3] && \text{for } M_b < \mu < M_t \\
c(x) &= \left(\frac{7}{2}\, x\right)^{\frac{4}{7}} [1 + 1.398x + 1.793\, x^2 - 0.6834\, x^3] && \text{for } M_t < \mu.
\end{aligned} \tag{3.57}$$

Chapter 4

Effective Bottom Yukawa Coupling

In this chapter we review the leading one-loop genuine SUSY-QCD and top-induced SUSY-electroweak corrections to processes that include bottom Yukawa couplings, as for example Higgs boson decays to $b\bar{b}$ pairs and Higgs radiation off bottom quarks. These corrections can be incorporated into effective bottom Yukawa couplings. The effective Yukawa couplings include the resummation of non-decoupling corrections for large values of tgβ. The calculation of these corrections is explained and the inclusion of the novel two-loop SUSY-QCD corrections is discussed.

4.1 Effective Lagrangian

In the MSSM the Higgs field H_1^0 couples to a pair of bottom-quarks via the Yukawa coupling λ_b^0

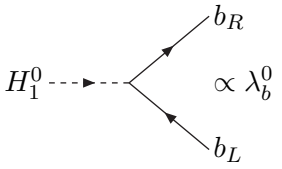

$$\mathcal{L} = -\lambda_b^0 \, \bar{b}_R^0 \, H_1^0 \, b_L^0 \; + \; \text{h.c.} \tag{4.1}$$

In the limit of vanishing Higgs- and bottom-momentum, i.e. in the low energy limit $m_b^2, M_H^2 \ll M_{SUSY}^2$, higher order corrections to this process can be included in a modification of the Yukawa coupling. In Figure 4.1 the Higgs-field H_2^0 couples to the bottom-quarks via (a) a bottom-squark and gluino loop and (b) a top-squark and Higgsino loop. Both diagrams are proportional to the bottom Yukawa coupling λ_b. In diagram (a) λ_b is included in the Higgs-sbottom coupling and in diagram (b) in one of the bottom-stop couplings depending on the chirality, see the corresponding Feynman rules in Appendix B.2. The Higgs Boson H_2^0 couples differently to up- and down-type squarks. In the case of up-type squarks, H_2^0 couples via the trilinear coupling A_u in the soft supersymmetry breaking Lagrangian (1.22), for down-type squarks via the parameter μ from the superpotential (1.20). The diagrams 4.1 (a) and (b) give rise to the effective Lagrangian

$$\mathcal{L}_{eff} = -\lambda_b \, \bar{b}_R \, [H_1^0 \; + \; \frac{\Delta m_b}{\text{tg}\beta} \, H_2^{0*}] \, b_L \; + \; \text{h.c.} \tag{4.2}$$

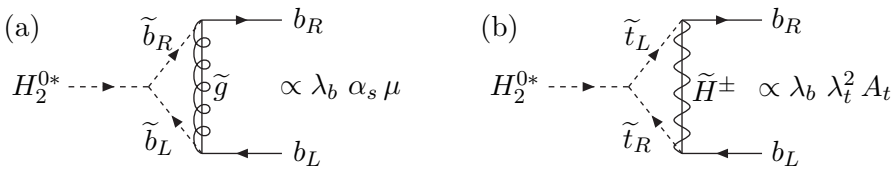

Figure 4.1: Loop-induced couplings of H_2^0 to bottom-quarks: (a) coupling via a sbottom-gluino loop and (b) coupling via a stop-Higgsino loop. The indicated values represent the contributions from the three vertices.

where the quark field renormalisation $\bar{b}_R^0 b_L^0 = Z_V \bar{b}_R b_L$ is absorbed into the Yukawa coupling. It should be noted, that the bottom wave-function renormalisation constants do not contain any leading non-decoupling contribution in μ or A_t. If the Higgs fields obtain their vacuum expectation values, the additional coupling involves a modification of the relation between the bottom Yukawa coupling λ_b and the bottom mass m_b:

$$m_b = \frac{\lambda_b}{\sqrt{2}}\, v_1\, [1 + \Delta m_b] \tag{4.3}$$

4.2 NLO Results

Including higher-order corrections to obtain effective couplings would usually require the calculation of diagrams as shown in Figure 4.1. This was done in [28, 100–102] to NLO. Here we use another approach, which exploits the low energy theorems discussed in section 3.1. The pole mass m_b of the bottom quark is given by

$$m_b = \frac{\lambda_b^0}{\sqrt{2}} v_1 + \Sigma_b(m_b) \tag{4.4}$$

where the leading terms of the self-energy $\Sigma_b(m_b)$ can be decomposed as

$$\Sigma_b(m_b) = \frac{\lambda_b^0}{\sqrt{2}}\, v_1\ \Delta m_b \quad , \quad \Delta m_b = \Delta m_b^{QCD} + \Delta m_b^{EW} \tag{4.5}$$

The terms Δm_b^{QCD} and Δm_b^{EW} in (4.5) can be obtained from mass insertions in the virtual sbottom and stop propagators, as is illustrated in Figure 4.2 at one-loop. These diagrams behave asymptotically as the integral $C_0(0,0;m_1,m_2,m_3)$ which is given in (A.11). The bottom momentum has been put to zero while keeping the bottom Yukawa coupling λ_b finite in the mass insertions. All supersymmetric particles are treated with full mass dependence. The finite result for Δm_b^{QCD} and Δm_b^{EW} at one-loop is:

$$\begin{aligned} \Delta m_b^{QCD\,(1)} &= \frac{C_F}{2}\,\frac{\alpha_s}{\pi}\, M_{\tilde{g}}\, \mu\, \mathrm{tg}\beta\ I(M^2_{\tilde{b}_1}, M^2_{\tilde{b}_2}, M^2_{\tilde{g}}) \\ \Delta m_b^{EW\,(1)} &= \frac{\lambda_t^2}{(4\pi)^2}\, A_t\, \mu\, \mathrm{tg}\beta\ I(M^2_{\tilde{t}_1}, M^2_{\tilde{t}_2}, \mu^2) \end{aligned} \tag{4.6}$$

with the scalar function

$$I(a,b,c) = -\frac{ab\log\frac{a}{b} + bc\log\frac{b}{c} + ca\log\frac{c}{a}}{(a-b)(b-c)(c-a)} \tag{4.7}$$

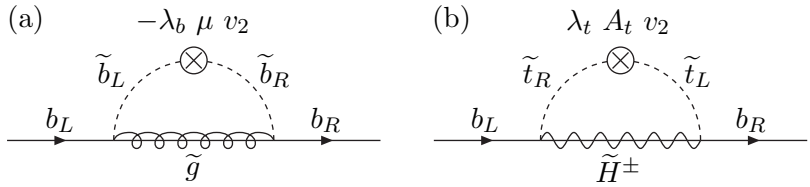

Figure 4.2: One-loop diagrams of (a) the SUSY-QCD and (b) the top-induced SUSY-electroweak contributions to the bottom self-energy with the off-diagonal mass insertions corresponding to the corrections Δm_b of the bottom Yukawa couplings. The virtual particles involve bottom quarks b and squarks $\widetilde{b}$, gluinos $\widetilde{g}$ and charged Higgsinos $\widetilde{H}^{\pm}$.

These corrections are non-decoupling in the sense that scaling all SUSY parameters in (4.6) leaves Δm_b invariant. In order to obtain the effective low-energy Lagrangian (4.2) from the expression (4.4) for the bottom mass, we have to perform the replacements $v_1 \to \sqrt{2}H_1^0$ and $v_2 \to \sqrt{2}H_2^{0*}$ in the corresponding bottom mass operator. These replacements lead to exact interactions with low-energy Higgs fields, i.e. in the limit of small Higgs boson momentum. We use the relation (4.3) together with equation (1.25) to express the fields H_1^0 and H_2^0 in the effective Lagrangian (4.2) in terms of physical Higgs fields:

$$\begin{aligned}\mathcal{L}_{eff} = &- m_b\,\bar{b}\left[1 + i\gamma_5\frac{G^0}{v}\right] b - \frac{m_b/v}{1+\Delta m_b}\,\bar{b}\Bigg[g_b^h\left(1 - \frac{\Delta m_b}{\mathrm{tg}\alpha\ \mathrm{tg}\beta}\right) h \\ &+ g_b^H\left(1 + \Delta m_b\frac{\mathrm{tg}\alpha}{\mathrm{tg}\beta}\right) H - g_b^A\left(1 - \frac{\Delta m_b}{\mathrm{tg}^2\beta}\right) i\gamma_5 A\Bigg] b \end{aligned} \tag{4.8}$$

with the couplings g_b^h, g_b^H, g_b^A from Table 2.1 and $v_1 = v\,\cos\beta$ with $v^2 = v_1^2 + v_2^2$. Defining modified couplings yields finally the following interaction terms:

$$\mathcal{L}_{eff} = -\frac{m_b}{v}\ \bar{b}\ [\ \tilde{g}_b^h\ h + \tilde{g}_b^H\ H - \tilde{g}_b^A\ i\gamma_5\ A\ ]\ b \tag{4.9}$$

with the effective couplings

$$\begin{aligned}\tilde{g}_b^h = \frac{g_b^h}{1+\Delta m_b}\left[1 - \Delta m_b\frac{1}{\mathrm{tg}\alpha\mathrm{tg}\beta}\right] \quad , \quad \tilde{g}_b^H = \frac{g_b^H}{1+\Delta m_b}\left[1 + \Delta m_b\frac{\mathrm{tg}\alpha}{\mathrm{tg}\beta}\right] \\ \tilde{g}_b^A = \frac{g_b^A}{1+\Delta m_b}\left[1 - \Delta m_b\frac{1}{\mathrm{tg}^2\beta}\right]\end{aligned} \tag{4.10}$$

Although the SUSY corrections Δm_b are loop suppressed, they turn out to be significant for large values of $\mathrm{tg}\beta$ and moderate or large μ values and in this case represent the dominant supersymmetric radiative corrections to the bottom Yukawa coupling. Nevertheless, the effective Lagrangian in (4.9) has been obtained by integrating out the heavy SUSY particles and is thus not restricted to large values of $\mathrm{tg}\beta$ only. In order to improve the perturbative result, all terms of $\mathcal{O}\left((\alpha_s\,\mu\,\mathrm{tg}\beta)^n\right)$ and $\mathcal{O}\left((\lambda_t^2\,A_t\,\mathrm{tg}\beta)^n\right)$ have been resummed [100]. The correctly resummed effective Lagrangian is given by equation (4.9). Apart from the correction Δm_b there is a second class of potentially large (non-decoupling) contributions at higher orders which may spoil the perturbative reliability of the results, namely the trilinear mixing parameter A_b which can be of similar size as $\mu\mathrm{tg}\beta$ as e.g. in no-mixing scenarios of the sbottom particles. However, it was shown that these contributions are small and of no phenomenological relevance [28].

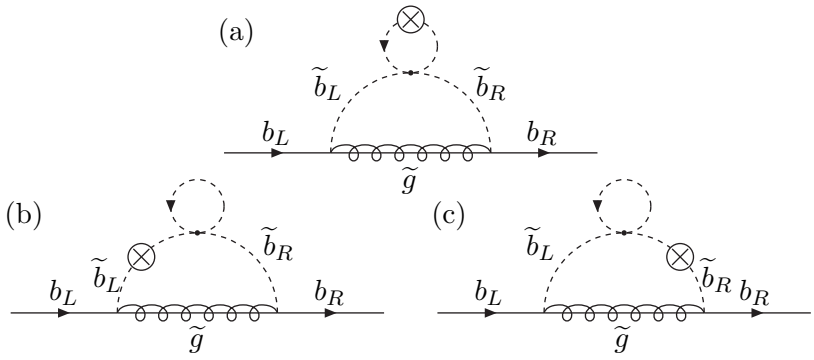

Figure 4.3: Two-loop contributions to the quantity Δm_b^{QCD}.

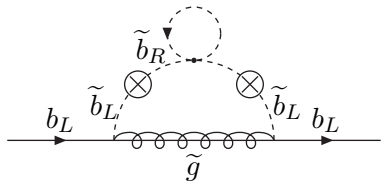

Figure 4.4: Two-loop diagram with additional mass insertion

4.3 Leading Terms for any Perturbative Order

Since our results are important for large tgβ scenarios, we want to show that contributions of order $\mathcal{O}\left(\mu^2 \mathrm{tg}^2\beta\right)$ or $\mathcal{O}\left(A_t^2 \mathrm{tg}^2\beta\right)$ do not exist or are suppressed at any order of perturbation theory. The structure of the self-energy can be derived from general arguments based on the asymptotic behavior of the corresponding Feynman diagrams in the low energy limit. At next-to-next-to-leading order (NNLO) the leading contributions involving μ are generated by e.g. the diagrams of Figure 4.3. The diagram 4.3 (a) behaves asymptotically as

$$\alpha_s^2\ \lambda_b\ \mu\ v_2\ M_{\tilde{g}}\ B_0(0; M_{\tilde{b}_1}, M_{\tilde{b}_1})\ C_0(0,0; M_{\tilde{b}_i}, M_{\tilde{b}_j}, M_{\tilde{g}})\ \sim\ \alpha_s^2\ m_b\ M_{\tilde{g}}\ \frac{\mu\,\mathrm{tg}\beta}{M_{SUSY}^2}$$

whereas diagrams (b) and (c) behave as

$$\alpha_s^2\ \lambda_b\ \mu\ v_2\ M_{\tilde{g}}\ A_0(M_{\tilde{b}_i})\ D_0(0,0,0; M_{\tilde{b}_1}, M_{\tilde{b}_2}, M_{\tilde{b}_j}, M_{\tilde{g}})\ \sim\ \alpha_s^2\ m_b\ M_{\tilde{g}}\ \frac{\mu\,\mathrm{tg}\beta}{M_{SUSY}^2}$$

Thus, the diagrams in Figure 4.3 contribute to the same order as the pure QCD corrections to the NLO results and do not generate terms of order $\mathcal{O}\left(\mu^2 \mathrm{tg}\beta^2\right)$. Also further mass insertions are non-leading, since they are suppressed by another power of m_b/M_{SUSY}. For example, the diagram in Figure 4.4, behaves asymptotically as

$$\sim\ \alpha_s^2\ m_b\ M_{\tilde{g}}\ \frac{(\mu\,\mathrm{tg}\beta)^2}{M_{SUSY}^3}\frac{m_b}{M_{SUSY}} \tag{4.11}$$

and is therefore non-leading. This suppression can be proven for any perturbative order. Due to the Kinoshita-Lee-Nauenberg theorem [103, 104], irreducible diagrams do not

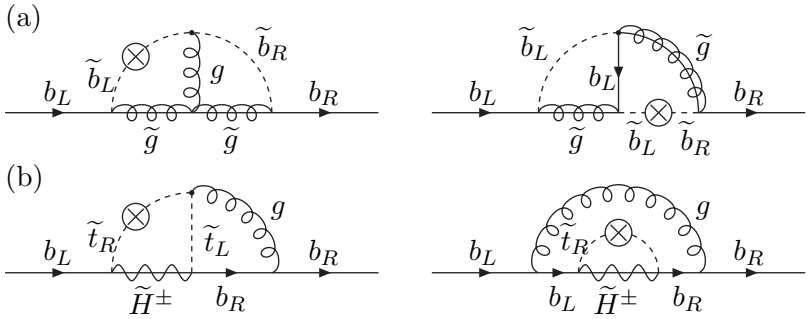

Figure 4.5: Typical two-loop diagrams of (a) the SUSY-QCD and (b) the top-induced SUSY-electroweak contributions to the bottom self-energy involving bottom quarks b, sbottom $\widetilde{b}$ and stop $\widetilde{t}$ squarks, gluons g, gluinos $\widetilde{g}$ and charged Higgsinos $\widetilde{H}^{\pm}$.

develop power-like divergences in the bottom mass for $m_b \to 0$. Thus any mass insertion in the sbottom propagators leads to the replacement

$$\frac{1}{q^2 - M^2_{\tilde{b}_i}} \to \frac{1}{q^2 - M^2_{\tilde{b}_1}}\; m_b\, \mu\, \mathrm{tg}\beta\; \frac{1}{q^2 - M^2_{\tilde{b}_2}} \;\sim\; -\frac{m_b\, \mu\, \mathrm{tg}\beta}{M^2_{SUSY}}\; \frac{1}{q^2 - M^2_{\tilde{b}_i}} \tag{4.12}$$

Therefore, the low-energy behavior of the mass-inserted diagram is modified by an additional power of $m_b \mu \mathrm{tg}\beta / M^2_{SUSY}$ and is thereby suppressed by m_b / M_{SUSY}, since μ is of order $\mathcal{O}(M_{SUSY})$. Hence, given a diagram of perturbative order n (i.e. with n-loops), the leading SUSY-QCD contributions will be of order

$$\mathcal{O}\Big(\frac{\alpha_s^n}{M_{SUSY}}\; \mu\, \mathrm{tg}\beta\Big) \quad , \quad \mathcal{O}\Big(\frac{\alpha_s^{n-1}}{M_{SUSY}}\; \lambda_t^2\, A_t\, \mathrm{tg}\beta\Big) \tag{4.13}$$

Consequently, at NLO, the diagrams of Figure 4.2 yield all leading powers of order $\mathcal{O}(\alpha_s \mu \mathrm{tg}\beta)$ and $\mathcal{O}\left(\lambda_t^2 A_t \mathrm{tg}\beta\right)$, and equation (4.6) constitutes the full result of the leading terms. At NNLO, only contributions of order $\mathcal{O}\left(\alpha_s^2 \mu \mathrm{tg}\beta\right)$ and $\mathcal{O}\left(\alpha_s \lambda_t^2 A_t \mathrm{tg}\beta\right)$ will arise.

4.4 Novel NNLO Corrections

The topic of this thesis is the calculation of the leading SUSY-QCD two-loop corrections to the effective bottom Yukawa coupling, i.e. the calculation of the SUSY-QCD corrections $\Delta m_b^{QCD\,(2)} \sim \mathcal{O}\left(\alpha_s^2 \mu \mathrm{tg}\beta / M_{SUSY}\right)$ and $\Delta m_b^{EW\,(2)} \sim \mathcal{O}\left(\alpha_s \lambda_t^2 A_t \mathrm{tg}\beta / M_{SUSY}\right)$. A typical sample of two-loop diagrams contributing to the bottom self-energy is shown in Figure 4.5 and the full set of calculated diagrams is given in Appendix C. The bottom momentum and its mass have been put to zero while keeping the bottom Yukawa coupling λ_b finite in the mass insertions. All supersymmetric particles as well as the top quark have been treated with full mass dependence. The two-loop integrals can be expressed in terms of the one-loop one-point integral $A_0(m)$ and the two-loop master integral $T_{134}(m_1, m_3, m_4)$ [105, 106], see section 3.4. The SUSY-QCD calculation was separated into three parts, each of which is proportional to a different colour factor C_F^2, $C_A C_F$ or $T_R C_F$ respectively. These were introduced in section 3.3. The SUSY-electroweak corrections are all proportional to C_F. Contrary to the one-loop corrections, the two-loop corrections $\Delta m_b^{(2)}$ are UV-divergent. To render the result finite, all masses and couplings

appearing at the one-loop order need to be renormalised, namely the bare parameters α_s^0, λ_t^0, A_t^0, $M_{\tilde{b}_1}^0$, $M_{\tilde{b}_2}^0$, $M_{\tilde{t}_1}^0$, $M_{\tilde{t}_2}^0$ and $M_{\tilde{g}}^0$. We separate these into physical parameters and counterterms $p^0 = p + \delta p$ as explained in section 3.6. The parameter μ^0 is not renormalised because its renormalisation is of a different order. The renormalisation can be written as:

$$\begin{aligned}\Delta m_b &= \Delta m_b^{(1)}(\bar{p}^0) + \Delta m_b^{(2)}(\bar{p}^0) = \Delta m_b^{(1)}(\bar{p}) + \sum_p \frac{\partial \Delta m_b^{(1)}}{\partial p}\delta p + \Delta m_b^{(2)}(\bar{p}) + \mathcal{O}\left(\alpha_s^3, \alpha_s^2\lambda_t\right) \\ &= \Delta m_b(\bar{p}) + \mathcal{O}\left(\alpha_s^3, \alpha_s^2\lambda_t\right) \end{aligned} \tag{4.14}$$

Here $\bar{p} = \{\alpha_s, \lambda_t, A_t, M_{\tilde{b}_1}^2, M_{\tilde{b}_2}^2, M_{\tilde{t}_1}^2, M_{\tilde{t}_2}^2, M_{\tilde{g}}\}$ is the tuple of all parameters that need to be renormalised and the counterterms δp are given in section 3.6.2. Thus, written in terms of physical parameters, Δm_b is finite. The strong coupling α_s and the top Yukawa coupling λ_t have been defined in the $\overline{MS}$ scheme with 5 active flavours, i.e. the top quark and the supersymmetric particles have been decoupled from the scale dependence of the strong coupling $\alpha_s(\mu_R)$ and the top Yukawa coupling $\lambda_t(\mu_R)$, see section 3.6.1. The obtained analytic result for $\Delta m_b^{(2)}$ is given in Appendix D. The numerical analysis of the newly obtained results follows in section 5.2.2.

Chapter 5

Results

In this final chapter we show numerical results to discuss the relevance of the obtained results. The goal of this work was the reduction of the remaining theoretical uncertainties in physical observables that involve the bottom Yukawa couplings $\tilde{g}_b^\Phi$. Part of these uncertainties stem from the variation of the corrections Δm_b with the renormalisation scale μ_R. So far at NLO, these uncertainties were sizable but are reduced significantly by our novel NNLO calculation. This is demonstrated for the partial decay width of Higgs bosons to bottom quarks. Branching ratios are shown for the dominant decay channels to bottom- and tau-pairs. Furthermore the reliability of the low-energy approximation is analysed.

5.1 Higgs Decays into Bottom Quark Pairs

At leading order the partial decay width $\Gamma_{LO}(\Phi \to b\bar{b})$ of the neutral Higgs bosons $\Phi = h, H, A$ into bottom quark pairs $b\bar{b}$ can be cast into the form

$$\Gamma_{LO}(\Phi \to b\bar{b}) = \begin{cases} \dfrac{3\mathrm{G_F} M_\Phi}{4\sqrt{2}\pi}\ m_b^2\ (g_b^\Phi)^2\ \beta^3\ , & \Phi = h, H \\ \dfrac{3\mathrm{G_F} M_\Phi}{4\sqrt{2}\pi}\ m_b^2\ (g_b^\Phi)^2\ \beta\ , & \Phi = A \end{cases} \tag{5.1}$$

with $\beta^2 = 1 - \tau$ and $\tau = 4m_b^2/M_\Phi^2$. The corresponding diagram is shown in the top left corner of Figure 5.1. The partial decay width $\Gamma_{LO}(\Phi \to b\bar{b})$ is illustrated in Figure 5.2 as a function of M_A.

5.1.1 QCD Corrections

The calculation of the QCD corrections [107–116] to the partial decay widths of the neutral Higgs bosons into bottom quark pairs, in the limit of large Higgs masses ($M_\Phi^2 \gg m_b^2$), yields the expression

$$\Gamma_{QCD}(\Phi \to b\bar{b}) = \frac{3\mathrm{G_F} M_\Phi}{4\sqrt{2}\pi}\ \overline{m}_b^2(M_\Phi)\ (g_b^\Phi)^2\ [\Delta_{QCD} + \Delta_t^\Phi] \tag{5.2}$$

where the couplings g_b^Φ are given in Table 2.1. The large logarithmic part of the QCD corrections, which emerges from the large scale difference between the Higgs mass and

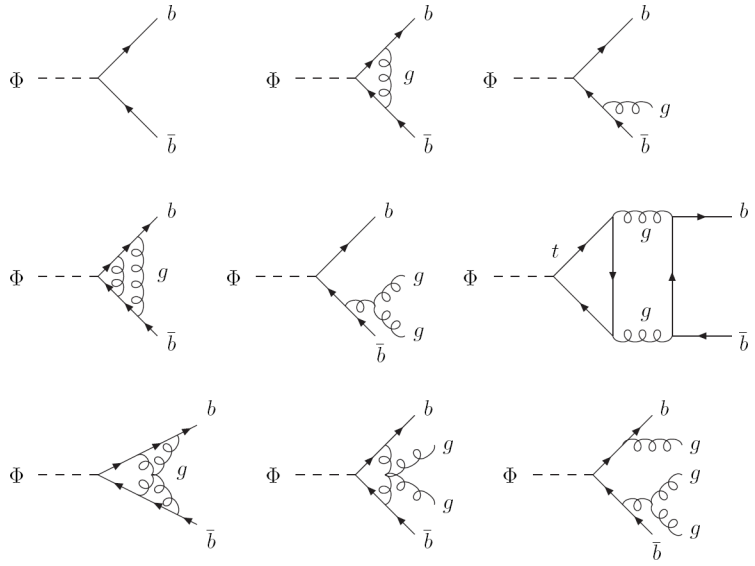

Figure 5.1: Typical diagrams contributing to $\Phi \to b\bar{b}$ at lowest order and one-, two- and three-loop QCD.

the bottom quark mass, has been absorbed in the running bottom quark mass $\overline{m}_b^2(M_\Phi)$ defined in the $\overline{MS}$-scheme at the scale of the corresponding Higgs boson mass M_Φ.

$$\overline{m}_b(M_\Phi^2) \;=\; m_b \left\{ 1 \;-\; \frac{\alpha_s(M_\Phi^2)}{\pi} C_F \big(1 + \frac{3}{4} \log \frac{M_\Phi^2}{m_b^2}\big) + \mathcal{O}\left(\alpha_s^2(M_\Phi^2)\right) \right\} \tag{5.3}$$

Neglecting regular quark mass effects, the NNNLO QCD corrections Δ_{QCD} are obtained by evaluating, amongst others, the diagrams shown in Figure 5.1.

$$\begin{aligned} \Delta_{QCD} = \; 1 + 5.67 \, \frac{\alpha_s(M_\Phi)}{\pi} + (35.94 - 1.36 N_F) \left(\frac{\alpha_s(M_\Phi)}{\pi} \right)^2 \\ + (164.14 - 25.77 N_F + 0.259 N_F^2) \left(\frac{\alpha_s(M_\Phi)}{\pi} \right)^3 \end{aligned} \tag{5.4}$$

Here $N_F = 5$ active flavours are taken into account. The top quark induced contributions Δ_t^Φ are

$$\Delta_t^\Phi = \begin{cases} \dfrac{g_t^\Phi}{g_b^\Phi} \left(\dfrac{\alpha_s(M_\Phi)}{\pi} \right)^2 \left[1.57 - \dfrac{2}{3} \log \left(\dfrac{M_\Phi^2}{m_t^2} \right) + \dfrac{1}{9} \log^2 \dfrac{\overline{m}_b^2(M_\Phi)}{M_\Phi^2} \right], & \Phi = h, H \\ \dfrac{g_t^\Phi}{g_b^\Phi} \left(\dfrac{\alpha_s(M_\Phi)}{\pi} \right)^2 \left[3.83 - \quad \log \left(\dfrac{M_\Phi^2}{m_t^2} \right) + \dfrac{1}{6} \log^2 \dfrac{\overline{m}_b^2(M_\Phi)}{M_\Phi^2} \right], & \Phi = A \end{cases} \tag{5.5}$$

In the intermediate and large Higgs boson mass regimes, the QCD corrections reduce the $b\bar{b}$ decay widths by about 50% due to the large logarithmic contributions. This can be inferred from Figure 5.2. The QCD corrected curve in Figure 5.2 is obtained by plotting $\Gamma_{QCD}(\Phi \to b\bar{b})$ as a function of M_A.

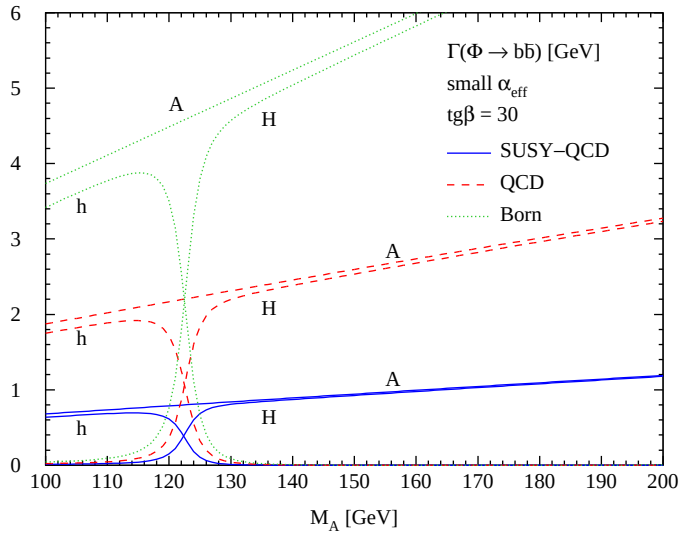

Figure 5.2: The partial decay width $\Gamma(\Phi \to b\bar{b})$ at leading order (Born), with QCD corrections and with SUSY-QCD corrections in the small α_{eff} scenario.

5.1.2 SUSY-QCD and SUSY-Electroweak Corrections

In the MSSM, the final result for the resummed partial decay widths $\tilde{\Gamma}$, valid in the low-energy limit $M_\Phi^2, M_Z^2, m_b^2 \ll M_{SUSY}^2$, can be obtained by replacing the couplings g_b^Φ in equation (5.2) with the new couplings $\tilde{g}_b^\Phi$ of equation (4.10).

$$\tilde{\Gamma}(\Phi \to b\bar{b}) = \frac{3\mathrm{G_F} M_\Phi}{4\sqrt{2}\pi}\, \overline{m}_b^2(M_\Phi)\, (\tilde{g}_b^\Phi)^2\, [\Delta_{QCD} + \Delta_t^\Phi] \tag{5.6}$$

To get an estimate of the reliability of the resummed decay width in equation (5.6), we want to analyse the difference between the partial decay width $\tilde{\Gamma}$, and the full SUSY-QCD and SUSY-electroweak corrections which are known at NLO [28, 100–102]. At NLO the full SUSY-QCD and SUSY-electroweak corrections can be incorporated into the partial decay widths (5.2) by an additional factor.

$$\Gamma(\Phi \to b\bar{b}) = \Gamma_{QCD}(\Phi \to b\bar{b})\, [1 + C_\Phi] \tag{5.7}$$

Replacing the couplings g_b^Φ with the resummed couplings $\tilde{g}_b^\Phi$ at NLO yields the expression

$$\Gamma(\Phi \to b\bar{b}) = \tilde{\Gamma}(\Phi \to b\bar{b})\, [1 + (C_\Phi - C_\Phi^{LE})] \tag{5.8}$$

The term $(C_\Phi - C_\Phi^{LE})$ is the difference between the full result and the low-energy approximation without resummation at NLO, which furnishes an estimate of the reliability of the corrected decay width in equation (5.6). This difference needs to be small, in order for the approximation to produce reliable results. This will be analysed quantitatively in section 5.2.1. In the following equations, we express C_Φ^{LE} in terms of known quantities.

$$\begin{aligned} \tilde{g}_b^\Phi &= g_b^\Phi \left[1 + \frac{1}{2} C_\Phi^{LE} + \mathcal{O}\left((\alpha_s \mathrm{tg}\beta)^2, (\lambda_t^2 \mathrm{tg}\beta)^2\right)\right] \quad , \quad C_\Phi^{LE} = -2\, \Delta m_b^{(1)}\, \kappa_\Phi \\ \kappa_h &= 1 + \frac{1}{\mathrm{tg}\alpha\, \mathrm{tg}\beta} \quad , \quad \kappa_H = 1 - \frac{\mathrm{tg}\alpha}{\mathrm{tg}\beta} \quad , \quad \kappa_A = 1 + \frac{1}{\mathrm{tg}^2\beta} \end{aligned} \tag{5.9}$$

Here, the $\mathcal{O}\left((\alpha_s \mathrm{tg}\beta)^2, (\lambda_t^2 \mathrm{tg}\beta)^2\right)$ terms stem from the resummation $1/(1+\Delta m_b)$ in the effective couplings $\tilde{g}_b^{\Phi}$ from equation (4.10) and $\Delta m_b^{(1)}$ is given in equation (4.6). Like the QCD corrections, the SUSY-QCD corrections are large for large values of tgβ. Figure 5.2 shows, that the SUSY-QCD corrections reduce the partial decay width, in the chosen scenario, by approximately a factor of 2 compared to the pure QCD corrections. The SUSY-QCD corrected curve in Figure 5.2 is obtained by plotting $\tilde{\Gamma}(\Phi \to b\bar{b})$ as a function of M_A.

5.2 Numerical Results

The numerical analysis of the neutral Higgs boson decays into bottom quark pairs is performed for four different MSSM scenarios [53] as representative cases. In the small α_{eff} scenario the mixing angle α goes to zero. In the maximal mixing scenario the mass of the light Higgs h obtains its maximal value. In the no-mixing scenario the mixing in the stop sector is zero ($X_t = 0$). In the gluophobic scenario the main production cross section for the light Higgs boson at the LHC $gg \to h$ is strongly suppressed.

The parameters of the **small α_{eff} scenario** are:

$$\begin{aligned} &\mathrm{tg}\beta = 30 \quad , \quad M_{\tilde{Q}} = 800 \text{ GeV} \quad , \quad M_{\tilde{g}} = 500 \text{ GeV} \\ &M_2 = 500 \text{ GeV} \quad , \quad A_b = A_t = -1133 \text{ GeV} \quad , \quad \mu = 2000 \text{ GeV} \end{aligned} \tag{5.10}$$

The parameters of the **maximal mixing scenario** are:

$$\begin{aligned} &\mathrm{tg}\beta = 30 \quad , \quad M_{\tilde{Q}} = 1000 \text{ GeV} \quad , \quad M_{\tilde{g}} = 800 \text{ GeV} \\ &M_2 = 200 \text{ GeV} \quad , \quad A_b = A_t = 2456 \text{ GeV} \quad , \quad \mu = 200 \text{ GeV} \end{aligned} \tag{5.11}$$

The parameters of the **no-mixing scenario** are:

$$\begin{aligned} &\mathrm{tg}\beta = 30 \quad , \quad M_{\tilde{Q}} = 2000 \text{ GeV} \quad , \quad M_{\tilde{g}} = 1600 \text{ GeV} \\ &M_2 = 200 \text{ GeV} \quad , \quad A_b = A_t = 7 \text{ GeV} \quad , \quad \mu = 200 \text{ GeV} \end{aligned} \tag{5.12}$$

The parameters of the **gluophobic scenario** are:

$$\begin{aligned} &\mathrm{tg}\beta = 30 \quad , \quad M_{\tilde{Q}} = 350 \text{ GeV} \quad , \quad M_{\tilde{g}} = 500 \text{ GeV} \\ &M_2 = 300 \text{ GeV} \quad , \quad A_b = A_t = -760 \text{ GeV} \quad , \quad \mu = 300 \text{ GeV} \end{aligned} \tag{5.13}$$

We use the RG-improved two-loop expressions of reference [117]. The bottom quark pole mass has been chosen to be $m_b = 4.60$ GeV, which corresponds to a $\overline{MS}$ mass $\overline{m}_b(\overline{m}_b) = 4.26$ GeV. The strong coupling constant has been normalized to $\alpha_s(M_Z) = 0.118$.

5.2.1 Validity of the Low-Energy Approximation

The **resummation effects** discussed in the previous section have been derived in the low-energy limit $M_\Phi^2, M_Z^2, m_b^2 \ll M_{SUSY}^2$. The question arises, how reliable this approximation works in phenomenological applications. In particular, the magnitude of

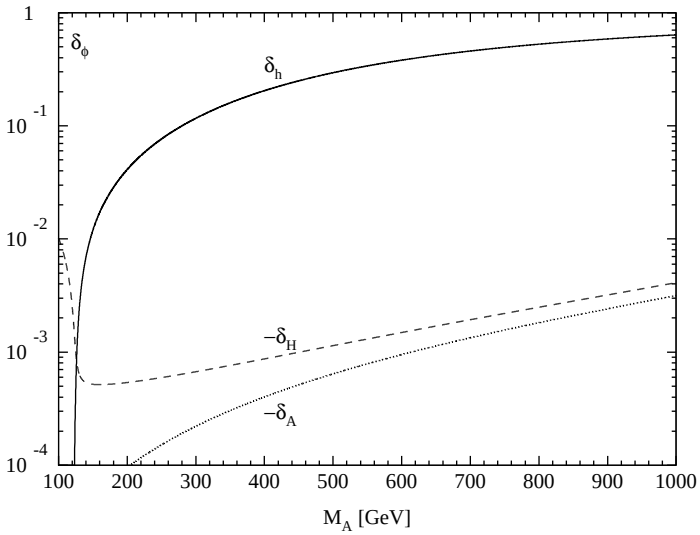

Figure 5.3: Relative deviations δ_Φ of the approximate low-energy one-loop result from the full NLO expression as a function of the pseudoscalar mass M_A in the small α_{eff} scenario for all neutral Higgs bosons. For the heavy scalar and pseudoscalar Higgs bosons the deviations are negative. The values shown have to be changed in sign.

$\mathcal{O}\left(M_\Phi^2/M_{SUSY}^2, M_Z^2/M_{SUSY}^2, m_b^2/M_{SUSY}^2\right)$ terms matters for sizable masses of the low-energy particles. This can be tested explicitly by comparing the approximate results of equation (5.9) with the full one-loop result. A typical example is depicted in Figure 5.3 for the small α_{eff} scenario, where the relative difference between the full and approximate one-loop contributions [see equation (5.8)]

$$\delta_\Phi = \frac{C_\Phi - C_\Phi^{LE}}{C_\Phi} \tag{5.14}$$

is shown for all neutral Higgs particles as a function of the pseudoscalar Higgs mass M_A. It is clearly visible that the approximation turns out to be sufficient for the heavy neutral Higgs particles H, A, but fails for the light scalar Higgs boson h in the decoupling limit $M_A \gg M_Z$ (discussed in section 2.2). However, in the decoupling limit the size of the approximate SUSY-QCD corrections strongly decreases, since $\mathrm{tg}\alpha \to -1/\mathrm{tg}\beta$ and thus

$$\tilde{g}_b^h = \frac{g_b^h}{1+\Delta m_b}\left(1 - \frac{\Delta m_b}{\mathrm{tg}\alpha\ \mathrm{tg}\beta}\right) \to g_b^h \tag{5.15}$$

so that the SUSY-QCD corrections become negligible. Due to this behaviour the low-energy approximation is sufficient for most phenomenological applications. This also explains the failure of the approximation in this case: the large non-decoupling contributions from Δm_b cancel to a large extent in the lightest Higgs boson couplings, leaving a small remainder of the same order as the non-leading contributions. On the other hand, this cancellation does not occur for the heavy Higgs bosons, and the effective Lagrangian approach yields a good approximation.

5.2.2 Novel NNLO Results

There are two basic sources of systematic uncertainties originating from the SUSY-QCD contributions:

(i) The MSSM masses and couplings involved in the SUSY-QCD and SUSY-electroweak corrections will only be known with a sizeable uncertainty at the LHC, while future e^+e^- linear colliders in the 500 GeV to 1 TeV range will enable precision measurements of the SUSY masses and couplings. These errors in the input parameters generate systematic uncertainties for the prediction of the partial decay widths.

(ii) Due to missing higher order results the scale dependence of the strong coupling constant α_s will not be compensated. The scale variation yields an estimate of the purely theoretical SUSY-QCD and SUSY-electroweak uncertainty.

The **scale dependences** of the corrections Δm_b^{QCD} and Δm_b^{EW} are displayed in Figure 5.4, Figure 5.5, Figure 5.6 and Figure 5.7 at the one-loop and two-loop order. The central scale of the SUSY-QCD part Δm_b^{QCD} and the SUSY-electroweak part Δm_b^{EW} is chosen as the average of the SUSY-particle masses at one-loop, i.e.

$$\mu_0^{QCD} = \frac{(M_{\tilde{b}_1} + M_{\tilde{b}_2} + M_{\tilde{g}})}{3} \quad , \quad \mu_0^{EW} = \frac{(M_{\tilde{t}_1} + M_{\tilde{t}_2} + \mu)}{3} \tag{5.16}$$

We obtain a significant reduction of the scale dependence at two-loop order and thus a large reduction of the theoretical uncertainty. Moreover a broad maximum/minimum develops at scales of about 1/4 to 1/3 of the chosen central scale in contrast to the monotonous scale dependence at one-loop order. In the small α_{eff} scenario the SUSY-QCD corrections are large and positive, while the SUSY-electroweak corrections are of moderate negative size. The two-loop corrections amount to $\mathcal{O}(10\%)$ in Δm_b^{QCD} and a few per cent in Δm_b^{EW} for the central scale choices. However, the sign and size of the corrections depends on the chosen MSSM scenario. For the maximal mixing scenario and the no-mixing scenario the SUSY-electroweak corrections are positive.

The results for the **partial decay widths** of equation (5.6) are shown in Figure 5.8, Figure 5.9, Figure 5.10 and Figure 5.11 for the four different scenarios. These results include the QCD corrections at three-loop order of equation (5.2) and the resummed couplings $\tilde{g}_b^{\Phi}$ of equation (4.10) at one-loop order (dashed blue curves) and at two-loop order (full red curves). The bands at one-loop order and two-loop order are obtained by varying the renormalisation scale between 1/2 and 2 times the corresponding central scale in (5.16) of the SUSY-QCD and SUSY-electroweak parts. It can be inferred from these figures, that the uncertainties at one-loop are typically of order $\mathcal{O}(10\%)$ but are reduced to the per-cent level at two-loop order. Since the included QCD corrections are of three-loop order, they are practically independent of the renormalisation scale and do not contribute to these uncertainties. The null of the partial decay width of the light scalar h at about $M_A \approx 150$ GeV is due to a null of the angle α, which provokes a change of sign in the Yukawa coupling $g_b^h = -\sin\alpha/\cos\beta$.

The uncertainties in the partial decay widths translate into systematic errors in the corresponding **branching ratios** of the neutral MSSM Higgs bosons. These errors cancel to a large extend in the branching ratio $BR(\Phi \to b\bar{b})$ due to its dominance, but are

sizable in the systematic uncertainties of the non-leading branching ratios at one-loop order. The branching ratios of the two dominant decay modes into $b\bar{b}$ and $\tau^+\tau^-$ pairs are depicted in Figure 5.12, Figure 5.13, Figure 5.14 and Figure 5.15 for the four different scenarios. In Figure 5.16 the branching ratios of the decay modes into $b\bar{b}$, $\tau^+\tau^-$, $t\bar{t}$ and gg pairs are shown for the small α_{eff} scenario. These Figures have been obtained with the program HDECAY [29, 118] after including the corrections obtained in this work. As in the case of the partial decay widths, the bands at one-loop order (dashed blue curves) and two-loop order (full red curves) are obtained by varying the renormalisation scale between 1/2 and 2 times the corresponding central scale in (5.16) of the SUSY-QCD and SUSY-electroweak parts. The uncertainties of the branching ratios reduce from $\mathcal{O}(10\%)$ at one-loop order to the per-cent level at two-loop order. The per-cent accuracy now matches the expected experimental accuracies at a future linear e^+e^- collider.

Since we have determined the effective resummed Yukawa coupling at two-loop order the results will also affect all other processes which are significantly induced by bottom Yukawa couplings, as e.g. MSSM Higgs radiation off bottom quarks at e^+e^- colliders and hadron colliders. The two-loop corrections can easily be included in the corresponding numerical programs.

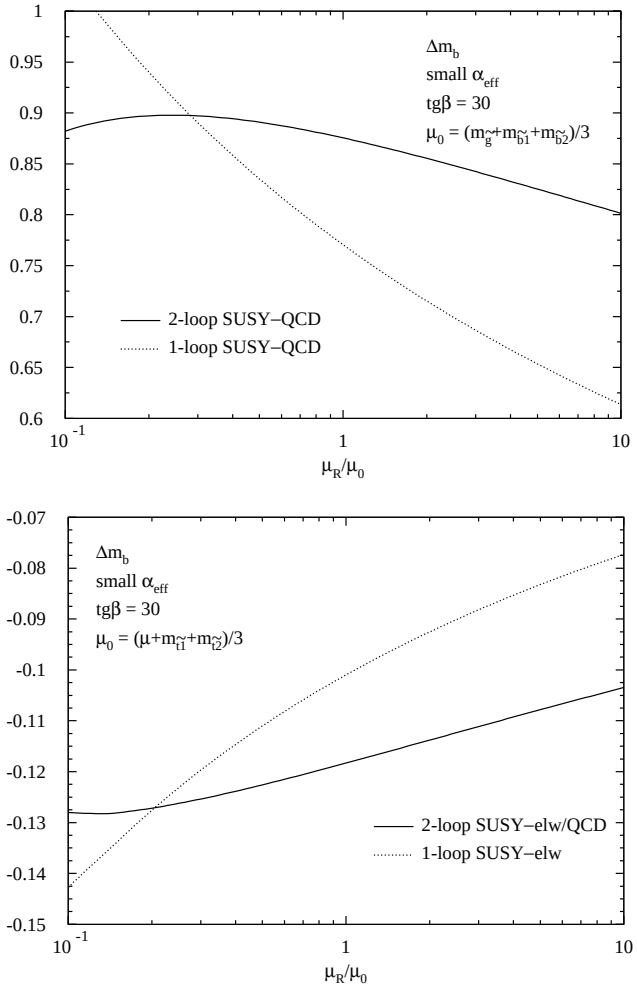

Figure 5.4: Scale dependence of the SUSY-QCD correction Δm_b^{QCD} and the SUSY-electroweak correction Δm_b^{EW} at one-loop and two-loop order in the small α_{eff} scenario.

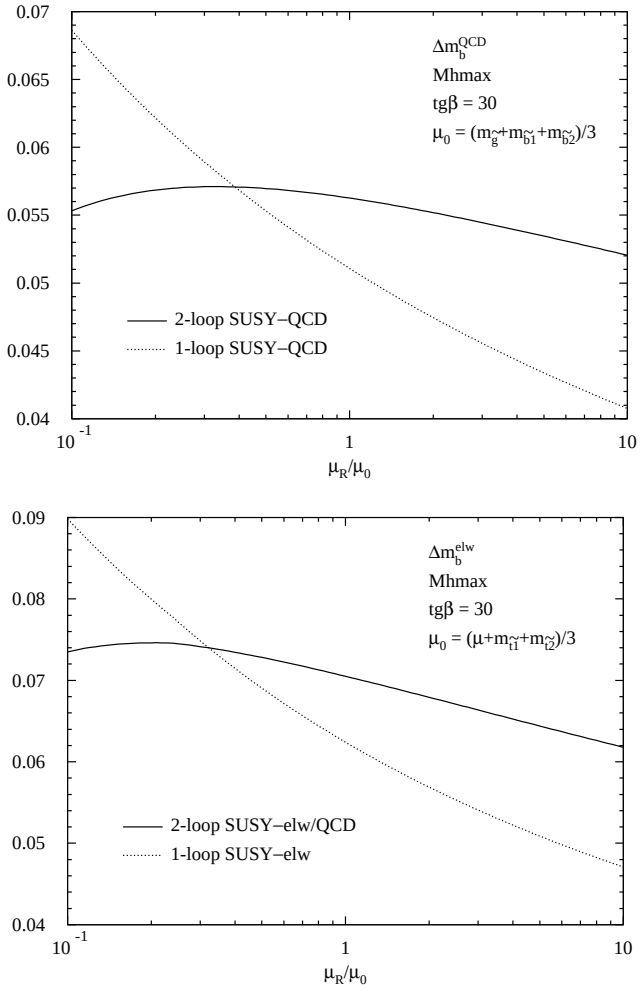

Figure 5.5: Scale dependence of the SUSY-QCD correction Δm_b^{QCD} and the SUSY-electroweak correction Δm_b^{EW} at one-loop and two-loop order in the maximal mixing scenario.

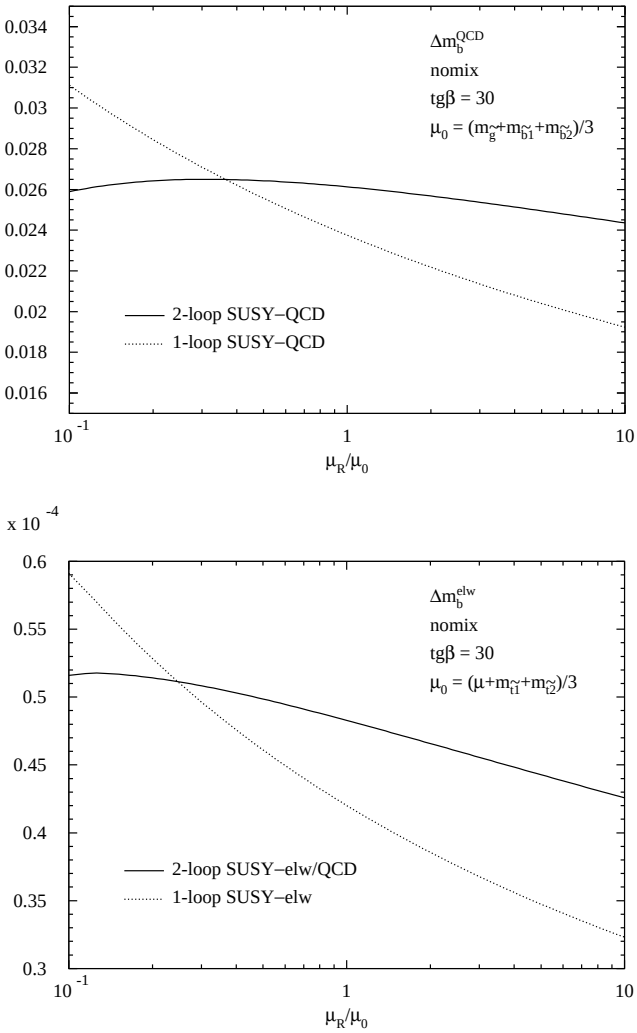

Figure 5.6: Scale dependence of the SUSY-QCD correction Δm_b^{QCD} and the SUSY-electroweak correction Δm_b^{EW} at one-loop and two-loop order in the no-mixing scenario.

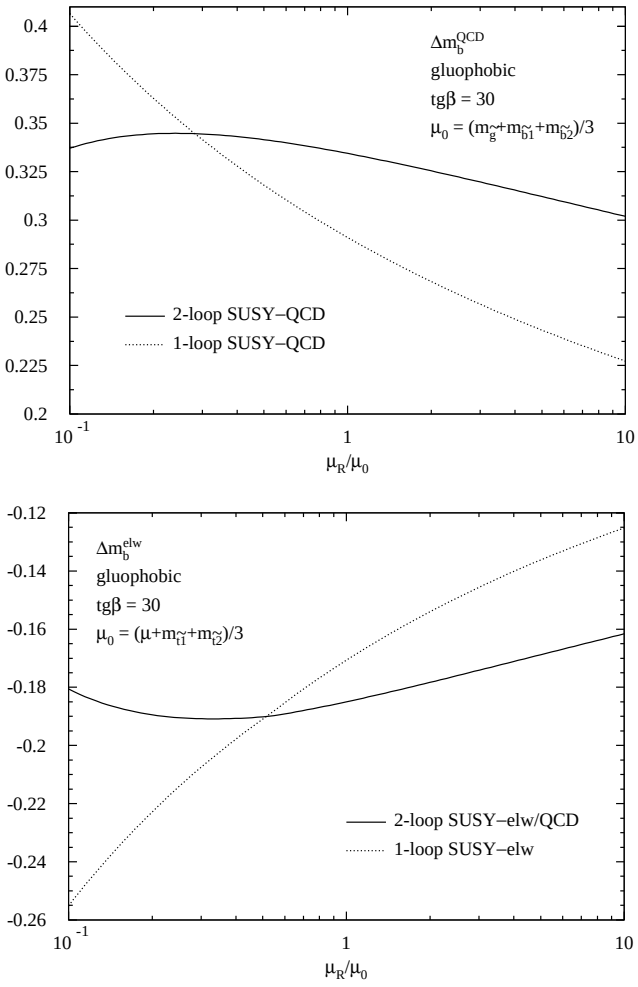

Figure 5.7: Scale dependence of the SUSY-QCD correction Δm_b^{QCD} and the SUSY-electroweak correction Δm_b^{EW} at one-loop and two-loop order in the gluophobic scenario.

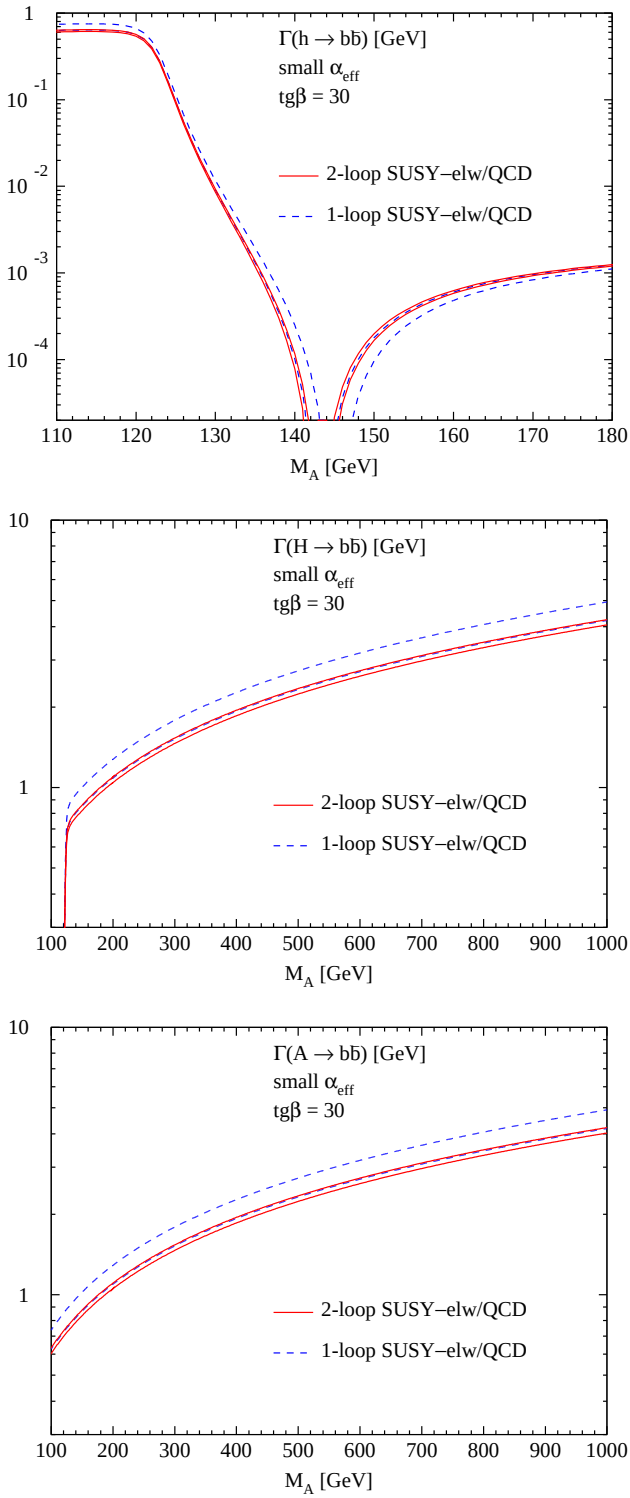

Figure 5.8: Partial decay widths $\Gamma(\Phi \to b\bar{b})$ of the light scalar h, the heavy scalar H and the pseudoscalar Higgs boson A in the small α_{eff} scenario. The dashed blue bands indicate the scale dependence at one-loop order and the full red bands at two-loop order by varying the renormalisation scale between 1/2 and 2 times the central scale given by an average of the SUSY particle masses.

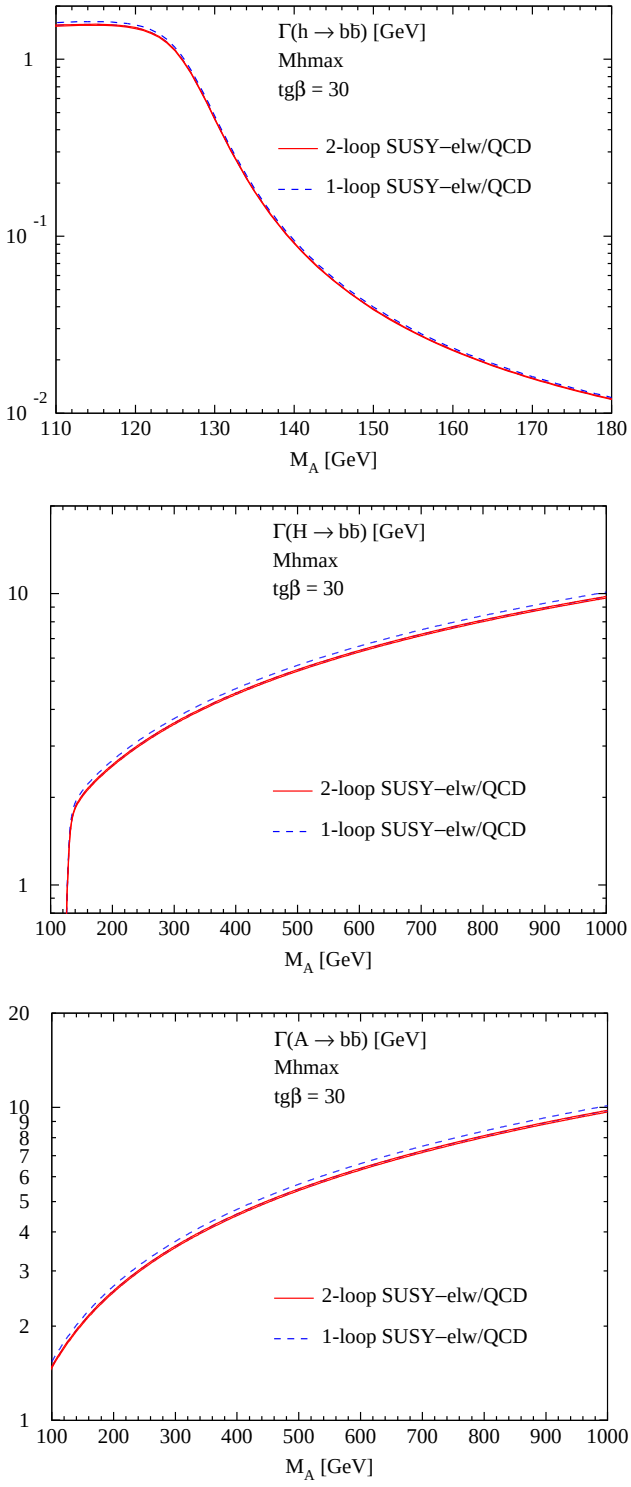

Figure 5.9: Partial decay widths $\Gamma(\Phi \to b\bar{b})$ of the light scalar h, the heavy scalar H and the pseudoscalar Higgs boson A in the maximal mixing scenario. The dashed blue bands indicate the scale dependence at one-loop order and the full red bands at two-loop order by varying the renormalisation scale between 1/2 and 2 times the central scale given by an average of the SUSY particle masses.

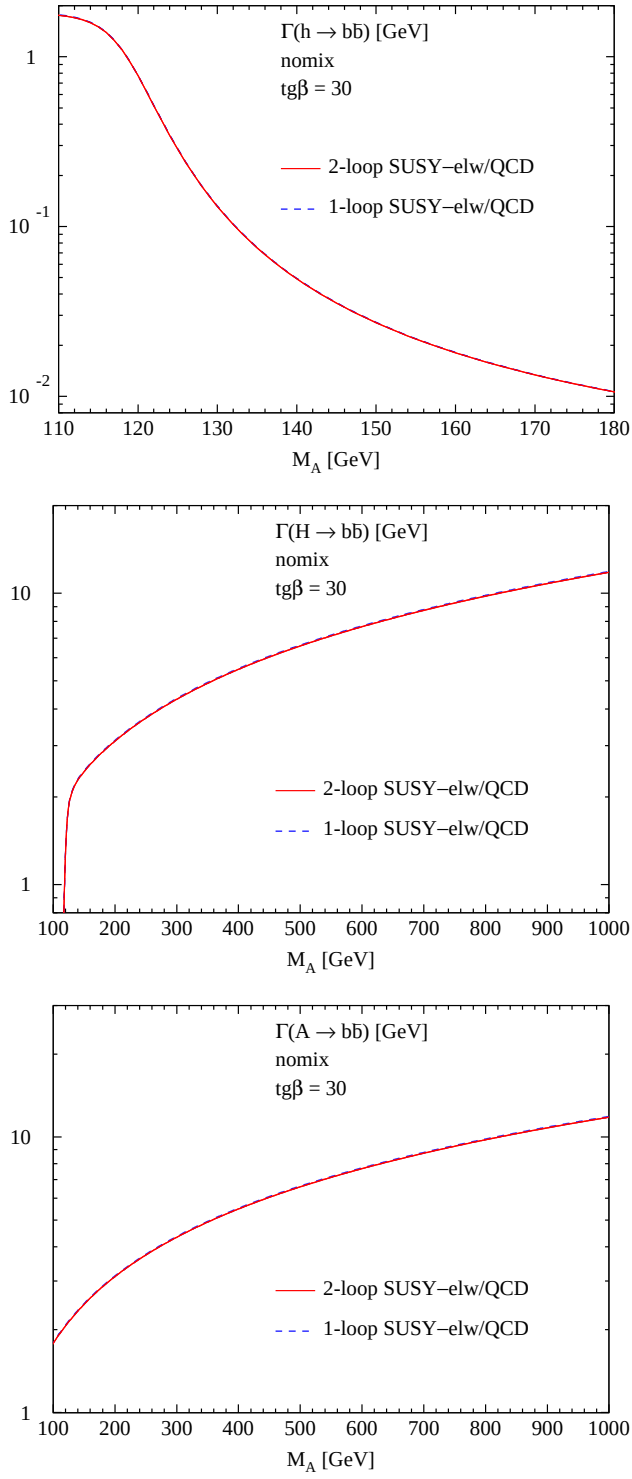

Figure 5.10: Partial decay widths $\Gamma(\Phi \to b\bar{b})$ of the light scalar h, the heavy scalar H and the pseudoscalar Higgs boson A in the no-mixing scenario. The dashed blue bands indicate the scale dependence at one-loop order and the full red bands at two-loop order by varying the renormalisation scale between 1/2 and 2 times the central scale given by an average of the SUSY particle masses.

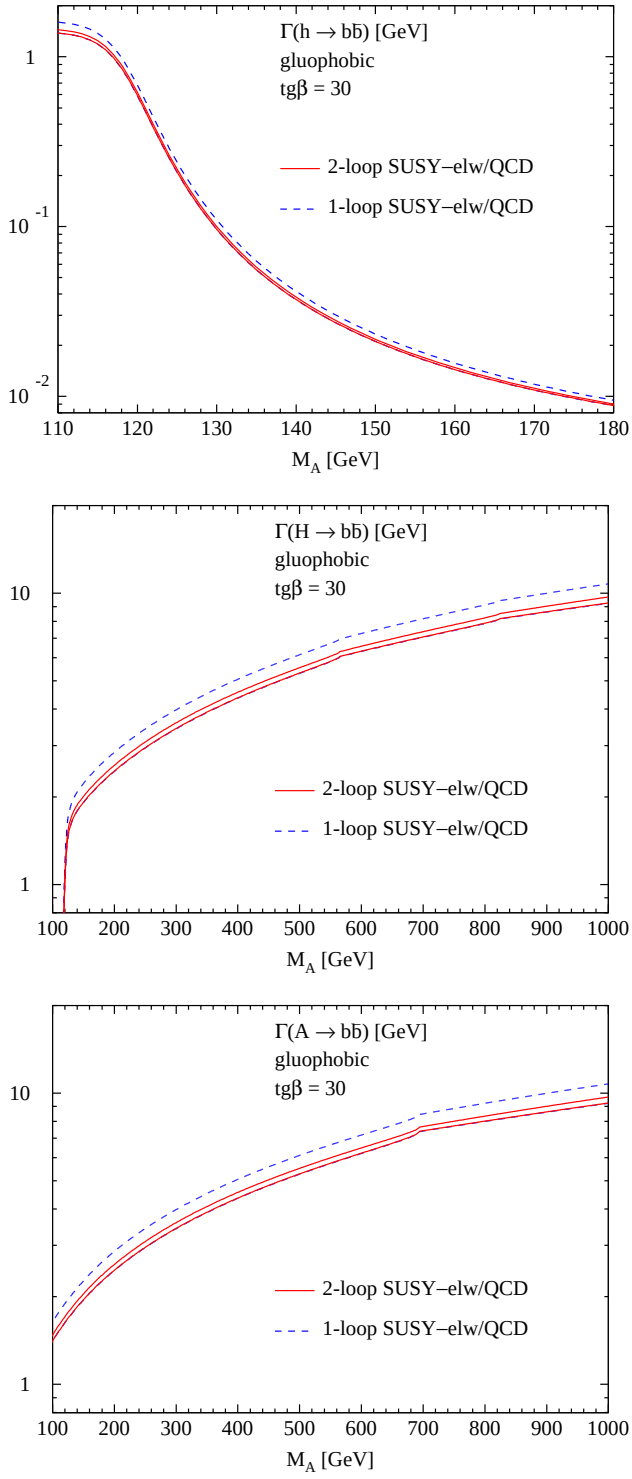

Figure 5.11: Partial decay widths $\Gamma(\Phi \to b\bar{b})$ of the light scalar h, the heavy scalar H and the pseudoscalar Higgs boson A in the gluophobic scenario. The dashed blue bands indicate the scale dependence at one-loop order and the full red bands at two-loop order by varying the renormalisation scale between 1/2 and 2 times the central scale given by an average of the SUSY particle masses.

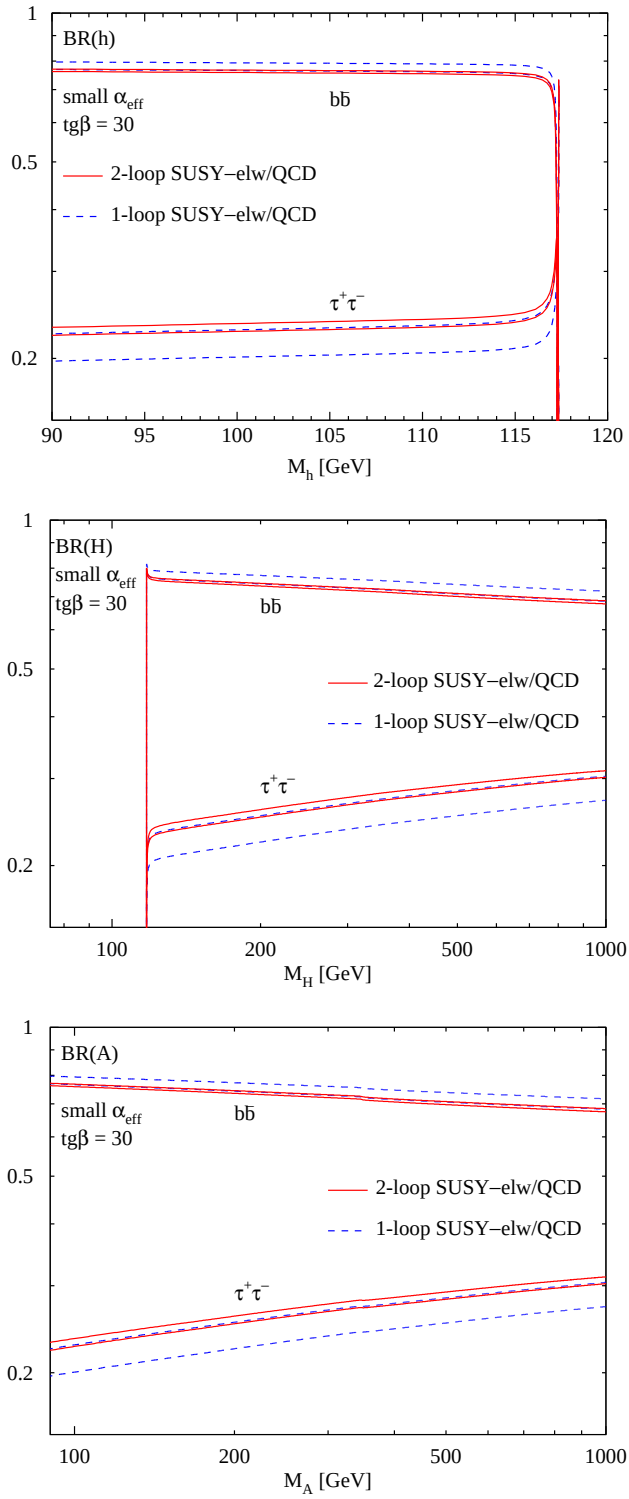

Figure 5.12: Branching ratios of the light scalar h, the heavy scalar H and the pseudoscalar A Higgs bosons to $b\bar{b}$ and $\tau^+\tau^-$ in the small α_{eff} scenario. The dashed blue bands indicate the scale dependence at one-loop order and the full red bands at two-loop order by varying the renormalisation scale between 1/2 and 2 times the central scale given by an average of the SUSY particle masses.

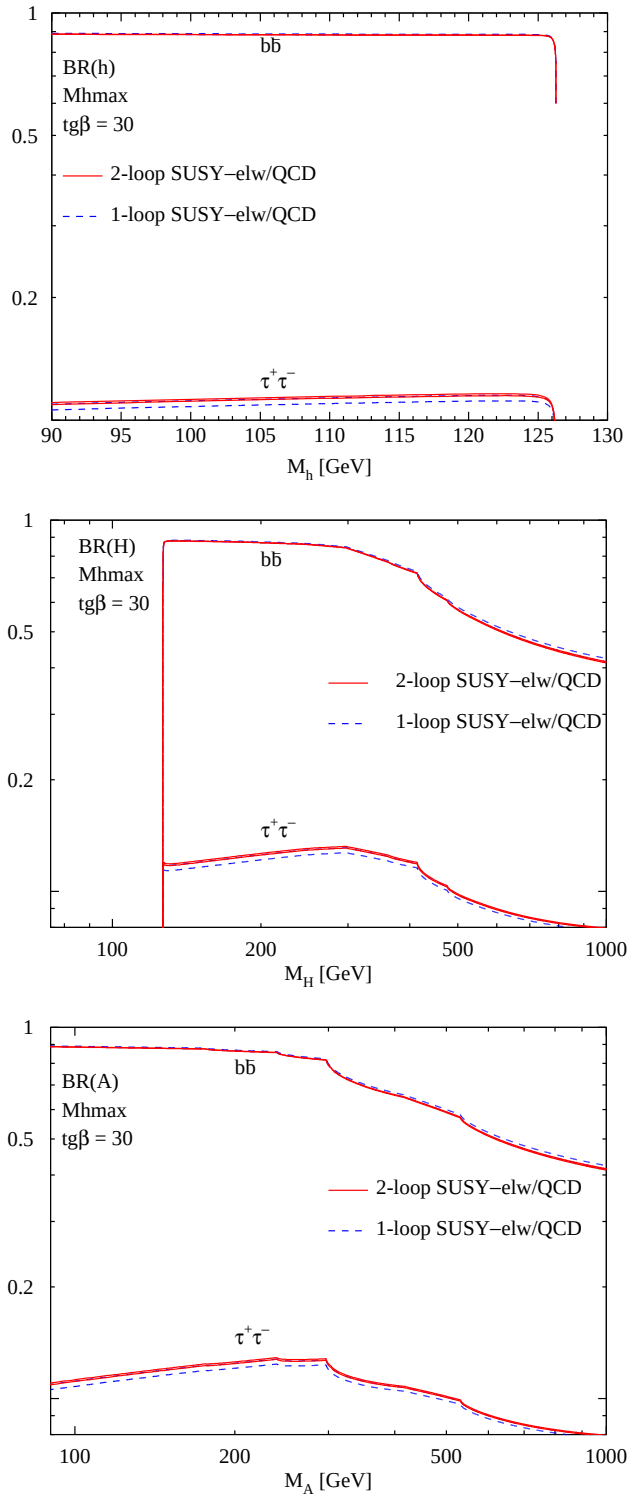

Figure 5.13: Branching ratios of the light scalar h, the heavy scalar H and the pseudoscalar A Higgs bosons to $b\bar{b}$ and $\tau^+\tau^-$ in the maximal mixing scenario. The dashed blue bands indicate the scale dependence at one-loop order and the full red bands at two-loop order by varying the renormalisation scale between 1/2 and 2 times the central scale given by an average of the SUSY particle masses.

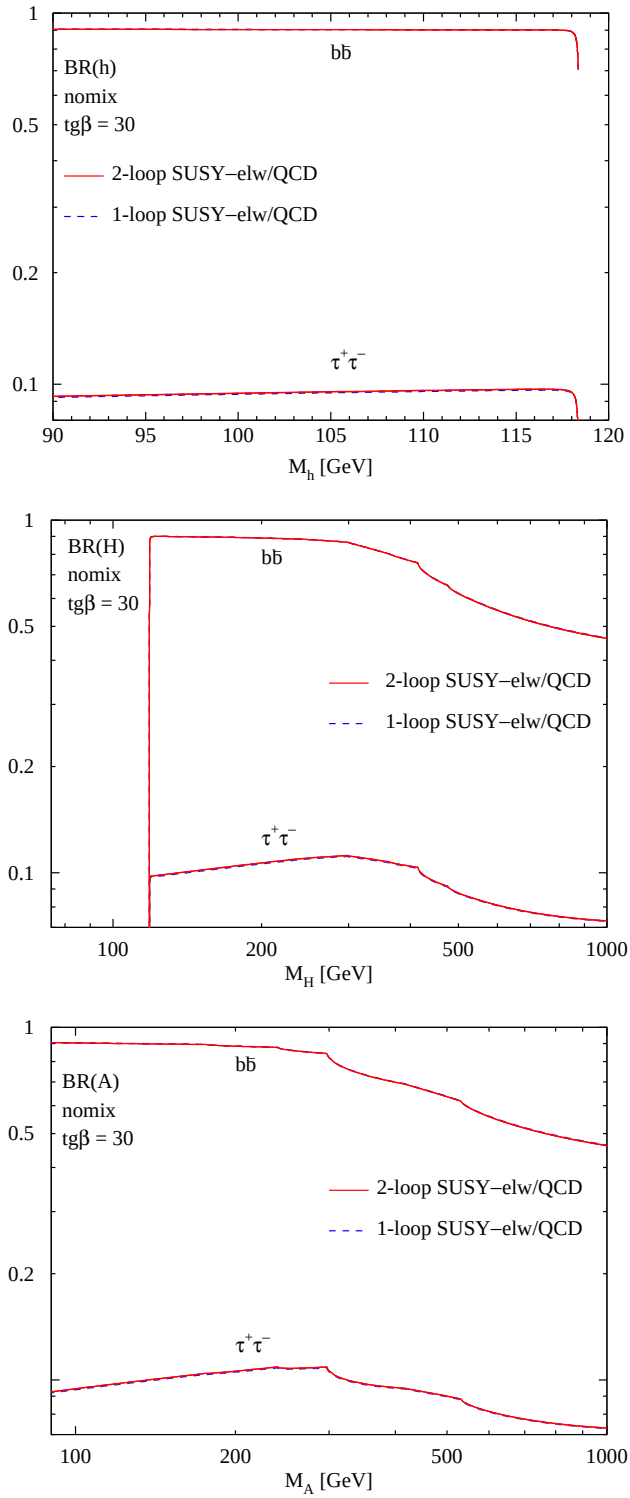

Figure 5.14: Branching ratios of the light scalar h, the heavy scalar H and the pseudoscalar A Higgs bosons to $b\bar{b}$ and $\tau^+\tau^-$ in the no-mixing scenario. The dashed blue bands indicate the scale dependence at one-loop order and the full red bands at two-loop order by varying the renormalisation scale between 1/2 and 2 times the central scale given by an average of the SUSY particle masses.

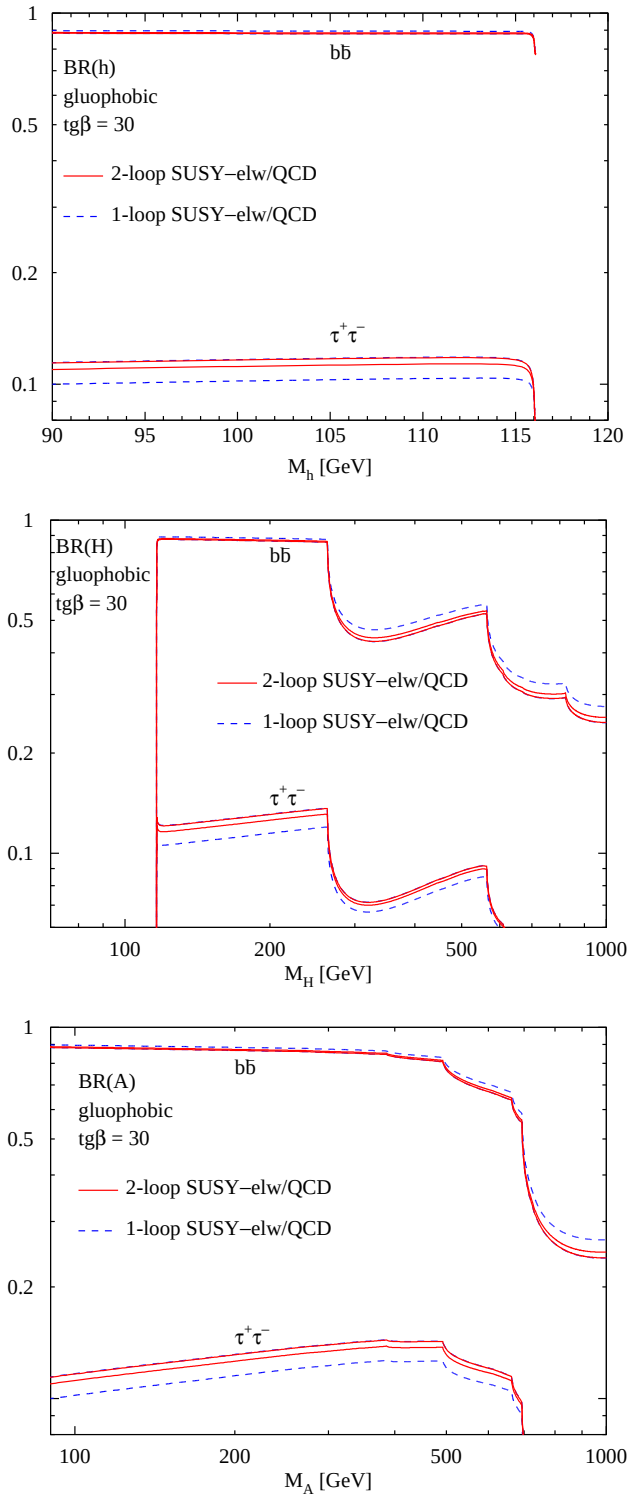

Figure 5.15: Branching ratios of the light scalar h, the heavy scalar H and the pseudoscalar A Higgs bosons to $b\bar{b}$ and $\tau^+\tau^-$ in the gluophobic scenario. The dashed blue bands indicate the scale dependence at one-loop order and the full red bands at two-loop order by varying the renormalisation scale between 1/2 and 2 times the central scale given by an average of the SUSY particle masses.

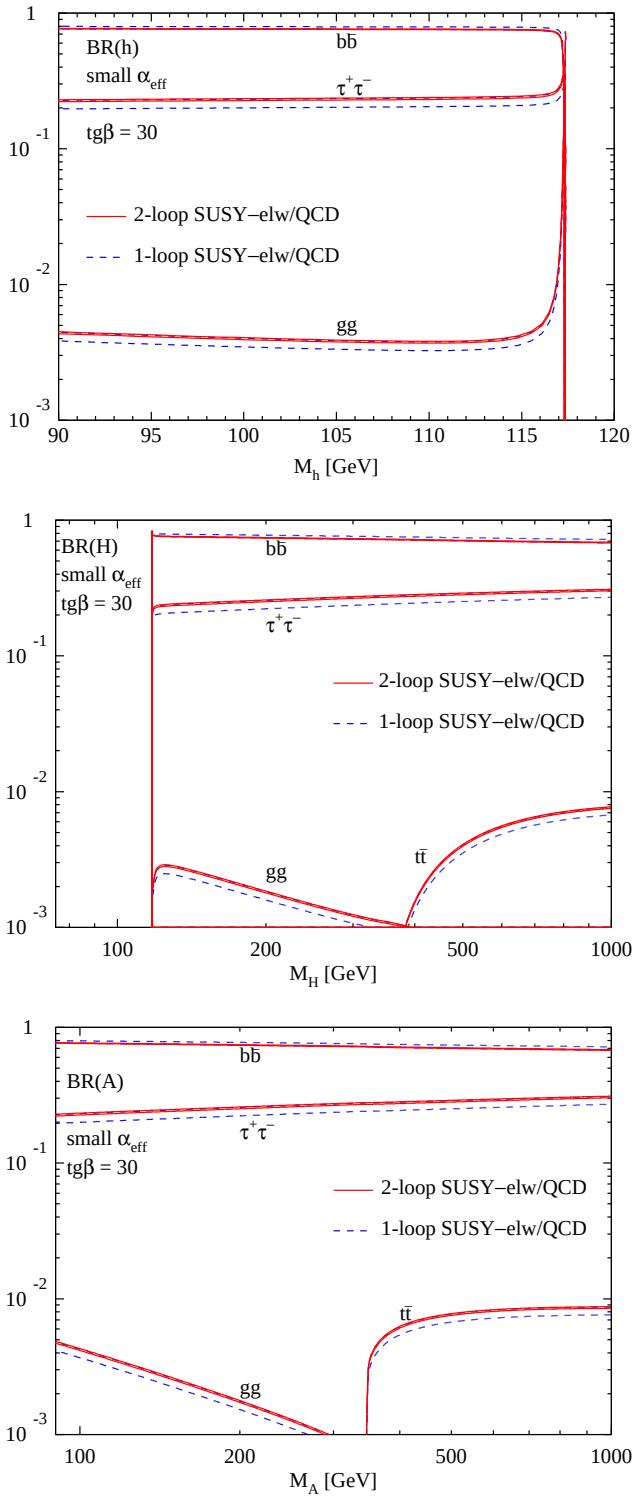

Figure 5.16: Branching ratios of the light scalar h, the heavy scalar H and the pseudoscalar A Higgs bosons in the small α_{eff} scenario with suppressed channels. The dashed blue bands indicate the scale dependence at one-loop order and the full red bands at two-loop order by varying the renormalisation scale between 1/2 and 2 times the central scale given by an average of the SUSY particle masses.

Chapter 6

Summary

The aim of this work was the determination of the NNLO order corrections to the effective bottom quark Yukawa couplings within supersymmetric theories for large values of tgβ, where the theoretical uncertainties were still sizable. The leading part of these SUSY-QCD and top-induced SUSY-electroweak corrections originates from factorisable contributions due to virtual squark, gluino and Higgsino exchange, which are absorbed in effective Yukawa couplings in a universal way. We have calculated the SUSY-QCD corrections to this leading part.
The framework of our calculation was an effective Lagrangian approach which is derived from a connection between the bottom-quark self-energy and the Yukawa coupling by means of low-energy theorems [85, 86] which have been proven to all orders in perturbation theory [119]. These low-energy theorems originate from the relation between matrix elements with and without scalar or pseudoscalar operator insertions at vanishing external momentum. They provide the first term of an expansion in small external momenta, which corresponds to a heavy mass expansion in the inverse virtual SUSY-particle masses. The procedure led to the simplification, that the bottom quark self-energy had to be computed at NNLO. We showed explicitly that the pseudoscalar part of the self-energy vanishes, as was to be expected and that the vectorial part and the axial vectorial part are suppressed. Therefore only the scalar part of the self-energy contributed to the calculation. In order to simplify the calculation, the scalar part of the self-energy was split into several parts, each proportional to another colour factor. After tensor reductions and heavy mass expansions, the occurring two-loop integrals could be expressed in terms of known master one-loop and two-loop integrals. Special attention had to be paid to the proper renormalisation, after connecting an external Higgs boson to the self-energy by means of the corresponding low-energy theorem. All occurring masses and the top trilinear coupling were renormalised in the on-shell scheme, whereas the strong coupling constant and the top Yukawa coupling were renormalised in the Collins-Wilczek-Zee scheme [92] with 5 active flavours. In this hybrid scheme, the $\overline{MS}$-scheme is used to renormalise the light flavours and the momentum subtraction scheme at zero momentum transfer is used to renormalise the heavy flavours, in order to decouple the heavy flavours from the renormalisation scale dependence of the couplings. As a next step, the results had to be incorporated in the resummation of the bottom Yukawa coupling. This required a proper proof that all leading and subleading contributions can be controlled by the obtained resummed effective Yukawa coupling up to all orders, and

is based on the power behaviour of the contributing multi-loop diagrams in the inverse heavy SUSY-particle masses [28, 100]. As a final step, the obtained results had to be included into existing programs to compute partial decay widths and branching ratios [29, 118].

In summary, the significant scale dependence of $\mathcal{O}(10\%)$ of the NLO predictions for processes involving the bottom quark Yukawa couplings of supersymmetric Higgs bosons required the inclusion of NNLO corrections. For the corrected Yukawa couplings, we find a reduction of the scale dependence to the per-cent level after the inclusion of our novel NNLO results. The improved NNLO predictions for the bottom Yukawa couplings can thus be taken as a base for experimental analyses at the Tevatron and the LHC as well as the ILC [120].

Appendix A

Integrals

In this Appendix all used one-loop and two-loop integrals are specified. Appendix A.1 lists the one-loop integrals, Appendix A.2 the two-loop integrals and Appendix A.3 shows some useful reductions to known integrals. All integrals are dimensionally regularised in $n = 4 - 2\epsilon$ space-time dimensions.

A.1 Scalar 1-loop Integrals

Definition (external momentum p and $n = 4 - 2\epsilon$)

$$A_0(m) = \int \frac{d^n k}{(2\pi)^n} \frac{1}{k^2 - m^2} \tag{A.1}$$

$$B_0(p; m_1, m_2) = \int \frac{d^n k}{(2\pi)^n} \frac{1}{k^2 - m_1^2} \frac{1}{(k+p)^2 - m_2^2} \tag{A.2}$$

$$C_0(p_1, p_2; m_1, m_2, m_3) = \int \frac{d^n k}{(2\pi)^n} \frac{1}{k^2 - m_1^2} \frac{1}{(k+p_1)^2 - m_2^2} \frac{1}{(k+p_2)^2 - m_3^2} \tag{A.3}$$

Integral $A_0(m)$

$$A_0(m) = i \frac{1}{(4\pi)^2} \Gamma(1+\epsilon) \left(\frac{4\pi}{m^2}\right)^{\epsilon} m^2 \left\{ \frac{1}{\epsilon} + 1 + \epsilon + \mathcal{O}\left(\epsilon^2\right) \right\} \tag{A.4}$$

$$A_0(0) = 0 \tag{A.5}$$

Integral $B_0(p; 0, m)$

$$B_0(p; 0, m) = i \frac{1}{(4\pi)^2} \Gamma(1+\epsilon) \left(\frac{4\pi}{m^2}\right)^{\epsilon} \left\{ \frac{1}{\epsilon} + \left[2 + \frac{1-\rho}{\rho} \log(1-\rho) \right] \right.$$
$$\left. + \epsilon \left[4 + \frac{1-\rho}{\rho} \left(Li_2\left(\frac{\rho}{\rho - 1}\right) - \frac{1}{2} \log^2(1-\rho) + 2 \log(1-\rho) \right) \right] + \mathcal{O}\left(\epsilon^2\right) \right\} \tag{A.6}$$

with $\rho = \frac{p^2}{m^2}$.

Integral $B_0(m;0,m)$

$$B_0(m;0,m) = i\,\frac{1}{(4\pi)^2}\,\Gamma(1+\epsilon)\left(\frac{4\pi}{m^2}\right)^{\epsilon}\left\{\frac{1}{\epsilon}+2+4\epsilon+\mathcal{O}\left(\epsilon^2\right)\right\} \tag{A.7}$$

Integral $B_0(0;m,m)$

$$B_0(0;m,m) = i\,\frac{1}{(4\pi)^2}\,\Gamma(1+\epsilon)\left(\frac{4\pi}{m^2}\right)^{\epsilon}\left\{\frac{1}{\epsilon}+\mathcal{O}\left(\epsilon^2\right)\right\} \tag{A.8}$$

Integral $B_0(p;m_1,m_2)$

$$\begin{aligned}
B_0(p;m_1,m_2) &= i\,\frac{1}{(4\pi)^2}\,\Gamma(1+\epsilon)\left(\frac{4\pi}{m_1^2}\right)^{\epsilon}\left\{\;\frac{1}{\epsilon}\right.\\
&+\left[2-\log\left(\frac{m_2^2}{m_1^2}\right)+\alpha_+\log\left(1-\frac{1}{\alpha_+}\right)+\alpha_-\log\left(1-\frac{1}{\alpha_-}\right)\right]\\
&+\frac{\epsilon}{2}\left[4-(\alpha_+-1)\left(\log\left(1-\frac{1}{\alpha_+}\right)-2\right)\log\left(1-\frac{1}{\alpha_+}\right)\right.\\
&-(\alpha_--1)\left(\log\left(1-\frac{1}{\alpha_-}\right)-2\right)\log\left(1-\frac{1}{\alpha_-}\right)+2\left((\alpha_+-1)\log\left(1-\frac{1}{\alpha_+}\right)\right.\\
&-(\alpha_+-1)\log\left(1-\frac{1}{\alpha_+}\right)\log\left(1-\frac{1}{\alpha_-}\right)+(\alpha_--1)\log\left(1-\frac{1}{\alpha_-}\right)\\
&+(\alpha_+-\alpha_-)\left(\log\left(1-\frac{1}{\alpha_-}\right)\log\left(1-\frac{\alpha_-}{\alpha_+}\right)\right.\\
&\left.\left.\left.\left.+Li_2\left(-\frac{\alpha_-}{\alpha_+-\alpha_-}\right)-Li_2\left(-\frac{\alpha_--1}{\alpha_+-\alpha_-}\right)\right)+2\right)\right]+\mathcal{O}\left(\epsilon^2\right)\left.\right\}
\end{aligned} \tag{A.9}$$

with

$$\alpha_\pm = \frac{p^2+m_1^2-m_2^2}{2p^2}\;\pm\;\sqrt{\left(\frac{p^2+m_1^2-m_2^2}{2p^2}\right)^2-\frac{m_1^2}{p^2}} \tag{A.10}$$

Integral $C_0(0,0;m_1,m_2,m_3)$

$$\begin{aligned}
C_0(0,0;m_1,m_2,m_3) = i\,\frac{1}{(4\pi)^2}\,\Gamma(1+\epsilon)\left(\frac{4\pi}{m_3^2}\right)^{\epsilon}\Big\{&-I(m_1^2,m_2^2,m_3^2)\\
&-\epsilon\left[I(m_1^2,m_2^2,m_3^2)+J(m_1^2,m_2^2,m_3^2)\right]+\mathcal{O}\left(\epsilon^2\right)\Big\}
\end{aligned} \tag{A.11}$$

with

$$I(a,b,c) = -\frac{ab\log\frac{a}{b}+bc\log\frac{b}{c}+ca\log\frac{c}{a}}{(a-b)(b-c)(c-a)} \tag{A.12}$$

$$J(a,b,c) = -\frac{1}{2}\,\frac{(ac-ab)\log^2\frac{a}{c}-(bc-ba)\log^2\frac{b}{c}}{(a-b)(b-c)(c-a)} \tag{A.13}$$

A.2 Scalar 2-loop Integrals

Definition (external momentum p and $n = 4 - 2\epsilon$)

$$T_{12345}(m_1, m_2, m_3, m_4, m_5) = \int \frac{d^n k}{(2\pi)^n} \frac{d^n q}{(2\pi)^n} \frac{1}{P_1\, P_2\, P_3\, P_4\, P_5} \tag{A.14}$$

The terms in the denominator are defined as

$$\begin{aligned} &P_1 = (k^2 - m_1^2)\ ,\ P_2 = ((k+p)^2 - m_2^2)\ ,\ P_3 = ((k-q)^2 - m_3^2) \\ &P_4 = (q^2 - m_4^2)\ ,\ P_5 = ((q+p)^2 - m_5^2) \end{aligned} \tag{A.15}$$

Integral $T_{134}(m_1, m_2, m_3)$

$$\begin{aligned} T_{134}(m_1, m_2, m_3) = &\frac{1}{(4\pi)^4}\, \Gamma^2(1+\epsilon)\, \left(\frac{4\pi}{m_3^2}\right)^{2\epsilon} \frac{1}{(1-\epsilon)(1-2\epsilon)}\, \frac{m_3^2}{2} \\ \Bigg\{ &-\frac{1}{\epsilon^2}\left(1 + \frac{m_1^2}{m_3^2} + \frac{m_2^2}{m_3^2}\right) + \frac{2}{\epsilon}\left(\frac{m_1^2}{m_3^2}\log\left(\frac{m_1^2}{m_3^2}\right) + \frac{m_2^2}{m_3^2}\log\left(\frac{m_2^2}{m_3^2}\right)\right) \\ &- \frac{m_1^2}{m_3^2}\log^2\left(\frac{m_1^2}{m_3^2}\right) - \frac{m_2^2}{m_3^2}\log^2\left(\frac{m_2^2}{m_3^2}\right) + \left(1 - \frac{m_1^2}{m_3^2} - \frac{m_2^2}{m_3^2}\right)\log\left(\frac{m_1^2}{m_3^2}\right)\log\left(\frac{m_2^2}{m_3^2}\right) \\ &- \lambda\left(\frac{m_1^2}{m_3^2}, \frac{m_2^2}{m_3^2}\right)\phi\left(\frac{m_1^2}{m_3^2}, \frac{m_2^2}{m_3^2}\right) \Bigg\} \end{aligned} \tag{A.16}$$

with

$$\begin{aligned} \lambda(x,y) = &\ \sqrt{(1-x-y)^2 - 4xy} \\ \phi(x,y) = &\ 2\,\log\left(\frac{1}{2}(1+x-y-\lambda(x,y))\right)\log\left(\frac{1}{2}(1-x+y-\lambda(x,y))\right) \\ &- 2\,Li_2\left(\frac{1}{2}(1+x-y-\lambda(x,y))\right) - 2Li_2\left(\frac{1}{2}(1-x+y-\lambda(x,y))\right) \\ &- \log(x)\log(y) + \frac{1}{3}\pi^2 \end{aligned} \tag{A.17}$$

Integral $T_{134}(0, m_1, m_2)$

$$\begin{aligned} T_{134}(0, m_1, m_2) = &\frac{1}{(4\pi)^4}\, \Gamma^2(1+\epsilon)\, \left(\frac{4\pi}{m_2^2}\right)^{2\epsilon} \frac{1}{(1-\epsilon)(1-2\epsilon)}\, \frac{m_2^2}{2} \\ &\Bigg\{ -\frac{1}{\epsilon^2}\left(1 + \frac{m_1^2}{m_2^2}\right) + \frac{2}{\epsilon}\left(\frac{m_1^2}{m_2^2}\log\left(\frac{m_1^2}{m_2^2}\right)\right) \\ &- \frac{m_1^2}{m_2^2}\log^2\left(\frac{m_1^2}{m_2^2}\right) - 2\left(1 - \frac{m_1^2}{m_2^2}\right) Li_2\left(1 - \frac{m_1^2}{m_2^2}\right) \Bigg\} \end{aligned} \tag{A.18}$$

A.3 Reductions

Integral $T_{1134}(0,0,m_1,m_2)$

$$T_{1134}(0,0,m_1,m_2) = \frac{1}{(m_1^2-m_2^2)^2}\Bigg\{(3-n)(m_1^2+m_2^2)T_{134}(0,m_1,m_2) - (2-n)A_0(m_1)A_0(m_2)\Bigg\} \tag{A.19}$$

Integral $T_{1134}(m_1,m_1,0,m_2)$

$$T_{1134}(m_1,m_1,0,m_2) = \frac{1}{(m_1^2-m_2^2)}\Bigg\{(n-3)T_{134}(0,m_1,m_2) + \frac{(2-n)}{2m_1^2}A_0(m_1)A_0(m_2)\Bigg\} \tag{A.20}$$

Integral $T_{1134}(m_1,m_1,m_3,m_4)$

$$\begin{aligned} T_{1134}(m_1,m_1,m_3,m_4) = & \frac{1}{(m_1^2+m_3^2+m_4^2-2m_1^2m_3^2-2m_1^2m_4^2-2m_3^2m_4^2)} \\ & \Bigg\{(m_1^2-m_3^2-m_4^2)\ (n-3)\ T_{134}(m_1,m_3,m_4) \\ & + \frac{(n-2)}{2}\Big(2A_0(m_3)A_0(m_4) - A_0(m_1)A_0(m_3) - A_0(m_1)A_0(m_4)\Big) \\ & - \frac{(n-2)}{2m_1^2}\Big(\big(m_3^2-m_4^2\big)\big(A_0(m_1)A_0(m_4) - A_0(m_1)A_0(m_3)\big)\Big)\Bigg\} \end{aligned} \tag{A.21}$$

Integral $T_{1134}(0,0,m,m)$

$$T_{1134}(0,0,m,m) \ = \frac{1}{(4m^4)}\ \frac{(n-2)}{(n-5)}\ A_0(m)^2 \tag{A.22}$$

Integral $T_{1134}(m,m,0,m)$

$$T_{1134}(m,m,0,m) \ = \frac{(n-2)}{(4m^4)}\ A_0(m)^2 \tag{A.23}$$

Appendix B

Feynman Rules

In this Appendix all used Feynman rules are specified. Appendix B.1 lists the Feynman rules for propagators, and Appendix B.2 lists the Feynman rules for the vertices. For several Feynman rules we specify the rule in the physical mass basis of the involved squarks as well as in the LR-basis.

B.1 Propagators

Quark Propagator

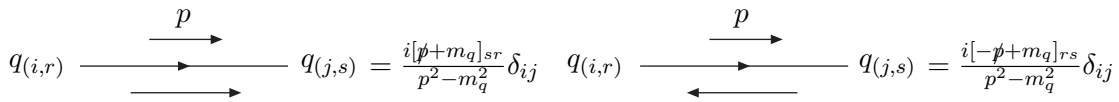

Gluon Propagator in Feynman Gauge

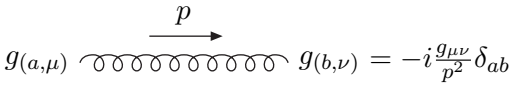

Gluino Propagator

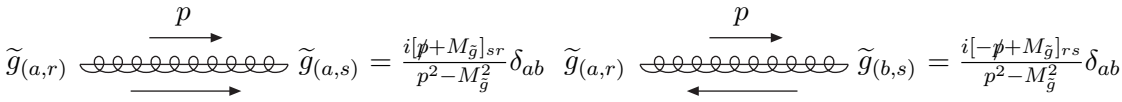

Higgsino Propagator

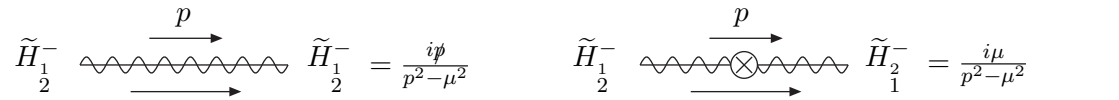

Squark Propagator ($\alpha = 1, 2$)

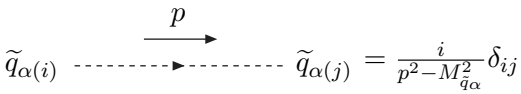

Squark Propagator in LR-Basis (α, $\beta = L$, R ; $M_{\alpha\beta}$ **defined in eq. (1.27)**)

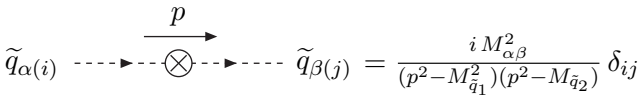

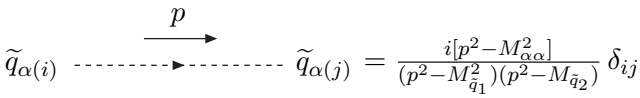

B.2 Vertices

2-Quark-Gluon Vertices

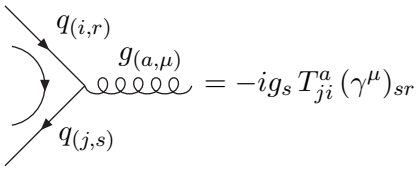

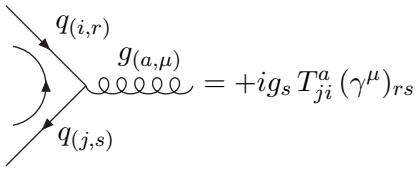

2-Gluino-gluon and 2-Squark-Gluon Vertices

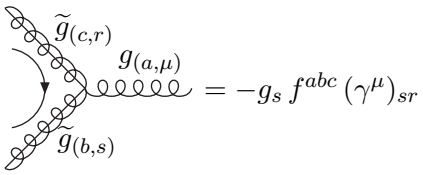

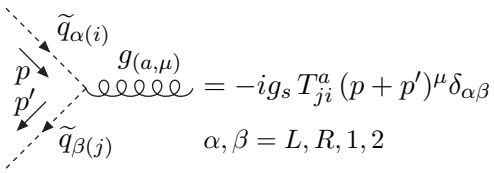

2-Squark-2-Gluon-Vertex

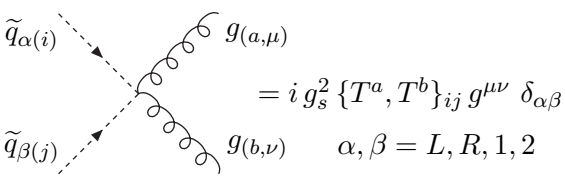

4-Squark-Vertex same flavour ($\alpha, \beta, \gamma, \delta = 1, 2$)

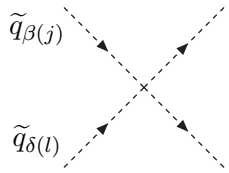

$$= -i\, g_s^2 \left\{ (T^a_{ij} T^a_{kl}) \mathbb{P}_{\alpha\beta} \mathbb{P}_{\gamma\delta} + (T^a_{il} T^a_{kj}) \mathbb{P}_{\alpha\delta} \mathbb{P}_{\gamma\beta} \right\}, \quad \mathbb{P} = \begin{pmatrix} +c_{2\widetilde{\theta}_q} & -s_{2\widetilde{\theta}_q} \\ -s_{2\widetilde{\theta}_q} & -c_{2\widetilde{\theta}_q} \end{pmatrix}$$

$\alpha, \beta, \gamma, \delta = 1, 2$

4 Squark Vertex different flavour ($\alpha, \beta, \gamma, \delta = 1, 2$)

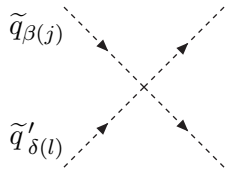

$$= -i\, g_s^2 \left\{ (T^a_{ij} T^a_{kl}) \mathbb{P}_{\alpha\beta} \mathbb{P}_{\gamma\delta} \right\}, \quad \mathbb{P} = \begin{pmatrix} +c_{2\widetilde{\theta}_q} & -s_{2\widetilde{\theta}_q} \\ -s_{2\widetilde{\theta}_q} & -c_{2\widetilde{\theta}_q} \end{pmatrix}$$

$\alpha, \beta, \gamma, \delta = 1, 2$

4-Squark-Vertex same flavour opposite helicities in LR-Basis

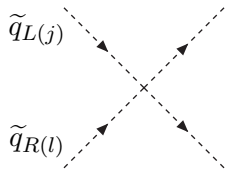

$$= +i\, g_s^2 \left\{ T^a_{ij} T^a_{kl} \right\}$$

4-Squark-Vertex same flavour same helicity in LR-Basis ($\alpha = L, R$)

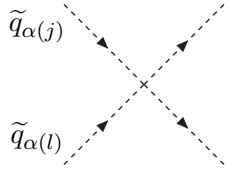

$$= -i g_s^2 \left\{ T^a_{ij} T^a_{kl} + T^a_{il} T^a_{kj} \right\}$$

4-Squark-Vertex different flavour in LR-Basis ($\alpha, \beta, \gamma, \delta = L, R$)

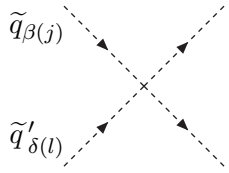

$$= \begin{cases} -i\, g_s^2 \left\{ (T^a_{ij} T^a_{kl}) \delta_{\alpha\beta} \delta_{\gamma\delta} \right\}, & \alpha = \gamma \\ +i\, g_s^2 \left\{ (T^a_{ij} T^a_{kl}) \delta_{\alpha\beta} \delta_{\gamma\delta} \right\}, & \alpha \neq \gamma \end{cases}$$

Gluino-Squark-Quark Vertex ($v_{1/2} = \pm c_{\widetilde{\theta}_q} - s_{\widetilde{\theta}_q}$, $a_{1/2} = c_{\widetilde{\theta}_q} \pm s_{\widetilde{\theta}_q}$)

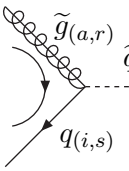

$= -i\frac{g_s}{\sqrt{2}} T^a_{ij} (v_\alpha + a_\alpha \gamma_5)_{sr}$ $\quad \alpha = 1,2$

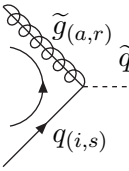

$= -i\frac{g_s}{\sqrt{2}} T^a_{ji} (v_\alpha - a_\alpha \gamma_5)_{rs}$ $\quad \alpha = 1,2$

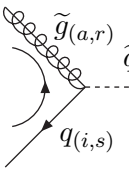

$= -i\frac{g_s}{\sqrt{2}} T^a_{ij} (v_\alpha + a_\alpha \gamma_5)_{rs}$ $\quad \alpha = 1,2$

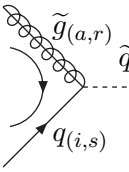

$= -i\frac{g_s}{\sqrt{2}} T^a_{ji} (v_\alpha - a_\alpha \gamma_5)_{sr}$ $\quad \alpha = 1,2$

Gluino-Squark-Quark Vertex in LR-Basis

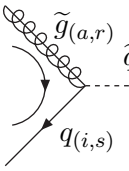

$= \begin{cases} -i\frac{g_s}{\sqrt{2}} T^a_{ij} (1+\gamma_5)_{sr} \text{ , L} \\ +i\frac{g_s}{\sqrt{2}} T^a_{ij} (1-\gamma_5)_{sr} \text{ , R} \end{cases}$

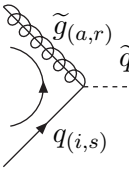

$= \begin{cases} -i\frac{g_s}{\sqrt{2}} T^a_{ji} (1-\gamma_5)_{rs} \text{ , L} \\ +i\frac{g_s}{\sqrt{2}} T^a_{ji} (1+\gamma_5)_{rs} \text{ , R} \end{cases}$

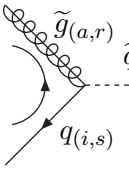

$= \begin{cases} -i\frac{g_s}{\sqrt{2}} T^a_{ij} (1+\gamma_5)_{rs} \text{ , L} \\ +i\frac{g_s}{\sqrt{2}} T^a_{ij} (1-\gamma_5)_{rs} \text{ , R} \end{cases}$

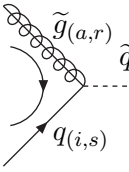

$= \begin{cases} -i\frac{g_s}{\sqrt{2}} T^a_{ji} (1-\gamma_5)_{sr} \text{ , L} \\ +i\frac{g_s}{\sqrt{2}} T^a_{ji} (1+\gamma_5)_{sr} \text{ , R} \end{cases}$

Higgsino-Squark-Quark Vertex

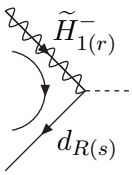

$= \lambda_b \frac{1}{2}(1-\gamma_5)_{sr}$

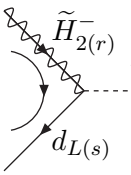

$= -\lambda_t \frac{1}{2}(1+\gamma_5)_{sr}$

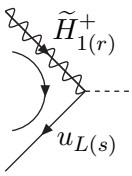

$= \lambda_b \frac{1}{2}(1+\gamma_5)_{sr}$

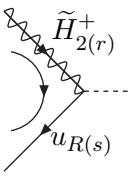

$= -\lambda_t \frac{1}{2}(1-\gamma_5)_{sr}$

Appendix C

Feynman Diagrams

In this Appendix all calculated two-loop diagrams are shown. Appendix C.1 lists the diagrams of the top-induced SUSY-electroweak contributions, and Appendix C.2 lists the diagrams of the SUSY-QCD contributions to the bottom quark self-energy. The particles involved are bottom quarks b, sbottom $\widetilde{b}$ and stop $\widetilde{t}$ squarks, gluons g, gluinos $\widetilde{g}$ and charged Higgsinos $\widetilde{H}^{\pm}$.

C.1 SUSY-Electroweak

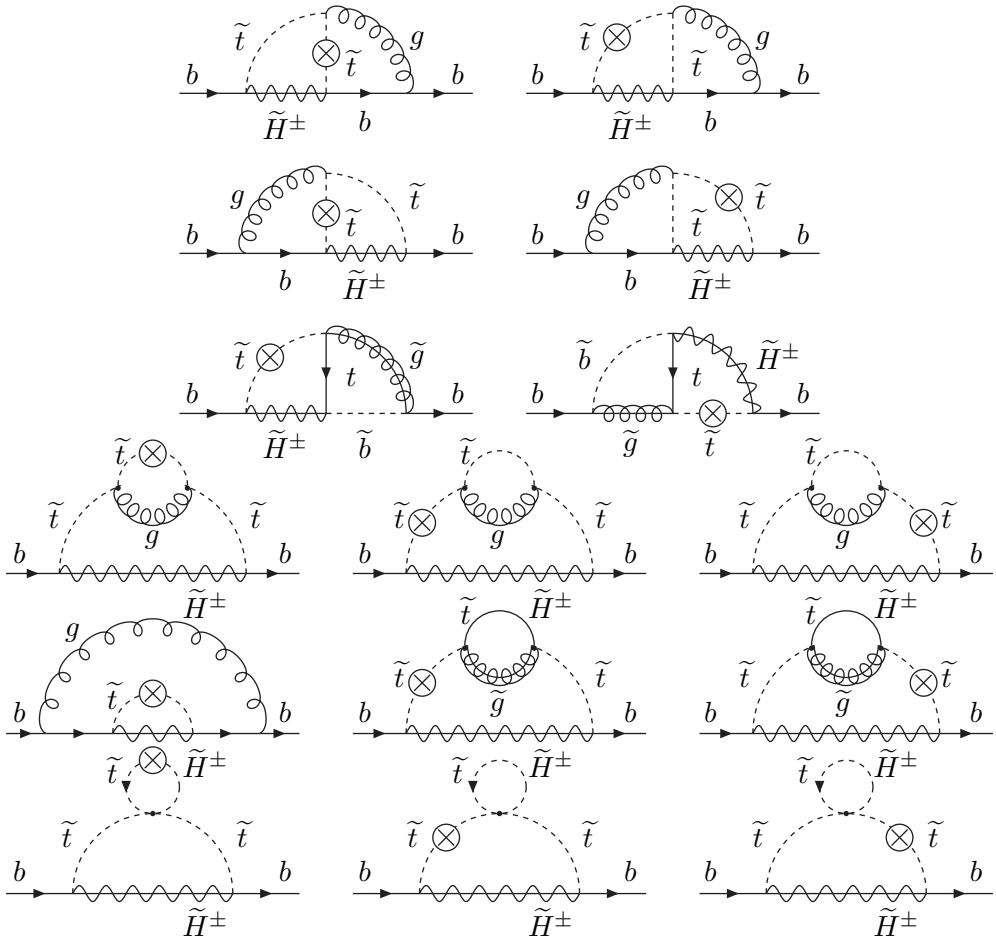

C.2 SUSY-QCD

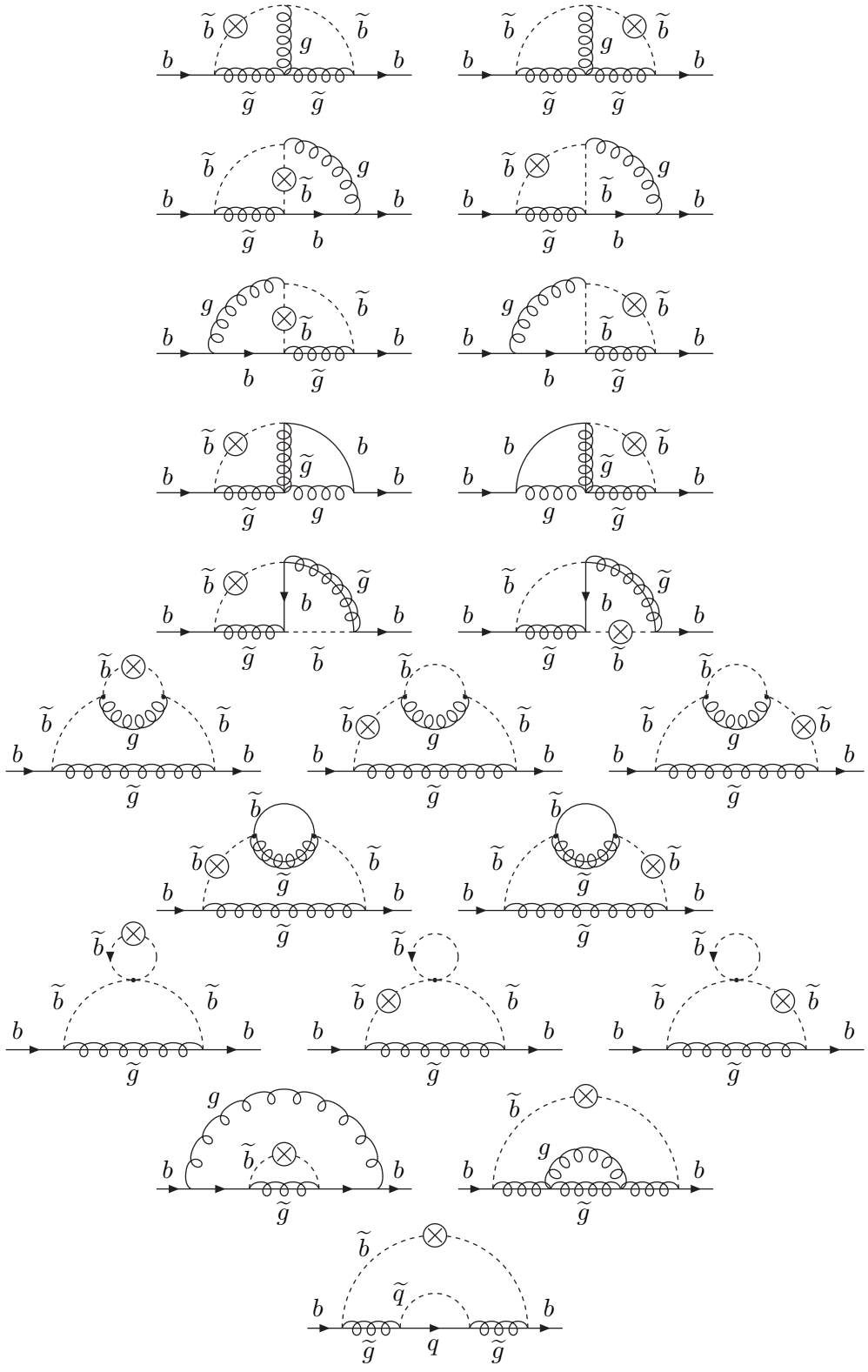
b̃ g b̃
b b
g̃ g̃
b̃ g b̃
b b
g̃ g̃
b̃ g b̃
b b
g̃ b
b̃ g b̃
b b
g̃ b
g b̃ b
b b
b g̃
g b̃ b
b b
g̃ g
b̃ g̃ b
b b
g̃ b
b̃ g̃ b
b b
g̃ b̃
b̃ b g̃
b b
g̃ b̃
b̃ b g̃
b b
g̃ b̃
b̃ g b̃
b b
g̃
b̃ g b̃
b b
g̃
b̃ g b̃
b b
g̃
b̃ g b̃
b b
g̃
b̃ g b̃
b b
g̃
b̃ g b̃
b b
g̃
g b̃
b b
g̃
b̃ g
b b
g̃
b̃ q̃
b b
g̃ q g̃

Appendix D

Analytic Results

In this Appendix the obtained analytic results for the 2-loop corrections to Δm_b are specified in terms of the 1-loop integral A_0 (A.3) and the 2-loop integral T_{134} (A.17). These corrections can be written as $\Delta m_b^{(2)} = \Delta m_b^{EW\,(2)} + \Delta m_b^{QCD\,(2)}$. Appendix D.1 specifies the analytic result for the top-induced SUSY-electroweak contribution $\Delta m_b^{EW\,(2)}$, and Appendix D.2 specifies the SUSY-QCD contribution $\Delta m_b^{QCD\,(2)}$. Involved parameters are the strong coupling α_s, the top mass m_t, the squark masses $M_{\tilde{q}_i}$, the gluino mass $M_{\tilde{g}}$, the Higgsino mass parameter μ, the top Yukawa coupling λ_t, the trilinear coupling A_t, the ratio of the two vacuum expectation values $\mathrm{tg}\beta = v_2/v_1$ and the number of dimensions $n = 4 - 2\epsilon$.

D.1 SUSY-Electroweak

In this section, the analytic result for the quantity $\Delta m_b^{EW\,(2)}$ is given in terms of integrals A_0 and T_{134}. The constant C_F is defined in section 3.3.

$$
\begin{aligned}
\Delta m_b^{EW\,(2)} \;=\; & C_F\,\alpha_s\,\lambda_t^2\,A_t\,\mu\,\mathrm{tg}\beta\,4\pi\,\Bigg\{ \\
& A_0(m_t)A_0(M_{\tilde{t}_1})\,\Bigg[\Big(2\Big(\Big(M_{\tilde{t}_1}^2(n-3)-\mu^2(n-2)\Big)m_t^4+ \\
& \quad \Big(-2(n-3)M_{\tilde{t}_1}^4+\left(2\mu^2(n-2)-M_{\tilde{g}}^2(n-4)\right)M_{\tilde{t}_1}^2+M_{\tilde{g}}^2\mu^2(n-2)\Big)m_t^2+ \\
& \quad M_{\tilde{t}_1}^2\left(M_{\tilde{t}_1}^2-M_{\tilde{g}}^2\right)\left((n-3)M_{\tilde{t}_1}^2+M_{\tilde{g}}^2-\mu^2(n-2)\right)\Big)\Big)\Big/ \\
& \quad \Big(\Big(M_{\tilde{t}_1}^2-M_{\tilde{t}_2}^2\Big)\Big(m_t^4-2\Big(M_{\tilde{t}_1}^2+M_{\tilde{g}}^2\Big)m_t^2+\Big(M_{\tilde{t}_1}^2-M_{\tilde{g}}^2\Big)^2\Big)\Big(M_{\tilde{t}_1}^3-M_{\tilde{t}_1}\mu^2\Big)^2\Big)\Bigg]+ \\
& A_0(M_{\tilde{b}_1})A_0(M_{\tilde{t}_1})\,\left[\frac{1}{\Big(M_{\tilde{t}_1}^2-M_{\tilde{t}_2}^2\Big)\Big(M_{\tilde{b}_1}^2-M_{\tilde{g}}^2\Big)\Big(M_{\tilde{t}_1}^2-\mu^2\Big)}\right]+ \\
& A_0(M_{\tilde{b}_2})A_0(M_{\tilde{t}_1})\,\left[\frac{1}{\Big(M_{\tilde{t}_1}^2-M_{\tilde{t}_2}^2\Big)\Big(M_{\tilde{b}_2}^2-M_{\tilde{g}}^2\Big)\Big(M_{\tilde{t}_1}^2-\mu^2\Big)}\right]+
\end{aligned}
$$

$$
\begin{aligned}
&A_0(M_{\tilde{t}_1})^2 \left[\frac{(3n-10)M_{\tilde{t}_1}^4 + \left(\mu^2(8-3n) - M_{\tilde{t}_2}^2(n-4)\right) M_{\tilde{t}_1}^2 + M_{\tilde{t}_2}^2\mu^2(n-2)}{M_{\tilde{t}_1}^2\left(M_{\tilde{t}_1}^2 - M_{\tilde{t}_2}^2\right)^2\left(M_{\tilde{t}_1}^2 - \mu^2\right)^2(n-3)}\right] + \\
&A_0(m_t)A_0(M_{\tilde{t}_2}\left[-\left(2\left(\left(M_{\tilde{t}_2}^2(n-3) - \mu^2(n-2)\right)m_t^4 + \right.\right.\right. \\
&\quad \left(-2(n-3)M_{\tilde{t}_2}^4 + \left(2\mu^2(n-2) - M_{\tilde{g}}^2(n-4)\right)M_{\tilde{t}_2}^2 + M_{\tilde{g}}^2\mu^2(n-2)\right)m_t^2 + \\
&\quad \left.\left.\left. M_{\tilde{t}_2}^2\left(M_{\tilde{t}_2}^2 - M_{\tilde{g}}^2\right)\left((n-3)M_{\tilde{t}_2}^2 + M_{\tilde{g}}^2 - \mu^2(n-2)\right)\right)\right)\Big/ \\
&\quad \left(\left(M_{\tilde{t}_1}^2 - M_{\tilde{t}_2}^2\right)\left(m_t^4 - 2\left(M_{\tilde{t}_2}^2 + M_{\tilde{g}}^2\right)m_t^2 + \left(M_{\tilde{t}_2}^2 - M_{\tilde{g}}^2\right)^2\right)\left(M_{\tilde{t}_2}^3 - M_{\tilde{t}_2}\mu^2\right)^2\right)\Bigg] + \\
&A_0(M_{\tilde{b}_1})A_0(M_{\tilde{t}_2})\left[-\frac{1}{\left(M_{\tilde{t}_1}^2 - M_{\tilde{t}_2}^2\right)\left(M_{\tilde{b}_1}^2 - M_{\tilde{g}}^2\right)\left(M_{\tilde{t}_2}^2 - \mu^2\right)}\right] + \\
&A_0(M_{\tilde{b}_2})A_0(M_{\tilde{t}_2})\left[-\frac{1}{\left(M_{\tilde{t}_1}^2 - M_{\tilde{t}_2}^2\right)\left(M_{\tilde{b}_2}^2 - M_{\tilde{g}}^2\right)\left(M_{\tilde{t}_2}^2 - \mu^2\right)}\right] + \\
&A_0(M_{\tilde{t}_1})A_0(M_{\tilde{t}_2})\left[-\frac{2\left(M_{\tilde{t}_1}^2 + M_{\tilde{t}_2}^2 - 2\mu^2\right)}{\left(M_{\tilde{t}_1}^2 - M_{\tilde{t}_2}^2\right)^2\left(M_{\tilde{t}_1}^2 - \mu^2\right)\left(M_{\tilde{t}_2}^2 - \mu^2\right)}\right] + \\
&A_0(M_{\tilde{t}_2})^2\left[\frac{\left(\mu^2(n-2) - M_{\tilde{t}_2}^2(n-4)\right)M_{\tilde{t}_1}^2 + M_{\tilde{t}_2}^2\left((3n-10)M_{\tilde{t}_2}^2 + \mu^2(8-3n)\right)}{M_{\tilde{t}_2}^2\left(M_{\tilde{t}_1}^2 - M_{\tilde{t}_2}^2\right)^2\left(M_{\tilde{t}_2}^2 - \mu^2\right)^2(n-3)}\right] + \\
&A_0(m_t)A_0(M_{\tilde{g}})\left[-\left(2\left(m_t^6 - \left(2M_{\tilde{t}_1}^2 + 2M_{\tilde{t}_2}^2 + M_{\tilde{g}}^2 - \mu^2\right)m_t^4 + \left(M_{\tilde{t}_1}^4 + \right.\right.\right. \right. \\
&\quad \left(3M_{\tilde{t}_2}^2 - 4M_{\tilde{g}}^2 - \mu^2\right)M_{\tilde{t}_1}^2 + M_{\tilde{t}_2}^4 - M_{\tilde{g}}^4 + 6M_{\tilde{g}}^2\mu^2 - M_{\tilde{t}_2}^2\left(4M_{\tilde{g}}^2 + \mu^2\right)\Big)m_t^2 + \\
&\quad \left.\left.\left.\left(M_{\tilde{t}_1}^2 - M_{\tilde{g}}^2\right)\left(M_{\tilde{g}}^2 - M_{\tilde{t}_2}^2\right)\left(M_{\tilde{t}_1}^2 + M_{\tilde{t}_2}^2 - M_{\tilde{g}}^2 - \mu^2\right)\right)(n-2)\right)\Big/ \\
&\quad \left(\left(m_t^4 - 2\left(M_{\tilde{t}_1}^2 + M_{\tilde{g}}^2\right)m_t^2 + \left(M_{\tilde{t}_1}^2 - M_{\tilde{g}}^2\right)^2\right)\right. \\
&\quad \left.\left(m_t^4 - 2\left(M_{\tilde{t}_2}^2 + M_{\tilde{g}}^2\right)m_t^2 + \left(M_{\tilde{t}_2}^2 - M_{\tilde{g}}^2\right)^2\right)\left(M_{\tilde{t}_1}^2 - \mu^2\right)\left(M_{\tilde{t}_2}^2 - \mu^2\right)\right)\Bigg] + \\
&A_0(M_{\tilde{t}_1})A_0(M_{\tilde{g}})\left[\left(M_{\tilde{t}_1}^2\left(\left(-2M_{\tilde{b}_2}^2 - M_{\tilde{t}_1}^2 + 2M_{\tilde{g}}^2 + \mu^2\right)M_{\tilde{b}_1}^2 - \right.\right.\right. \\
&\quad 2M_{\tilde{g}}^2\left(-M_{\tilde{t}_1}^2 + M_{\tilde{g}}^2 + \mu^2\right) + M_{\tilde{b}_2}^2\left(-M_{\tilde{t}_1}^2 + 2M_{\tilde{g}}^2 + \mu^2\right)\Big)m_t^4 - \\
&\quad 2\left(M_{\tilde{t}_1}^2 + M_{\tilde{g}}^2\right)\left(\left(-M_{\tilde{t}_1}^4 + \left(\mu^2 - M_{\tilde{g}}^2(n-4)\right)M_{\tilde{t}_1}^2 + \right.\right. \\
&\quad \left.\left.M_{\tilde{b}_2}^2\left(M_{\tilde{t}_1}^2(n-4) - \mu^2(n-2)\right) + M_{\tilde{g}}^2\mu^2(n-2)\right)M_{\tilde{b}_1}^2 + \right. \\
&\quad M_{\tilde{g}}^2\left(2M_{\tilde{t}_1}^4 + \left(M_{\tilde{g}}^2(n-4) - 2\mu^2\right)M_{\tilde{t}_1}^2 - M_{\tilde{g}}^2\mu^2(n-2)\right) + \\
&\quad \left.M_{\tilde{b}_2}^2\left(-M_{\tilde{t}_1}^4 + \left(\mu^2 - M_{\tilde{g}}^2(n-4)\right)M_{\tilde{t}_1}^2 + M_{\tilde{g}}^2\mu^2(n-2)\right)\right)m_t^2 + \\
&\quad \left(M_{\tilde{t}_1}^2 - M_{\tilde{g}}^2\right)^2\left(\left(-M_{\tilde{t}_1}^4 + \left(\mu^2 - 2M_{\tilde{g}}^2(n-3)\right)M_{\tilde{t}_1}^2 + \right.\right. \\
&\quad \left.\left.2M_{\tilde{b}_2}^2\left(M_{\tilde{t}_1}^2(n-3) - \mu^2(n-2)\right) + 2M_{\tilde{g}}^2\mu^2(n-2)\right)M_{\tilde{b}_1}^2 + \right.
\end{aligned}
$$

$$
\begin{aligned}
&2M_{\tilde{g}}^2\left(M_{\tilde{t}_1}^4+\left(M_{\tilde{g}}^2(n-3)-\mu^2\right)M_{\tilde{t}_1}^2-M_{\tilde{g}}^2\mu^2(n-2)\right)+\\
&M_{\tilde{b}_2}^2\left(-M_{\tilde{t}_1}^4+\left(\mu^2-2M_{\tilde{g}}^2(n-3)\right)M_{\tilde{t}_1}^2+2M_{\tilde{g}}^2\mu^2(n-2)\right)\Big)\Big)\Big/\\
&\left(\left(M_{\tilde{t}_1}^2-M_{\tilde{t}_2}^2\right)\left(M_{\tilde{b}_1}^2-M_{\tilde{g}}^2\right)\left(M_{\tilde{b}_2}^2-M_{\tilde{g}}^2\right)\right.\\
&\left.\left(m_t^4-2\left(M_{\tilde{t}_1}^2+M_{\tilde{g}}^2\right)m_t^2+\left(M_{\tilde{t}_1}^2-M_{\tilde{g}}^2\right)^2\right)\left(M_{\tilde{t}_1}^3-M_{\tilde{t}_1}\mu^2\right)^2\right)\Bigg]+
\end{aligned}
$$

$$
\begin{aligned}
A_0(M_{\tilde{t}_2})A_0(M_{\tilde{g}})\Bigg[&\left(M_{\tilde{t}_2}^2\left(\left(2M_{\tilde{b}_2}^2+M_{\tilde{t}_2}^2-2M_{\tilde{g}}^2-\mu^2\right)M_{\tilde{b}_1}^2+\right.\right.\\
&\left.M_{\tilde{b}_2}^2\left(M_{\tilde{t}_2}^2-2M_{\tilde{g}}^2-\mu^2\right)+2M_{\tilde{g}}^2\left(-M_{\tilde{t}_2}^2+M_{\tilde{g}}^2+\mu^2\right)\right)m_t^4+\\
&2\left(M_{\tilde{t}_2}^2+M_{\tilde{g}}^2\right)\left(\left(-M_{\tilde{t}_2}^4+\left(\mu^2-M_{\tilde{g}}^2(n-4)\right)M_{\tilde{t}_2}^2+\right.\right.\\
&\left.M_{\tilde{b}_2}^2\left(M_{\tilde{t}_2}^2(n-4)-\mu^2(n-2)\right)+M_{\tilde{g}}^2\mu^2(n-2)\right)M_{\tilde{b}_1}^2+\\
&M_{\tilde{g}}^2\left(2M_{\tilde{t}_2}^4+\left(M_{\tilde{g}}^2(n-4)-2\mu^2\right)M_{\tilde{t}_2}^2-M_{\tilde{g}}^2\mu^2(n-2)\right)+\\
&\left.M_{\tilde{b}_2}^2\left(-M_{\tilde{t}_2}^4+\left(\mu^2-M_{\tilde{g}}^2(n-4)\right)M_{\tilde{t}_2}^2+M_{\tilde{g}}^2\mu^2(n-2)\right)\right)m_t^2-\\
&\left(M_{\tilde{t}_2}^2-M_{\tilde{g}}^2\right)^2\left(\left(-M_{\tilde{t}_2}^4+\left(\mu^2-2M_{\tilde{g}}^2(n-3)\right)M_{\tilde{t}_2}^2+\right.\right.\\
&\left.2M_{\tilde{b}_2}^2\left(M_{\tilde{t}_2}^2(n-3)-\mu^2(n-2)\right)+2M_{\tilde{g}}^2\mu^2(n-2)\right)M_{\tilde{b}_1}^2+\\
&2M_{\tilde{g}}^2\left(M_{\tilde{t}_2}^4+\left(M_{\tilde{g}}^2(n-3)-\mu^2\right)M_{\tilde{t}_2}^2-M_{\tilde{g}}^2\mu^2(n-2)\right)+\\
&\left.M_{\tilde{b}_2}^2\left(-M_{\tilde{t}_2}^4+\left(\mu^2-2M_{\tilde{g}}^2(n-3)\right)M_{\tilde{t}_2}^2+2M_{\tilde{g}}^2\mu^2(n-2)\right)\right)\Big)\Big/\\
&\left(\left(M_{\tilde{t}_2}^2-M_{\tilde{t}_1}^2\right)\left(M_{\tilde{b}_1}^2-M_{\tilde{g}}^2\right)\left(M_{\tilde{g}}^2-M_{\tilde{b}_2}^2\right)\right.\\
&\left.\left(m_t^4-2\left(M_{\tilde{t}_2}^2+M_{\tilde{g}}^2\right)m_t^2+\left(M_{\tilde{t}_2}^2-M_{\tilde{g}}^2\right)^2\right)\left(M_{\tilde{t}_2}^3-M_{\tilde{t}_2}\mu^2\right)^2\right)\Bigg]+
\end{aligned}
$$

$$
A_0(m_t)A_0(\mu)\left[-\frac{2\left(M_{\tilde{t}_1}^2+M_{\tilde{t}_2}^2-2\mu^2\right)}{\left(M_{\tilde{t}_1}^2-\mu^2\right)^2\left(M_{\tilde{t}_2}^2-\mu^2\right)^2}\right]+
$$

$$
A_0(M_{\tilde{b}_1})A_0(\mu)\left[\frac{1}{\left(M_{\tilde{b}_1}^2-M_{\tilde{g}}^2\right)\left(M_{\tilde{t}_1}^2-\mu^2\right)\left(M_{\tilde{t}_2}^2-\mu^2\right)}\right]+
$$

$$
A_0(M_{\tilde{b}_2})A_0(\mu)\left[\frac{1}{\left(M_{\tilde{b}_2}^2-M_{\tilde{g}}^2\right)\left(M_{\tilde{t}_1}^2-\mu^2\right)\left(M_{\tilde{t}_2}^2-\mu^2\right)}\right]+
$$

$$
A_0(M_{\tilde{t}_1})A_0(\mu)\left[\frac{2M_{\tilde{t}_1}^2-\mu^2(n-2)^2+M_{\tilde{t}_2}^2\left(n^2-4n+2\right)}{\left(M_{\tilde{t}_1}^2-M_{\tilde{t}_2}^2\right)\left(M_{\tilde{t}_1}^2-\mu^2\right)^2\left(M_{\tilde{t}_2}^2-\mu^2\right)}\right]+
$$

$$
A_0(M_{\tilde{t}_2})A_0(\mu)\left[\frac{-\left(n^2-4n+2\right)M_{\tilde{t}_1}^2-2M_{\tilde{t}_2}^2+\mu^2(n-2)^2}{\left(M_{\tilde{t}_1}^2-M_{\tilde{t}_2}^2\right)\left(M_{\tilde{t}_1}^2-\mu^2\right)\left(M_{\tilde{t}_2}^2-\mu^2\right)^2}\right]+
$$

$$
\begin{aligned}
A_0(M_{\tilde{g}})A_0(\mu)\Bigg[&\frac{1}{\left(M_{\tilde{b}_1}^2-M_{\tilde{g}}^2\right)\left(M_{\tilde{b}_2}^2-M_{\tilde{g}}^2\right)\left(M_{\tilde{t}_1}^2-\mu^2\right)^2\left(M_{\tilde{t}_2}^2-\mu^2\right)^2}\\
&\Big(\Big(-\mu^4+M_{\tilde{t}_2}^2\mu^2-4M_{\tilde{g}}^2\mu^2+2M_{\tilde{t}_2}^2M_{\tilde{g}}^2-2M_{\tilde{b}_2}^2\left(M_{\tilde{t}_1}^2+M_{\tilde{t}_2}^2-2\mu^2\right)+
\end{aligned}
$$

$$
\begin{aligned}
&M_{\tilde{t}_1}^2\left(-M_{\tilde{t}_2}^2+2M_{\tilde{g}}^2+\mu^2\right)\Big)M_{\tilde{b}_1}^2-2M_{\tilde{g}}^2\\
&\Big(\left(-M_{\tilde{t}_2}^2+M_{\tilde{g}}^2+\mu^2\right)M_{\tilde{t}_1}^2+M_{\tilde{t}_2}^2\left(M_{\tilde{g}}^2+\mu^2\right)-\mu^2\left(2M_{\tilde{g}}^2+\mu^2\right)\Big)+M_{\tilde{b}_2}^2\\
&\Big(\left(-M_{\tilde{t}_2}^2+2M_{\tilde{g}}^2+\mu^2\right)M_{\tilde{t}_1}^2+M_{\tilde{t}_2}^2\left(2M_{\tilde{g}}^2+\mu^2\right)-\mu^2\left(4M_{\tilde{g}}^2+\mu^2\right)\Big)\Big)\Bigg]+
\end{aligned}
$$

$$
\sum_{i=1,2}T_{134}(0,M_{\tilde{t}_i},\mu)\left[-\frac{\left(M_{\tilde{t}_i}^2+\mu^2\right)\left(n^2-5n+4\right)}{\left(M_{\tilde{t}_1}^2-M_{\tilde{t}_2}^2\right)\left(M_{\tilde{t}_i}^2-\mu^2\right)^2}\right]+
$$

$$
T_{134}(m_t,M_{\tilde{b}_1},M_{\tilde{t}_1})\left[\frac{m_t^2+M_{\tilde{b}_1}^2-M_{\tilde{t}_1}^2}{\left(M_{\tilde{t}_1}^2-M_{\tilde{t}_2}^2\right)\left(M_{\tilde{b}_1}^2-M_{\tilde{g}}^2\right)\left(M_{\tilde{t}_1}^2-\mu^2\right)}\right]+
$$

$$
T_{134}(m_t,M_{\tilde{b}_1},M_{\tilde{t}_2})\left[\frac{m_t^2+M_{\tilde{b}_1}^2-M_{\tilde{t}_2}^2}{\left(M_{\tilde{t}_2}^2-M_{\tilde{t}_1}^2\right)\left(M_{\tilde{b}_1}^2-M_{\tilde{g}}^2\right)\left(M_{\tilde{t}_2}^2-\mu^2\right)}\right]+
$$

$$
T_{134}(m_t,M_{\tilde{b}_1},\mu)\left[\frac{m_t^2+M_{\tilde{b}_1}^2-\mu^2}{\left(M_{\tilde{b}_1}^2-M_{\tilde{g}}^2\right)\left(M_{\tilde{t}_1}^2-\mu^2\right)\left(M_{\tilde{t}_2}^2-\mu^2\right)}\right]+
$$

$$
T_{134}(m_t,M_{\tilde{b}_2},M_{\tilde{t}_1})\left[\frac{m_t^2+M_{\tilde{b}_2}^2-M_{\tilde{t}_1}^2}{\left(M_{\tilde{t}_1}^2-M_{\tilde{t}_2}^2\right)\left(M_{\tilde{b}_2}^2-M_{\tilde{g}}^2\right)\left(M_{\tilde{t}_1}^2-\mu^2\right)}\right]+
$$

$$
T_{134}(m_t,M_{\tilde{b}_2},M_{\tilde{t}_2})\left[\frac{m_t^2+M_{\tilde{b}_2}^2-M_{\tilde{t}_2}^2}{\left(M_{\tilde{t}_2}^2-M_{\tilde{t}_1}^2\right)\left(M_{\tilde{b}_2}^2-M_{\tilde{g}}^2\right)\left(M_{\tilde{t}_2}^2-\mu^2\right)}\right]+
$$

$$
T_{134}(m_t,M_{\tilde{b}_2},\mu)\left[\frac{m_t^2+M_{\tilde{b}_2}^2-\mu^2}{\left(M_{\tilde{b}_2}^2-M_{\tilde{g}}^2\right)\left(M_{\tilde{t}_1}^2-\mu^2\right)\left(M_{\tilde{t}_2}^2-\mu^2\right)}\right]+
$$

$$
\begin{aligned}
&T_{134}(m_t,M_{\tilde{t}_1},M_{\tilde{g}})\Bigg[\Big(\Big(\Big(-2M_{\tilde{b}_2}^2-M_{\tilde{t}_1}^2+2M_{\tilde{g}}^2+\mu^2\Big)M_{\tilde{b}_1}^2-\\
&\quad 2M_{\tilde{g}}^2\left(-M_{\tilde{t}_1}^2+M_{\tilde{g}}^2+\mu^2\right)+M_{\tilde{b}_2}^2\left(-M_{\tilde{t}_1}^2+2M_{\tilde{g}}^2+\mu^2\right)\Big)m_t^6+\\
&\quad \Big(\Big(3M_{\tilde{t}_1}^4+\left(M_{\tilde{g}}^2(2n-9)-3\mu^2\right)M_{\tilde{t}_1}^2+M_{\tilde{g}}^2\left(\mu^2(3-2n)-2M_{\tilde{g}}^2\right)+\\
&\quad 2M_{\tilde{b}_2}^2\left(-(n-5)M_{\tilde{t}_1}^2+M_{\tilde{g}}^2+\mu^2(n-2)\right)\Big)M_{\tilde{b}_1}^2+\\
&\quad 2M_{\tilde{g}}^2\left(-3M_{\tilde{t}_1}^4+\left(3\mu^2-M_{\tilde{g}}^2(n-4)\right)M_{\tilde{t}_1}^2+M_{\tilde{g}}^2\left(M_{\tilde{g}}^2+\mu^2(n-1)\right)\right)+\\
&\quad M_{\tilde{b}_2}^2\left(3M_{\tilde{t}_1}^4+\left(M_{\tilde{g}}^2(2n-9)-3\mu^2\right)M_{\tilde{t}_1}^2+M_{\tilde{g}}^2\left(\mu^2(3-2n)-2M_{\tilde{g}}^2\right)\right)\Big)m_t^4+\\
&\quad \Big(\Big(-3M_{\tilde{t}_1}^6+\left(3\mu^2-4M_{\tilde{g}}^2(n-4)\right)M_{\tilde{t}_1}^4+M_{\tilde{g}}^2\left((4n-19)M_{\tilde{g}}^2+2\mu^2(2n-5)\right)\\
&\quad M_{\tilde{t}_1}^2+M_{\tilde{g}}^4\left(\mu^2(15-4n)-2M_{\tilde{g}}^2\right)+2M_{\tilde{b}_2}^2\Big((2n-7)M_{\tilde{t}_1}^4-2\\
&\quad \left((n-5)M_{\tilde{g}}^2+\mu^2(n-2)\right)M_{\tilde{t}_1}^2+M_{\tilde{g}}^2\left(M_{\tilde{g}}^2+2\mu^2(n-4)\right)\Big)\Big)\\
&\quad M_{\tilde{b}_1}^2+2M_{\tilde{g}}^2\Big(3M_{\tilde{t}_1}^6+\left(M_{\tilde{g}}^2(2n-9)-3\mu^2\right)M_{\tilde{t}_1}^4+M_{\tilde{g}}^2\\
&\quad \left(M_{\tilde{g}}^2(9-2n)-2\mu^2(n-3)\right)M_{\tilde{t}_1}^2+M_{\tilde{g}}^4\left(M_{\tilde{g}}^2+\mu^2(2n-7)\right)\Big)+\\
&\quad M_{\tilde{b}_2}^2\Big(-3M_{\tilde{t}_1}^6+\left(3\mu^2-4M_{\tilde{g}}^2(n-4)\right)M_{\tilde{t}_1}^4+M_{\tilde{g}}^2\left((4n-19)M_{\tilde{g}}^2+\right.\\
&\quad \left.2\mu^2(2n-5)\right)M_{\tilde{t}_1}^2+M_{\tilde{g}}^4\left(\mu^2(15-4n)-2M_{\tilde{g}}^2\right)\Big)\Big)m_t^2-
\end{aligned}
$$

$$\left(M_{\tilde{t}_1}^2 - M_{\tilde{g}}^2\right)^2 \left(\left(-M_{\tilde{t}_1}^4 + \left((7-2n)M_{\tilde{g}}^2 + \mu^2\right) M_{\tilde{t}_1}^2 + 2M_{\tilde{b}_2}^2 \left((n-3)M_{\tilde{t}_1}^2 + M_{\tilde{g}}^2 - \mu^2(n-2)\right) + M_{\tilde{g}}^2 \left(\mu^2(2n-5) - 2M_{\tilde{g}}^2\right)\right) M_{\tilde{b}_1}^2 + 2M_{\tilde{g}}^2 \left(M_{\tilde{t}_1}^4 + \left(M_{\tilde{g}}^2(n-4) - \mu^2\right) M_{\tilde{t}_1}^2 + M_{\tilde{g}}^2 \left(M_{\tilde{g}}^2 - \mu^2(n-3)\right)\right) - M_{\tilde{b}_2}^2 \left(M_{\tilde{t}_1}^4 + \left(M_{\tilde{g}}^2(2n-7) - \mu^2\right) M_{\tilde{t}_1}^2 + M_{\tilde{g}}^2 \left(2M_{\tilde{g}}^2 + \mu^2(5-2n)\right)\right)\right)\Big/ \left(\left(M_{\tilde{t}_1}^2 - M_{\tilde{t}_2}^2\right)\left(M_{\tilde{b}_1}^2 - M_{\tilde{g}}^2\right)\left(M_{\tilde{b}_2}^2 - M_{\tilde{g}}^2\right) \left(m_t^4 - 2\left(M_{\tilde{t}_1}^2 + M_{\tilde{g}}^2\right) m_t^2 + \left(M_{\tilde{t}_1}^2 - M_{\tilde{g}}^2\right)^2\right)\left(M_{\tilde{t}_1}^2 - \mu^2\right)^2\right) \Bigg] +$$

$$T_{134}(m_t, M_{\tilde{t}_2}, M_{\tilde{g}}) \Bigg[\left(\left(\left(2M_{\tilde{b}_2}^2 + M_{\tilde{t}_2}^2 - 2M_{\tilde{g}}^2 - \mu^2\right) M_{\tilde{b}_1}^2 + M_{\tilde{b}_2}^2 \left(M_{\tilde{t}_2}^2 - 2M_{\tilde{g}}^2 - \mu^2\right) + 2M_{\tilde{g}}^2 \left(-M_{\tilde{t}_2}^2 + M_{\tilde{g}}^2 + \mu^2\right)\right) m_t^6 + \left(\left(-3M_{\tilde{t}_2}^4 + \left((9-2n)M_{\tilde{g}}^2 + 3\mu^2\right) M_{\tilde{t}_2}^2 + 2M_{\tilde{b}_2}^2 \left((n-5)M_{\tilde{t}_2}^2 - M_{\tilde{g}}^2 - \mu^2(n-2)\right) + M_{\tilde{g}}^2 \left(2M_{\tilde{g}}^2 + \mu^2(2n-3)\right)\right) M_{\tilde{b}_1}^2 - 2M_{\tilde{g}}^2 \left(-3M_{\tilde{t}_2}^4 + \left(3\mu^2 - M_{\tilde{g}}^2(n-4)\right) M_{\tilde{t}_2}^2 + M_{\tilde{g}}^2 \left(M_{\tilde{g}}^2 + \mu^2(n-1)\right)\right) + M_{\tilde{b}_2}^2 \left(-3M_{\tilde{t}_2}^4 + \left((9-2n)M_{\tilde{g}}^2 + 3\mu^2\right) M_{\tilde{t}_2}^2 + M_{\tilde{g}}^2 \left(2M_{\tilde{g}}^2 + \mu^2(2n-3)\right)\right)\right) m_t^4 + \left(\left(3M_{\tilde{t}_2}^6 + \left(4M_{\tilde{g}}^2(n-4) - 3\mu^2\right) M_{\tilde{t}_2}^4 + M_{\tilde{g}}^2 \left((19-4n)M_{\tilde{g}}^2 + 2\mu^2(5-2n)\right) M_{\tilde{t}_2}^2 - 2M_{\tilde{b}_2}^2 \left((2n-7)M_{\tilde{t}_2}^4 - 2\left((n-5)M_{\tilde{g}}^2 + \mu^2(n-2)\right) M_{\tilde{t}_2}^2 + M_{\tilde{g}}^2 \left(M_{\tilde{g}}^2 + 2\mu^2(n-4)\right)\right) + M_{\tilde{g}}^4 \left(2M_{\tilde{g}}^2 + \mu^2(4n-15)\right)\right) M_{\tilde{b}_1}^2 - 2M_{\tilde{g}}^2 \left(3M_{\tilde{t}_2}^6 + \left(M_{\tilde{g}}^2(2n-9) - 3\mu^2\right) M_{\tilde{t}_2}^4 + M_{\tilde{g}}^2 \left(M_{\tilde{g}}^2(9-2n) - 2\mu^2(n-3)\right) M_{\tilde{t}_2}^2 + M_{\tilde{g}}^4 \left(M_{\tilde{g}}^2 + \mu^2(2n-7)\right)\right) + M_{\tilde{b}_2}^2 \left(3M_{\tilde{t}_2}^6 + \left(4M_{\tilde{g}}^2(n-4) - 3\mu^2\right) M_{\tilde{t}_2}^4 + M_{\tilde{g}}^2 \left((19-4n)M_{\tilde{g}}^2 + 2\mu^2(5-2n)\right) M_{\tilde{t}_2}^2 + M_{\tilde{g}}^4 \left(2M_{\tilde{g}}^2 + \mu^2(4n-15)\right)\right)\right) m_t^2 + \left(M_{\tilde{t}_2}^2 - M_{\tilde{g}}^2\right)^2 \left(\left(-M_{\tilde{t}_2}^4 + \left((7-2n)M_{\tilde{g}}^2 + \mu^2\right) M_{\tilde{t}_2}^2 + 2M_{\tilde{b}_2}^2 \left((n-3)M_{\tilde{t}_2}^2 + M_{\tilde{g}}^2 - \mu^2(n-2)\right) + M_{\tilde{g}}^2 \left(\mu^2(2n-5) - 2M_{\tilde{g}}^2\right)\right) M_{\tilde{b}_1}^2 + 2M_{\tilde{g}}^2 \left(M_{\tilde{t}_2}^4 + \left(M_{\tilde{g}}^2(n-4) - \mu^2\right) M_{\tilde{t}_2}^2 + M_{\tilde{g}}^2 \left(M_{\tilde{g}}^2 - \mu^2(n-3)\right)\right) - M_{\tilde{b}_2}^2 \left(M_{\tilde{t}_2}^4 + \left(M_{\tilde{g}}^2(2n-7) - \mu^2\right) M_{\tilde{t}_2}^2 + M_{\tilde{g}}^2 \left(2M_{\tilde{g}}^2 + \mu^2(5-2n)\right)\right)\right)\Big/ \left(\left(M_{\tilde{t}_1}^2 - M_{\tilde{t}_2}^2\right)\left(M_{\tilde{b}_1}^2 - M_{\tilde{g}}^2\right)\left(M_{\tilde{b}_2}^2 - M_{\tilde{g}}^2\right)\left(m_t^4 - 2\left(M_{\tilde{t}_2}^2 + M_{\tilde{g}}^2\right) m_t^2 + \left(M_{\tilde{t}_2}^2 - M_{\tilde{g}}^2\right)^2\right)\left(M_{\tilde{t}_2}^2 - \mu^2\right)^2\right) \Bigg] +$$

$$T_{134}(m_t, M_{\tilde{g}}, \mu) \Bigg[\left(\left(m_t^2 + M_{\tilde{g}}^2 - \mu^2\right) \left(\left(-\mu^4 + M_{\tilde{t}_2}^2\mu^2 - 4M_{\tilde{g}}^2\mu^2 + 2M_{\tilde{t}_2}^2 M_{\tilde{g}}^2 - 2M_{\tilde{b}_2}^2 \left(M_{\tilde{t}_1}^2 + M_{\tilde{t}_2}^2 - 2\mu^2\right) + M_{\tilde{t}_1}^2 \left(-M_{\tilde{t}_2}^2 + 2M_{\tilde{g}}^2 + \mu^2\right)\right) M_{\tilde{b}_1}^2 - 2M_{\tilde{g}}^2 \left(\left(-M_{\tilde{t}_2}^2 + M_{\tilde{g}}^2 + \mu^2\right) M_{\tilde{t}_1}^2 + M_{\tilde{t}_2}^2 \left(M_{\tilde{g}}^2 + \mu^2\right) - \mu^2 \left(2M_{\tilde{g}}^2 + \mu^2\right)\right) + M_{\tilde{b}_2}^2 \left(\left(-M_{\tilde{t}_2}^2 + 2M_{\tilde{g}}^2 + \mu^2\right) M_{\tilde{t}_1}^2 +$$

$$M_{\tilde{t}_2}^2\left(2M_{\tilde{g}}^2+\mu^2\right)-\mu^2\left(4M_{\tilde{g}}^2+\mu^2\right)\Big)\Big)\Big/$$
$$\left(\left(M_{\tilde{b}_1}^2-M_{\tilde{g}}^2\right)\left(M_{\tilde{b}_2}^2-M_{\tilde{g}}^2\right)\left(M_{\tilde{t}_1}^2-\mu^2\right)^2\left(M_{\tilde{t}_2}^2-\mu^2\right)^2\right)\Bigg]\Bigg\}$$

D.2 SUSY-QCD

In this section, the analytic result for the quantity $\Delta m_b^{QCD\,(2)}$ is given in terms of integrals A_0 and T_{134}. These corrections are split into three parts, each of which is proportional to a different colour factor, namely C_AC_F, C_F^2 and T_RC_F (section 3.3) respectively. Therefore we write $\Delta m_b^{QCD\,(2)} = \Delta m_b^{QCD\,(2)}\Big|_{C_AC_F} + \Delta m_b^{QCD\,(2)}\Big|_{C_F^2} + \Delta m_b^{QCD\,(2)}\Big|_{T_RC_F}$.

SUSY-QCD corrections proportional to C_AC_F

$$\Delta m_b^{QCD\,(2)}\Big|_{C_AC_F} = -C_AC_F\left(\frac{\alpha_s}{4\pi}\right)^2 M_{\tilde{g}}\,\mu\,\mathrm{tg}\beta\,\pi^4\Bigg\{$$
$$A_0(M_{\tilde{g}})^2\Bigg[-\Big(256(n-2)\Big(\Big(M_{\tilde{b}_2}^2(n-1)^2-M_{\tilde{g}}^2\left(n^2-4n+5\right)\Big)M_{\tilde{b}_1}^2+$$
$$M_{\tilde{g}}^2\left(M_{\tilde{g}}^2(n-3)^2-M_{\tilde{b}_2}^2\left(n^2-4n+5\right)\right)\Big)\Big)\Big/$$
$$\left(M_{\tilde{g}}^2\left(M_{\tilde{b}_1}^2-M_{\tilde{g}}^2\right)^2\left(M_{\tilde{b}_2}^2-M_{\tilde{g}}^2\right)^2(n-3)\right)\Bigg]+$$
$$A_0(M_{\tilde{b}_1})^2\left[-\frac{512(n-2)}{\left(M_{\tilde{b}_1}^2-M_{\tilde{b}_2}^2\right)\left(M_{\tilde{b}_1}^2-M_{\tilde{g}}^2\right)^2(n-3)}\right]+$$
$$A_0(M_{\tilde{b}_2})^2\left[\frac{512(n-2)}{\left(M_{\tilde{b}_1}^2-M_{\tilde{b}_2}^2\right)\left(M_{\tilde{b}_2}^2-M_{\tilde{g}}^2\right)^2(n-3)}\right]+$$
$$A_0(M_{\tilde{b}_1})A_0(M_{\tilde{g}})\left[-\frac{512(n-2)}{\left(M_{\tilde{b}_1}^2-M_{\tilde{b}_2}^2\right)\left(M_{\tilde{b}_1}^2-M_{\tilde{g}}^2\right)^2}\right]+$$
$$A_0(M_{\tilde{b}_2})A_0(M_{\tilde{g}})\left[\frac{512(n-2)}{\left(M_{\tilde{b}_1}^2-M_{\tilde{b}_2}^2\right)\left(M_{\tilde{b}_2}^2-M_{\tilde{g}}^2\right)^2}\right]+$$
$$T_{134}(0,M_{\tilde{b}_1},M_{\tilde{b}_2})\left[\frac{512}{\left(M_{\tilde{b}_1}^2-M_{\tilde{g}}^2\right)\left(M_{\tilde{g}}^2-M_{\tilde{b}_2}^2\right)}\right]+$$
$$T_{134}(0,M_{\tilde{b}_1},M_{\tilde{g}})\left[\frac{512\left(M_{\tilde{b}_1}^2+M_{\tilde{g}}^2(n-2)-M_{\tilde{b}_2}^2(n-1)\right)}{\left(M_{\tilde{b}_1}^2-M_{\tilde{b}_2}^2\right)\left(M_{\tilde{b}_1}^2-M_{\tilde{g}}^2\right)\left(M_{\tilde{b}_2}^2-M_{\tilde{g}}^2\right)}\right]+$$
$$T_{134}(0,M_{\tilde{b}_2},M_{\tilde{g}})\left[\frac{512\left((n-1)M_{\tilde{b}_1}^2-M_{\tilde{b}_2}^2-M_{\tilde{g}}^2(n-2)\right)}{\left(M_{\tilde{b}_1}^2-M_{\tilde{b}_2}^2\right)\left(M_{\tilde{b}_1}^2-M_{\tilde{g}}^2\right)\left(M_{\tilde{b}_2}^2-M_{\tilde{g}}^2\right)}\right]\Bigg\}$$

SUSY-QCD corrections proportional to C_F^2

$$
\begin{aligned}
&\Delta m_b^{QCD\,(2)}\Big|_{C_F^2} = -C_F^2\left(\frac{\alpha_s}{4\pi}\right)^2 M_{\tilde g}\,\mu\,\mathrm{tg}\beta\,\pi^4\left\{\right.\\
&A_0(M_{\tilde b_1})^2\left[-\frac{512\left((2n-7)M_{\tilde b_1}^4+\left(M_{\tilde b_2}^2+M_{\tilde g}^2(8-3n)\right)M_{\tilde b_1}^2+M_{\tilde b_2}^2M_{\tilde g}^2(n-2)\right)}{M_{\tilde b_1}^2\left(M_{\tilde b_1}^2-M_{\tilde b_2}^2\right)^2\left(M_{\tilde b_1}^2-M_{\tilde g}^2\right)^2(n-3)}\right]+\\
&A_0(M_{\tilde b_1})A_0(M_{\tilde b_2})\left[\frac{1024\left(M_{\tilde b_1}^2+M_{\tilde b_2}^2-2M_{\tilde g}^2\right)}{\left(M_{\tilde b_1}^2-M_{\tilde b_2}^2\right)^2\left(M_{\tilde b_1}^2-M_{\tilde g}^2\right)\left(M_{\tilde b_2}^2-M_{\tilde g}^2\right)}\right]+\\
&A_0(M_{\tilde b_2})^2\left[-\frac{512\left(\left(M_{\tilde b_2}^2+M_{\tilde g}^2(n-2)\right)M_{\tilde b_1}^2+M_{\tilde b_2}^2\left((2n-7)M_{\tilde b_2}^2+M_{\tilde g}^2(8-3n)\right)\right)}{M_{\tilde b_2}^2\left(M_{\tilde b_1}^2-M_{\tilde b_2}^2\right)^2\left(M_{\tilde b_2}^2-M_{\tilde g}^2\right)^2(n-3)}\right]+\\
&A_0(M_{\tilde b_1})A_0(M_{\tilde g})\left[-\left(512\left(2M_{\tilde b_1}^4+\left(M_{\tilde b_2}^2\left(n^2-2n-2\right)-M_{\tilde g}^2(n-2)n\right)M_{\tilde b_1}^2+\right.\right.\right.\\
&\qquad\left.\left.\left.2M_{\tilde g}^2\left(M_{\tilde g}^2-M_{\tilde b_2}^2\right)(n-2)\right)\right)\Big/\left(\left(M_{\tilde b_1}^2-M_{\tilde b_2}^2\right)\left(M_{\tilde b_2}^2-M_{\tilde g}^2\right)\left(M_{\tilde b_1}^3-M_{\tilde b_1}M_{\tilde g}^2\right)^2\right)\right]+\\
&A_0(M_{\tilde b_2})A_0(M_{\tilde g})\left[\left(512\left(2M_{\tilde b_2}^4-M_{\tilde g}^2(n-2)nM_{\tilde b_2}^2+2M_{\tilde g}^4(n-2)+\right.\right.\right.\\
&\qquad\left.\left.M_{\tilde b_1}^2\left(M_{\tilde b_2}^2\left(n^2-2n-2\right)-2M_{\tilde g}^2(n-2)\right)\right)\right)\Big/\\
&\qquad\left.\left(\left(M_{\tilde b_1}^2-M_{\tilde b_2}^2\right)\left(M_{\tilde b_1}^2-M_{\tilde g}^2\right)\left(M_{\tilde b_2}^3-M_{\tilde b_2}M_{\tilde g}^2\right)^2\right)\right]+\\
&A_0(M_{\tilde g})^2\left[\frac{512\left(M_{\tilde b_1}^2+M_{\tilde b_2}^2-2M_{\tilde g}^2\right)}{\left(M_{\tilde b_1}^2-M_{\tilde g}^2\right)^2\left(M_{\tilde b_2}^2-M_{\tilde g}^2\right)^2}\right]+\\
&T_{134}(0,M_{\tilde b_1},M_{\tilde b_2})\left[\frac{1024}{\left(M_{\tilde b_1}^2-M_{\tilde g}^2\right)\left(M_{\tilde b_2}^2-M_{\tilde g}^2\right)}\right]+\\
&T_{134}(0,M_{\tilde b_1},M_{\tilde g})\left[\left(512\left(-2M_{\tilde b_1}^4+\left(\left(n^2-3n-2\right)M_{\tilde b_2}^2+M_{\tilde g}^2\left(-n^2+3n+6\right)\right)M_{\tilde b_1}^2+\right.\right.\right.\\
&\qquad\left.\left.M_{\tilde g}^2\left(M_{\tilde b_2}^2\left(n^2-7n+10\right)-M_{\tilde g}^2\left(n^2-7n+12\right)\right)\right)\right)\Big/\\
&\qquad\left.\left(\left(M_{\tilde b_1}^2-M_{\tilde b_2}^2\right)\left(M_{\tilde b_1}^2-M_{\tilde g}^2\right)^2\left(M_{\tilde b_2}^2-M_{\tilde g}^2\right)\right)\right]+\\
&T_{134}(0,M_{\tilde b_2},M_{\tilde g})\left[-\left(512\left(-2M_{\tilde b_2}^4+M_{\tilde g}^2\left(-n^2+3n+6\right)M_{\tilde b_2}^2-M_{\tilde g}^4\left(n^2-7n+12\right)+\right.\right.\right.\\
&\qquad\left.\left.M_{\tilde b_1}^2\left(\left(n^2-3n-2\right)M_{\tilde b_2}^2+M_{\tilde g}^2\left(n^2-7n+10\right)\right)\right)\right)\Big/\\
&\qquad\left.\left.\left(\left(M_{\tilde b_1}^2-M_{\tilde b_2}^2\right)\left(M_{\tilde b_1}^2-M_{\tilde g}^2\right)\left(M_{\tilde b_2}^2-M_{\tilde g}^2\right)^2\right)\right]\right\}
\end{aligned}
$$

SUSY-QCD corrections proportional to $T_R C_F$

$$
\begin{aligned}
\Delta m_b^{QCD\,(2)}\Big|_{T_R C_F} = & -T_R C_F \left(\frac{\alpha_s}{4\pi}\right)^2 M_{\tilde{g}}\,\mu\,\mathrm{tg}\beta\,\pi^4 \Bigg\{ \\
& A_0(m_t) A_0(M_{\tilde{b}_1}) \left[-\frac{2048}{\left(M^2_{\tilde{b}_1} - M^2_{\tilde{b}_2}\right)\left(M^2_{\tilde{b}_1} - M^2_{\tilde{g}}\right)^2} \right] + \\
& A_0(M_{\tilde{b}_1})^2 \left[\frac{1024}{\left(M^2_{\tilde{b}_1} - M^2_{\tilde{b}_2}\right)\left(M^2_{\tilde{b}_1} - M^2_{\tilde{g}}\right)^2} \right] + \\
& A_0(m_t) A_0(M_{\tilde{b}_2}) \left[\frac{2048}{\left(M^2_{\tilde{b}_1} - M^2_{\tilde{b}_2}\right)\left(M^2_{\tilde{b}_2} - M^2_{\tilde{g}}\right)^2} \right] + \\
& A_0(M_{\tilde{b}_1}) A_0(M_{\tilde{b}_2}) \left[-\frac{1024\left(M^2_{\tilde{b}_1} + M^2_{\tilde{b}_2} - 2M^2_{\tilde{g}}\right)}{\left(M^2_{\tilde{b}_1} - M^2_{\tilde{g}}\right)^2\left(M^2_{\tilde{b}_2} - M^2_{\tilde{g}}\right)^2} \right] + \\
& A_0(M_{\tilde{b}_2})^2 \left[-\frac{1024}{\left(M^2_{\tilde{b}_1} - M^2_{\tilde{b}_2}\right)\left(M^2_{\tilde{b}_2} - M^2_{\tilde{g}}\right)^2} \right] + \\
& A_0(M_{\tilde{b}_1}) A_0(M_{\tilde{c}_1}) \left[\frac{1024}{\left(M^2_{\tilde{b}_1} - M^2_{\tilde{b}_2}\right)\left(M^2_{\tilde{b}_1} - M^2_{\tilde{g}}\right)^2} \right] + \\
& A_0(M_{\tilde{b}_2}) A_0(M_{\tilde{c}_1}) \left[-\frac{1024}{\left(M^2_{\tilde{b}_1} - M^2_{\tilde{b}_2}\right)\left(M^2_{\tilde{b}_2} - M^2_{\tilde{g}}\right)^2} \right] + \\
& A_0(M_{\tilde{b}_1}) A_0(M_{\tilde{c}_2}) \left[\frac{1024}{\left(M^2_{\tilde{b}_1} - M^2_{\tilde{b}_2}\right)\left(M^2_{\tilde{b}_1} - M^2_{\tilde{g}}\right)^2} \right] + \\
& A_0(M_{\tilde{b}_2}) A_0(M_{\tilde{c}_2}) \left[-\frac{1024}{\left(M^2_{\tilde{b}_1} - M^2_{\tilde{b}_2}\right)\left(M^2_{\tilde{b}_2} - M^2_{\tilde{g}}\right)^2} \right] + \\
& A_0(M_{\tilde{b}_1}) A_0(M_{\tilde{d}_1}) \left[\frac{1024}{\left(M^2_{\tilde{b}_1} - M^2_{\tilde{b}_2}\right)\left(M^2_{\tilde{b}_1} - M^2_{\tilde{g}}\right)^2} \right] + \\
& A_0(M_{\tilde{b}_2}) A_0(M_{\tilde{d}_1}) \left[-\frac{1024}{\left(M^2_{\tilde{b}_1} - M^2_{\tilde{b}_2}\right)\left(M^2_{\tilde{b}_2} - M^2_{\tilde{g}}\right)^2} \right] + \\
& A_0(M_{\tilde{b}_1}) A_0(M_{\tilde{d}_2}) \left[\frac{1024}{\left(M^2_{\tilde{b}_1} - M^2_{\tilde{b}_2}\right)\left(M^2_{\tilde{b}_1} - M^2_{\tilde{g}}\right)^2} \right] + \\
& A_0(M_{\tilde{b}_2}) A_0(M_{\tilde{d}_2}) \left[-\frac{1024}{\left(M^2_{\tilde{b}_1} - M^2_{\tilde{b}_2}\right)\left(M^2_{\tilde{b}_2} - M^2_{\tilde{g}}\right)^2} \right] + \\
& A_0(M_{\tilde{b}_1}) A_0(M_{\tilde{s}_1}) \left[\frac{1024}{\left(M^2_{\tilde{b}_1} - M^2_{\tilde{b}_2}\right)\left(M^2_{\tilde{b}_1} - M^2_{\tilde{g}}\right)^2} \right] + \\
\end{aligned}
$$

$$
\begin{aligned}
&A_0(M_{\tilde{b}_2})A_0(M_{\tilde{s}_1})\left[-\frac{1024}{\left(M_{\tilde{b}_1}^2-M_{\tilde{b}_2}^2\right)\left(M_{\tilde{b}_2}^2-M_{\tilde{g}}^2\right)^2}\right]+\\
&A_0(M_{\tilde{b}_1})A_0(M_{\tilde{s}_2})\left[\frac{1024}{\left(M_{\tilde{b}_1}^2-M_{\tilde{b}_2}^2\right)\left(M_{\tilde{b}_1}^2-M_{\tilde{g}}^2\right)^2}\right]+\\
&A_0(M_{\tilde{b}_2})A_0(M_{\tilde{s}_2})\left[-\frac{1024}{\left(M_{\tilde{b}_1}^2-M_{\tilde{b}_2}^2\right)\left(M_{\tilde{b}_2}^2-M_{\tilde{g}}^2\right)^2}\right]+\\
&A_0(m_t)A_0(M_{\tilde{t}_1})\left[\frac{1024\left(m_t^2-M_{\tilde{t}_1}^2+M_{\tilde{g}}^2\right)(n-2)\left(\left(M_{\tilde{b}_1}^2-M_{\tilde{g}}^2\right)\left(M_{\tilde{b}_2}^2-M_{\tilde{g}}^2\right)\right)^{-1}}{\left(m_t^4-2\left(M_{\tilde{t}_1}^2+M_{\tilde{g}}^2\right)m_t^2+\left(M_{\tilde{t}_1}^2-M_{\tilde{g}}^2\right)^2\right)}\right]+\\
&A_0(M_{\tilde{b}_1})A_0(M_{\tilde{t}_1})\left[\frac{1024}{\left(M_{\tilde{b}_1}^2-M_{\tilde{b}_2}^2\right)\left(M_{\tilde{b}_1}^2-M_{\tilde{g}}^2\right)^2}\right]+\\
&A_0(M_{\tilde{b}_2})A_0(M_{\tilde{t}_1})\left[-\frac{1024}{\left(M_{\tilde{b}_1}^2-M_{\tilde{b}_2}^2\right)\left(M_{\tilde{b}_2}^2-M_{\tilde{g}}^2\right)^2}\right]+\\
&A_0(m_t)A_0(M_{\tilde{t}_2})\left[\frac{1024\left(m_t^2-M_{\tilde{t}_2}^2+M_{\tilde{g}}^2\right)(n-2)\left(\left(M_{\tilde{b}_1}^2-M_{\tilde{g}}^2\right)\left(M_{\tilde{b}_2}^2-M_{\tilde{g}}^2\right)\right)^{-1}}{\left(m_t^4-2\left(M_{\tilde{t}_2}^2+M_{\tilde{g}}^2\right)m_t^2+\left(M_{\tilde{t}_2}^2-M_{\tilde{g}}^2\right)^2\right)}\right]+\\
&A_0(M_{\tilde{b}_1})A_0(M_{\tilde{t}_2})\left[\frac{1024}{\left(M_{\tilde{b}_1}^2-M_{\tilde{b}_2}^2\right)\left(M_{\tilde{b}_1}^2-M_{\tilde{g}}^2\right)^2}\right]+\\
&A_0(M_{\tilde{b}_2})A_0(M_{\tilde{t}_2})\left[-\frac{1024}{\left(M_{\tilde{b}_1}^2-M_{\tilde{b}_2}^2\right)\left(M_{\tilde{b}_2}^2-M_{\tilde{g}}^2\right)^2}\right]+\\
&A_0(M_{\tilde{b}_1})A_0(M_{\tilde{u}_1})\left[\frac{1024}{\left(M_{\tilde{b}_1}^2-M_{\tilde{b}_2}^2\right)\left(M_{\tilde{b}_1}^2-M_{\tilde{g}}^2\right)^2}\right]+\\
&A_0(M_{\tilde{b}_2})A_0(M_{\tilde{u}_1})\left[-\frac{1024}{\left(M_{\tilde{b}_1}^2-M_{\tilde{b}_2}^2\right)\left(M_{\tilde{b}_2}^2-M_{\tilde{g}}^2\right)^2}\right]+\\
&A_0(M_{\tilde{b}_1})A_0(M_{\tilde{u}_2})\left[\frac{1024}{\left(M_{\tilde{b}_1}^2-M_{\tilde{b}_2}^2\right)\left(M_{\tilde{b}_1}^2-M_{\tilde{g}}^2\right)^2}\right]+\\
&A_0(M_{\tilde{b}_2})A_0(M_{\tilde{u}_2})\left[-\frac{1024}{\left(M_{\tilde{b}_1}^2-M_{\tilde{b}_2}^2\right)\left(M_{\tilde{b}_2}^2-M_{\tilde{g}}^2\right)^2}\right]+\\
&A_0(m_t)A_0(M_{\tilde{g}})\left[\left(1024\left(-2\left(M_{\tilde{b}_1}^2+M_{\tilde{b}_2}^2-2M_{\tilde{g}}^2\right)m_t^8+2\left(\left((n-2)M_{\tilde{b}_2}^2+\right.\right.\right.\right.\\
&\quad 2M_{\tilde{t}_1}^2+2M_{\tilde{t}_2}^2+6M_{\tilde{g}}^2-M_{\tilde{g}}^2n\Big)M_{\tilde{b}_1}^2+M_{\tilde{g}}^2\left(-4M_{\tilde{t}_1}^2-4M_{\tilde{t}_2}^2+M_{\tilde{g}}^2(n-10)\right)+\\
&\quad \left.\left.\left.\left.M_{\tilde{b}_2}^2\left(2M_{\tilde{t}_1}^2+2M_{\tilde{t}_2}^2-M_{\tilde{g}}^2(n-6)\right)\right)\right)m_t^6-\right.
\end{aligned}
$$

$$
\begin{aligned}
&\Big(\Big(2M_{\tilde{t}_1}^4+\Big(8M_{\tilde{t}_2}^2-M_{\tilde{g}}^2(n-6)\Big)M_{\tilde{t}_1}^2+2M_{\tilde{t}_2}^4+24M_{\tilde{g}}^4+6M_{\tilde{t}_2}^2M_{\tilde{g}}^2+\\
&M_{\tilde{b}_2}^2\Big(M_{\tilde{t}_1}^2+M_{\tilde{t}_2}^2+6M_{\tilde{g}}^2\Big)(n-2)-6M_{\tilde{g}}^4n-M_{\tilde{t}_2}^2M_{\tilde{g}}^2n\Big)M_{\tilde{b}_1}^2+\\
&M_{\tilde{g}}^2\Big(-4M_{\tilde{t}_1}^4+\Big(M_{\tilde{g}}^2(n-10)-16M_{\tilde{t}_2}^2\Big)M_{\tilde{t}_1}^2-4M_{\tilde{t}_2}^4+M_{\tilde{t}_2}^2M_{\tilde{g}}^2\\
&(n-10)+6M_{\tilde{g}}^4(n-6)\Big)+M_{\tilde{b}_2}^2\Big(2M_{\tilde{t}_1}^4+\Big(8M_{\tilde{t}_2}^2-M_{\tilde{g}}^2(n-6)\Big)\\
&M_{\tilde{t}_1}^2+2M_{\tilde{t}_2}^4-M_{\tilde{t}_2}^2M_{\tilde{g}}^2(n-6)-6M_{\tilde{g}}^4(n-4)\Big)\Big)m_t^4+\\
&\Big(\Big(\Big(\Big(4M_{\tilde{t}_2}^2-M_{\tilde{g}}^2(n-6)\Big)M_{\tilde{t}_1}^4+2\Big(2M_{\tilde{t}_2}^4+2M_{\tilde{g}}^2(n-6)M_{\tilde{t}_2}^2+M_{\tilde{g}}^4(n-4)\Big)\\
&M_{\tilde{t}_1}^2+M_{\tilde{g}}^2\Big(-(n-6)M_{\tilde{t}_2}^4+2M_{\tilde{g}}^2(n-4)M_{\tilde{t}_2}^2+\\
&2M_{\tilde{g}}^4(10-3n)\Big)+M_{\tilde{b}_2}^2\Big(M_{\tilde{t}_1}^4-2\Big(2M_{\tilde{t}_2}^2+M_{\tilde{g}}^2\Big)M_{\tilde{t}_1}^2+\\
&M_{\tilde{t}_2}^4+6M_{\tilde{g}}^4-2M_{\tilde{t}_2}^2M_{\tilde{g}}^2\Big)(n-2)\Big)M_{\tilde{b}_1}^2+\\
&M_{\tilde{b}_2}^2\Big(\Big(4M_{\tilde{t}_2}^2-M_{\tilde{g}}^2(n-6)\Big)M_{\tilde{t}_1}^4+2\Big(2M_{\tilde{t}_2}^4+2M_{\tilde{g}}^2(n-6)M_{\tilde{t}_2}^2+\\
&M_{\tilde{g}}^4(n-4)\Big)M_{\tilde{t}_1}^2+M_{\tilde{g}}^2\Big(-(n-6)M_{\tilde{t}_2}^4+2M_{\tilde{g}}^2(n-4)M_{\tilde{t}_2}^2+\\
&2M_{\tilde{g}}^4(10-3n)\Big)\Big)+M_{\tilde{g}}^2\Big(\Big(M_{\tilde{g}}^2(n-10)-8M_{\tilde{t}_2}^2\Big)M_{\tilde{t}_1}^4-\\
&2\Big(4M_{\tilde{t}_2}^4+2M_{\tilde{g}}^2(n-10)M_{\tilde{t}_2}^2+M_{\tilde{g}}^4(n-6)\Big)M_{\tilde{t}_1}^2+\\
&M_{\tilde{g}}^2\Big((n-10)M_{\tilde{t}_2}^4-2M_{\tilde{g}}^2(n-6)M_{\tilde{t}_2}^2+2M_{\tilde{g}}^4(3n-14)\Big)\Big)\Big)m_t^2+\\
&\Big(M_{\tilde{t}_1}^2-M_{\tilde{g}}^2\Big)\Big(M_{\tilde{t}_2}^2-M_{\tilde{g}}^2\Big)\Big(-2nM_{\tilde{g}}^6+8M_{\tilde{g}}^6-6M_{\tilde{t}_1}^2M_{\tilde{g}}^4-\\
&6M_{\tilde{t}_2}^2M_{\tilde{g}}^4+M_{\tilde{t}_1}^2nM_{\tilde{g}}^4+M_{\tilde{t}_2}^2nM_{\tilde{g}}^4+4M_{\tilde{t}_1}^2M_{\tilde{t}_2}^2M_{\tilde{g}}^2-\\
&M_{\tilde{b}_2}^2\Big(\Big(2M_{\tilde{t}_2}^2+M_{\tilde{g}}^2(n-4)\Big)M_{\tilde{t}_1}^2+M_{\tilde{g}}^2\Big(M_{\tilde{t}_2}^2(n-4)-2M_{\tilde{g}}^2(n-3)\Big)\Big)+\\
&M_{\tilde{b}_1}^2\Big(\Big(M_{\tilde{t}_1}^2+M_{\tilde{t}_2}^2-2M_{\tilde{g}}^2\Big)(n-2)M_{\tilde{b}_2}^2-\\
&M_{\tilde{t}_1}^2\Big(2M_{\tilde{t}_2}^2+M_{\tilde{g}}^2(n-4)\Big)-M_{\tilde{g}}^2\Big(M_{\tilde{t}_2}^2(n-4)-2M_{\tilde{g}}^2(n-3)\Big)\Big)\Big)\Big)\Big)\Big/\\
&\Big(\Big(M_{\tilde{b}_1}^2-M_{\tilde{g}}^2\Big)^2\Big(M_{\tilde{b}_2}^2-M_{\tilde{g}}^2\Big)^2\Big(m_t^4-2\Big(M_{\tilde{t}_1}^2+M_{\tilde{g}}^2\Big)m_t^2+\Big(M_{\tilde{t}_1}^2-M_{\tilde{g}}^2\Big)^2\Big)\\
&\Big(m_t^4-2\Big(M_{\tilde{t}_2}^2+M_{\tilde{g}}^2\Big)m_t^2+\Big(M_{\tilde{t}_2}^2-M_{\tilde{g}}^2\Big)^2\Big)\Big)\Big]+
\end{aligned}
$$

$$
A_0(M_{\tilde{b}_1})A_0(M_{\tilde{g}})\left[\frac{1024\left(M_{\tilde{b}_1}^2+M_{\tilde{b}_2}^2-2M_{\tilde{g}}^2\right)}{\left(M_{\tilde{b}_1}^2-M_{\tilde{g}}^2\right)^2\left(M_{\tilde{b}_2}^2-M_{\tilde{g}}^2\right)^2}\right]+
$$

$$
A_0(M_{\tilde{b}_2})A_0(M_{\tilde{g}})\left[\frac{1024\left(M_{\tilde{b}_1}^2+M_{\tilde{b}_2}^2-2M_{\tilde{g}}^2\right)}{\left(M_{\tilde{b}_1}^2-M_{\tilde{g}}^2\right)^2\left(M_{\tilde{b}_2}^2-M_{\tilde{g}}^2\right)^2}\right]+
$$

$$
A_0(M_{\tilde{c}_1})A_0(M_{\tilde{g}})\left[\frac{1024\left(M_{\tilde{b}_1}^2+M_{\tilde{b}_2}^2-2M_{\tilde{g}}^2\right)}{\left(M_{\tilde{b}_1}^2-M_{\tilde{g}}^2\right)^2\left(M_{\tilde{b}_2}^2-M_{\tilde{g}}^2\right)^2}\right]+
$$

$$
A_0(M_{\tilde{c}_2})A_0(M_{\tilde{g}})\left[\frac{1024\left(M_{\tilde{b}_1}^2+M_{\tilde{b}_2}^2-2M_{\tilde{g}}^2\right)}{\left(M_{\tilde{b}_1}^2-M_{\tilde{g}}^2\right)^2\left(M_{\tilde{b}_2}^2-M_{\tilde{g}}^2\right)^2}\right]+
$$

$$
\begin{aligned}
&A_0(M_{\tilde{d}_1})A_0(M_{\tilde{g}}) \left[\frac{1024\left(M_{\tilde{b}_1}^2+M_{\tilde{b}_2}^2-2M_{\tilde{g}}^2\right)}{\left(M_{\tilde{b}_1}^2-M_{\tilde{g}}^2\right)^2\left(M_{\tilde{b}_2}^2-M_{\tilde{g}}^2\right)^2}\right]+\\
&A_0(M_{\tilde{d}_2})A_0(M_{\tilde{g}}) \left[\frac{1024\left(M_{\tilde{b}_1}^2+M_{\tilde{b}_2}^2-2M_{\tilde{g}}^2\right)}{\left(M_{\tilde{b}_1}^2-M_{\tilde{g}}^2\right)^2\left(M_{\tilde{b}_2}^2-M_{\tilde{g}}^2\right)^2}\right]+\\
&A_0(M_{\tilde{s}_1})A_0(M_{\tilde{g}}) \left[\frac{1024\left(M_{\tilde{b}_1}^2+M_{\tilde{b}_2}^2-2M_{\tilde{g}}^2\right)}{\left(M_{\tilde{b}_1}^2-M_{\tilde{g}}^2\right)^2\left(M_{\tilde{b}_2}^2-M_{\tilde{g}}^2\right)^2}\right]+\\
&A_0(M_{\tilde{s}_2})A_0(M_{\tilde{g}}) \left[\frac{1024\left(M_{\tilde{b}_1}^2+M_{\tilde{b}_2}^2-2M_{\tilde{g}}^2\right)}{\left(M_{\tilde{b}_1}^2-M_{\tilde{g}}^2\right)^2\left(M_{\tilde{b}_2}^2-M_{\tilde{g}}^2\right)^2}\right]+\\
&A_0(M_{\tilde{t}_1})A_0(M_{\tilde{g}}) \left[\left(1024\left(\left(M_{\tilde{b}_1}^2+M_{\tilde{b}_2}^2-2M_{\tilde{g}}^2\right)m_t^4-2\left(nM_{\tilde{g}}^4-4M_{\tilde{g}}^4-2M_{\tilde{t}_1}^2M_{\tilde{g}}^2+\right.\right.\right.\\
&\quad M_{\tilde{b}_2}^2\left(M_{\tilde{t}_1}^2-M_{\tilde{g}}^2(n-3)\right)+M_{\tilde{b}_1}^2\left((n-2)M_{\tilde{b}_2}^2+M_{\tilde{t}_1}^2-M_{\tilde{g}}^2(n-3)\right)\Big)\\
&\quad \left.\left.m_t^2+\left(M_{\tilde{b}_1}^2+M_{\tilde{b}_2}^2-2M_{\tilde{g}}^2\right)\left(M_{\tilde{t}_1}^2-M_{\tilde{g}}^2\right)^2\right)\right)\Big/\\
&\quad \left.\left(\left(M_{\tilde{b}_1}^2-M_{\tilde{g}}^2\right)^2\left(M_{\tilde{b}_2}^2-M_{\tilde{g}}^2\right)^2\left(m_t^4-2\left(M_{\tilde{t}_1}^2+M_{\tilde{g}}^2\right)m_t^2+\left(M_{\tilde{t}_1}^2-M_{\tilde{g}}^2\right)^2\right)\right)\right]+\\
&A_0(M_{\tilde{t}_2})A_0(M_{\tilde{g}}) \left[\left(1024\left(\left(M_{\tilde{b}_1}^2+M_{\tilde{b}_2}^2-2M_{\tilde{g}}^2\right)m_t^4-2\left(nM_{\tilde{g}}^4-4M_{\tilde{g}}^4-2M_{\tilde{t}_2}^2M_{\tilde{g}}^2+\right.\right.\right.\\
&\quad M_{\tilde{b}_2}^2\left(M_{\tilde{t}_2}^2-M_{\tilde{g}}^2(n-3)\right)+M_{\tilde{b}_1}^2\left((n-2)M_{\tilde{b}_2}^2+M_{\tilde{t}_2}^2-M_{\tilde{g}}^2(n-3)\right)\Big)\\
&\quad \left.\left.m_t^2+\left(M_{\tilde{b}_1}^2+M_{\tilde{b}_2}^2-2M_{\tilde{g}}^2\right)\left(M_{\tilde{t}_2}^2-M_{\tilde{g}}^2\right)^2\right)\right)\Big/\\
&\quad \left.\left(\left(M_{\tilde{b}_1}^2-M_{\tilde{g}}^2\right)^2\left(M_{\tilde{b}_2}^2-M_{\tilde{g}}^2\right)^2\left(m_t^4-2\left(M_{\tilde{t}_2}^2+M_{\tilde{g}}^2\right)m_t^2+\left(M_{\tilde{t}_2}^2-M_{\tilde{g}}^2\right)^2\right)\right)\right]+\\
&A_0(M_{\tilde{u}_1})A_0(M_{\tilde{g}}) \left[\frac{1024\left(M_{\tilde{b}_1}^2+M_{\tilde{b}_2}^2-2M_{\tilde{g}}^2\right)}{\left(M_{\tilde{b}_1}^2-M_{\tilde{g}}^2\right)^2\left(M_{\tilde{b}_2}^2-M_{\tilde{g}}^2\right)^2}\right]+\\
&A_0(M_{\tilde{u}_2})A_0(M_{\tilde{g}}) \left[\frac{1024\left(M_{\tilde{b}_1}^2+M_{\tilde{b}_2}^2-2M_{\tilde{g}}^2\right)}{\left(M_{\tilde{b}_1}^2-M_{\tilde{g}}^2\right)^2\left(M_{\tilde{b}_2}^2-M_{\tilde{g}}^2\right)^2}\right]+\\
&T_{134}(0,M_{\tilde{b}_1},M_{\tilde{b}_2}) \left[\frac{1024\left(M_{\tilde{b}_1}^4-2M_{\tilde{g}}^2M_{\tilde{b}_1}^2+M_{\tilde{b}_2}^4+2M_{\tilde{g}}^4-2M_{\tilde{b}_2}^2M_{\tilde{g}}^2\right)}{\left(M_{\tilde{b}_1}^2-M_{\tilde{g}}^2\right)^2\left(M_{\tilde{b}_2}^2-M_{\tilde{g}}^2\right)^2}\right]+\\
&T_{134}(0,M_{\tilde{b}_1},M_{\tilde{c}_1}) \left[\frac{1024\left(M_{\tilde{b}_1}^2-M_{\tilde{c}_1}^2\right)}{\left(M_{\tilde{b}_1}^2-M_{\tilde{b}_2}^2\right)\left(M_{\tilde{b}_1}^2-M_{\tilde{g}}^2\right)^2}\right]+\\
&T_{134}(0,M_{\tilde{b}_1},M_{\tilde{c}_2}) \left[\frac{1024\left(M_{\tilde{b}_1}^2-M_{\tilde{c}_2}^2\right)}{\left(M_{\tilde{b}_1}^2-M_{\tilde{b}_2}^2\right)\left(M_{\tilde{b}_1}^2-M_{\tilde{g}}^2\right)^2}\right]+
\end{aligned}
$$

$$
\begin{aligned}
&T_{134}(0, M_{\tilde{b}_1}, M_{\tilde{d}_1}) \left[\frac{1024 \left(M_{\tilde{b}_1}^2 - M_{\tilde{d}_1}^2 \right)}{\left(M_{\tilde{b}_1}^2 - M_{\tilde{b}_2}^2 \right) \left(M_{\tilde{b}_1}^2 - M_{\tilde{g}}^2 \right)^2} \right] + \\
&T_{134}(0, M_{\tilde{b}_1}, M_{\tilde{d}_2}) \left[\frac{1024 \left(M_{\tilde{b}_1}^2 - M_{\tilde{d}_2}^2 \right)}{\left(M_{\tilde{b}_1}^2 - M_{\tilde{b}_2}^2 \right) \left(M_{\tilde{b}_1}^2 - M_{\tilde{g}}^2 \right)^2} \right] + \\
&T_{134}(0, M_{\tilde{b}_1}, M_{\tilde{s}_1}) \left[\frac{1024 \left(M_{\tilde{b}_1}^2 - M_{\tilde{s}_1}^2 \right)}{\left(M_{\tilde{b}_1}^2 - M_{\tilde{b}_2}^2 \right) \left(M_{\tilde{b}_1}^2 - M_{\tilde{g}}^2 \right)^2} \right] + \\
&T_{134}(0, M_{\tilde{b}_1}, M_{\tilde{s}_2}) \left[\frac{1024 \left(M_{\tilde{b}_1}^2 - M_{\tilde{s}_2}^2 \right)}{\left(M_{\tilde{b}_1}^2 - M_{\tilde{b}_2}^2 \right) \left(M_{\tilde{b}_1}^2 - M_{\tilde{g}}^2 \right)^2} \right] + \\
&T_{134}(0, M_{\tilde{b}_1}, M_{\tilde{u}_1}) \left[\frac{1024 \left(M_{\tilde{b}_1}^2 - M_{\tilde{u}_1}^2 \right)}{\left(M_{\tilde{b}_1}^2 - M_{\tilde{b}_2}^2 \right) \left(M_{\tilde{b}_1}^2 - M_{\tilde{g}}^2 \right)^2} \right] + \\
&T_{134}(0, M_{\tilde{b}_1}, M_{\tilde{u}_2}) \left[\frac{1024 \left(M_{\tilde{b}_1}^2 - M_{\tilde{u}_2}^2 \right)}{\left(M_{\tilde{b}_1}^2 - M_{\tilde{b}_2}^2 \right) \left(M_{\tilde{b}_1}^2 - M_{\tilde{g}}^2 \right)^2} \right] + \\
&T_{134}(0, M_{\tilde{b}_1}, M_{\tilde{g}}) \left[- \frac{1024 \left(M_{\tilde{b}_1}^2 + M_{\tilde{g}}^2 (n-4) - M_{\tilde{b}_2}^2 (n-3) \right)}{\left(M_{\tilde{b}_1}^2 - M_{\tilde{g}}^2 \right) \left(M_{\tilde{b}_2}^2 - M_{\tilde{g}}^2 \right)^2} \right] + \\
&T_{134}(0, M_{\tilde{b}_2}, M_{\tilde{c}_1}) \left[- \frac{1024 \left(M_{\tilde{b}_2}^2 - M_{\tilde{c}_1}^2 \right)}{\left(M_{\tilde{b}_1}^2 - M_{\tilde{b}_2}^2 \right) \left(M_{\tilde{b}_2}^2 - M_{\tilde{g}}^2 \right)^2} \right] + \\
&T_{134}(0, M_{\tilde{b}_2}, M_{\tilde{c}_2}) \left[- \frac{1024 \left(M_{\tilde{b}_2}^2 - M_{\tilde{c}_2}^2 \right)}{\left(M_{\tilde{b}_1}^2 - M_{\tilde{b}_2}^2 \right) \left(M_{\tilde{b}_2}^2 - M_{\tilde{g}}^2 \right)^2} \right] + \\
&T_{134}(0, M_{\tilde{b}_2}, M_{\tilde{d}_1}) \left[- \frac{1024 \left(M_{\tilde{b}_2}^2 - M_{\tilde{d}_1}^2 \right)}{\left(M_{\tilde{b}_1}^2 - M_{\tilde{b}_2}^2 \right) \left(M_{\tilde{b}_2}^2 - M_{\tilde{g}}^2 \right)^2} \right] + \\
&T_{134}(0, M_{\tilde{b}_2}, M_{\tilde{d}_2}) \left[- \frac{1024 \left(M_{\tilde{b}_2}^2 - M_{\tilde{d}_2}^2 \right)}{\left(M_{\tilde{b}_1}^2 - M_{\tilde{b}_2}^2 \right) \left(M_{\tilde{b}_2}^2 - M_{\tilde{g}}^2 \right)^2} \right] + \\
&T_{134}(0, M_{\tilde{b}_2}, M_{\tilde{s}_1}) \left[- \frac{1024 \left(M_{\tilde{b}_2}^2 - M_{\tilde{s}_1}^2 \right)}{\left(M_{\tilde{b}_1}^2 - M_{\tilde{b}_2}^2 \right) \left(M_{\tilde{b}_2}^2 - M_{\tilde{g}}^2 \right)^2} \right] + \\
&T_{134}(0, M_{\tilde{b}_2}, M_{\tilde{s}_2}) \left[- \frac{1024 \left(M_{\tilde{b}_2}^2 - M_{\tilde{s}_2}^2 \right)}{\left(M_{\tilde{b}_1}^2 - M_{\tilde{b}_2}^2 \right) \left(M_{\tilde{b}_2}^2 - M_{\tilde{g}}^2 \right)^2} \right] + \\
&T_{134}(0, M_{\tilde{b}_2}, M_{\tilde{u}_1}) \left[- \frac{1024 \left(M_{\tilde{b}_2}^2 - M_{\tilde{u}_1}^2 \right)}{\left(M_{\tilde{b}_1}^2 - M_{\tilde{b}_2}^2 \right) \left(M_{\tilde{b}_2}^2 - M_{\tilde{g}}^2 \right)^2} \right] + \\
\end{aligned}
$$

$$
\begin{aligned}
&T_{134}(0,M_{\tilde{b}_2},M_{\tilde{u}_2})\left[-\frac{1024\left(M_{\tilde{b}_2}^2-M_{\tilde{u}_2}^2\right)}{\left(M_{\tilde{b}_1}^2-M_{\tilde{b}_2}^2\right)\left(M_{\tilde{b}_2}^2-M_{\tilde{g}}^2\right)^2}\right]+\\
&T_{134}(0,M_{\tilde{b}_2},M_{\tilde{g}})\left[\frac{1024\left((n-3)M_{\tilde{b}_1}^2-M_{\tilde{b}_2}^2-M_{\tilde{g}}^2(n-4)\right)}{\left(M_{\tilde{b}_1}^2-M_{\tilde{g}}^2\right)^2\left(M_{\tilde{b}_2}^2-M_{\tilde{g}}^2\right)}\right]+\\
&T_{134}(0,M_{\tilde{c}_1},M_{\tilde{g}})\left[-\left(1024\left(-nM_{\tilde{g}}^4+4M_{\tilde{g}}^4-2M_{\tilde{c}_1}^2M_{\tilde{g}}^2+M_{\tilde{b}_2}^2\left(M_{\tilde{c}_1}^2+M_{\tilde{g}}^2(n-3)\right)+\right.\right.\right.\\
&\qquad\left.\left.\left.M_{\tilde{b}_1}^2\left(-(n-2)M_{\tilde{b}_2}^2+M_{\tilde{c}_1}^2+M_{\tilde{g}}^2(n-3)\right)\right)\right)\Big/\\
&\qquad\left(\left(M_{\tilde{b}_1}^2-M_{\tilde{g}}^2\right)^2\left(M_{\tilde{b}_2}^2-M_{\tilde{g}}^2\right)^2\right)\Bigg]+\\
&T_{134}(0,M_{\tilde{c}_2},M_{\tilde{g}})\Bigg[-\left(1024\left(-nM_{\tilde{g}}^4+4M_{\tilde{g}}^4-2M_{\tilde{c}_2}^2M_{\tilde{g}}^2+M_{\tilde{b}_2}^2\left(M_{\tilde{c}_2}^2+M_{\tilde{g}}^2(n-3)\right)+M_{\tilde{b}_1}^2\right.\right.\\
&\qquad\left.\left.\left(-(n-2)M_{\tilde{b}_2}^2+M_{\tilde{c}_2}^2+M_{\tilde{g}}^2(n-3)\right)\right)\right)/\left(\left(M_{\tilde{b}_1}^2-M_{\tilde{g}}^2\right)^2\left(M_{\tilde{b}_2}^2-M_{\tilde{g}}^2\right)^2\right)\Bigg]+\\
&T_{134}(0,M_{\tilde{d}_1},M_{\tilde{g}})\left[-\left(1024\left(-nM_{\tilde{g}}^4+4M_{\tilde{g}}^4-2M_{\tilde{d}_1}^2M_{\tilde{g}}^2+\right.\right.\right.\\
&\qquad M_{\tilde{b}_2}^2\left(M_{\tilde{d}_1}^2+M_{\tilde{g}}^2(n-3)\right)+M_{\tilde{b}_1}^2\left.\left.\left(-(n-2)M_{\tilde{b}_2}^2+M_{\tilde{d}_1}^2+M_{\tilde{g}}^2(n-3)\right)\right)\right)\Big/\\
&\qquad\left(\left(M_{\tilde{b}_1}^2-M_{\tilde{g}}^2\right)^2\left(M_{\tilde{b}_2}^2-M_{\tilde{g}}^2\right)^2\right)\Bigg]+\\
&T_{134}(0,M_{\tilde{d}_2},M_{\tilde{g}})\Bigg[-\left(1024\left(-nM_{\tilde{g}}^4+4M_{\tilde{g}}^4-2M_{\tilde{d}_2}^2M_{\tilde{g}}^2+M_{\tilde{b}_2}^2\left(M_{\tilde{d}_2}^2+M_{\tilde{g}}^2(n-3)\right)+M_{\tilde{b}_1}^2\right.\right.\\
&\qquad\left.\left.\left(-(n-2)M_{\tilde{b}_2}^2+M_{\tilde{d}_2}^2+M_{\tilde{g}}^2(n-3)\right)\right)\right)/\left(\left(M_{\tilde{b}_1}^2-M_{\tilde{g}}^2\right)^2\left(M_{\tilde{b}_2}^2-M_{\tilde{g}}^2\right)^2\right)\Bigg]+\\
&T_{134}(0,M_{\tilde{s}_1},M_{\tilde{g}})\left[-\left(1024\left(-nM_{\tilde{g}}^4+4M_{\tilde{g}}^4-2M_{\tilde{s}_1}^2M_{\tilde{g}}^2+\right.\right.\right.\\
&\qquad M_{\tilde{b}_2}^2\left(M_{\tilde{s}_1}^2+M_{\tilde{g}}^2(n-3)\right)+M_{\tilde{b}_1}^2\left.\left.\left(-(n-2)M_{\tilde{b}_2}^2+M_{\tilde{s}_1}^2+M_{\tilde{g}}^2(n-3)\right)\right)\right)\Big/\\
&\qquad\left(\left(M_{\tilde{b}_1}^2-M_{\tilde{g}}^2\right)^2\left(M_{\tilde{b}_2}^2-M_{\tilde{g}}^2\right)^2\right)\Bigg]+\\
&T_{134}(0,M_{\tilde{s}_2},M_{\tilde{g}})\Bigg[-\left(1024\left(-nM_{\tilde{g}}^4+4M_{\tilde{g}}^4-2M_{\tilde{s}_2}^2M_{\tilde{g}}^2+M_{\tilde{b}_2}^2\left(M_{\tilde{s}_2}^2+M_{\tilde{g}}^2(n-3)\right)+\right.\right.\\
&\qquad\left.\left.M_{\tilde{b}_1}^2\left(-(n-2)M_{\tilde{b}_2}^2+M_{\tilde{s}_2}^2+M_{\tilde{g}}^2(n-3)\right)\right)\right)\Big/\\
&\qquad\left(\left(M_{\tilde{b}_1}^2-M_{\tilde{g}}^2\right)^2\left(M_{\tilde{b}_2}^2-M_{\tilde{g}}^2\right)^2\right)\Bigg]+\\
&T_{134}(0,M_{\tilde{u}_1},M_{\tilde{g}})\Bigg[-\left(1024\left(-nM_{\tilde{g}}^4+4M_{\tilde{g}}^4-2M_{\tilde{u}_1}^2M_{\tilde{g}}^2+M_{\tilde{b}_2}^2\left(M_{\tilde{u}_1}^2+M_{\tilde{g}}^2(n-3)\right)+\right.\right.\\
&\qquad\left.\left.M_{\tilde{b}_1}^2\left(-(n-2)M_{\tilde{b}_2}^2+M_{\tilde{u}_1}^2+M_{\tilde{g}}^2(n-3)\right)\right)\right)\Big/
\end{aligned}
$$

$$\left(\left(M_{\tilde{b}_1}^2 - M_{\tilde{g}}^2\right)^2 \left(M_{\tilde{b}_2}^2 - M_{\tilde{g}}^2\right)^2\right)\Bigg] +$$

$$T_{134}(0, M_{\tilde{u}_2}, M_{\tilde{g}})\Bigg[-\Big(1024\left(-nM_{\tilde{g}}^4 + 4M_{\tilde{g}}^4 - 2M_{\tilde{u}_2}^2 M_{\tilde{g}}^2 + M_{\tilde{b}_2}^2\left(M_{\tilde{u}_2}^2 + M_{\tilde{g}}^2(n-3)\right) + M_{\tilde{b}_1}^2\right.$$
$$\left.\left(-(n-2)M_{\tilde{b}_2}^2 + M_{\tilde{u}_2}^2 + M_{\tilde{g}}^2(n-3)\right)\right)\Big) \Big/ \left(\left(M_{\tilde{b}_1}^2 - M_{\tilde{g}}^2\right)^2 \left(M_{\tilde{b}_2}^2 - M_{\tilde{g}}^2\right)^2\right)\Bigg] +$$

$$T_{134}(m_t, M_{\tilde{b}_1}, M_{\tilde{t}_1})\left[\frac{1024\left(m_t^2 + M_{\tilde{b}_1}^2 - M_{\tilde{t}_1}^2\right)}{\left(M_{\tilde{b}_1}^2 - M_{\tilde{b}_2}^2\right)\left(M_{\tilde{b}_1}^2 - M_{\tilde{g}}^2\right)^2}\right] +$$

$$T_{134}(m_t, M_{\tilde{b}_1}, M_{\tilde{t}_2})\left[\frac{1024\left(m_t^2 + M_{\tilde{b}_1}^2 - M_{\tilde{t}_2}^2\right)}{\left(M_{\tilde{b}_1}^2 - M_{\tilde{b}_2}^2\right)\left(M_{\tilde{b}_1}^2 - M_{\tilde{g}}^2\right)^2}\right] +$$

$$T_{134}(m_t, M_{\tilde{b}_2}, M_{\tilde{t}_1})\left[-\frac{1024\left(m_t^2 + M_{\tilde{b}_2}^2 - M_{\tilde{t}_1}^2\right)}{\left(M_{\tilde{b}_1}^2 - M_{\tilde{b}_2}^2\right)\left(M_{\tilde{b}_2}^2 - M_{\tilde{g}}^2\right)^2}\right] +$$

$$T_{134}(m_t, M_{\tilde{b}_2}, M_{\tilde{t}_2})\left[-\frac{1024\left(m_t^2 + M_{\tilde{b}_2}^2 - M_{\tilde{t}_2}^2\right)}{\left(M_{\tilde{b}_1}^2 - M_{\tilde{b}_2}^2\right)\left(M_{\tilde{b}_2}^2 - M_{\tilde{g}}^2\right)^2}\right] +$$

$$T_{134}(m_t, M_{\tilde{t}_1}, M_{\tilde{g}})\Bigg[-\Big(1024\Big(-\left(M_{\tilde{b}_1}^2 + M_{\tilde{b}_2}^2 - 2M_{\tilde{g}}^2\right)m_t^6 - \left(-nM_{\tilde{g}}^4 + 6M_{\tilde{g}}^4 +\right.$$
$$6M_{\tilde{t}_1}^2 M_{\tilde{g}}^2 + M_{\tilde{b}_2}^2\left(M_{\tilde{g}}^2(n-5) - 3M_{\tilde{t}_1}^2\right) + M_{\tilde{b}_1}^2\left(-(n-4)M_{\tilde{b}_2}^2 - 3M_{\tilde{t}_1}^2 + M_{\tilde{g}}^2(n-5)\right)\Big)$$
$$m_t^4 - \Big(-6M_{\tilde{g}}^2 M_{\tilde{t}_1}^4 + 2M_{\tilde{g}}^4 M_{\tilde{t}_1}^2 + M_{\tilde{b}_2}^2\left(3M_{\tilde{t}_1}^4 + M_{\tilde{g}}^4\right) +$$
$$M_{\tilde{b}_1}^2\left(3M_{\tilde{t}_1}^4 + M_{\tilde{g}}^4 - 2M_{\tilde{b}_2}^2\left(M_{\tilde{t}_1}^2 + M_{\tilde{g}}^2\right)\right)\Big)m_t^2 -$$
$$\left(M_{\tilde{t}_1}^2 - M_{\tilde{g}}^2\right)^2\Big(nM_{\tilde{g}}^4 - 4M_{\tilde{g}}^4 + 2M_{\tilde{t}_1}^2 M_{\tilde{g}}^2 - M_{\tilde{b}_2}^2\left(M_{\tilde{t}_1}^2 + M_{\tilde{g}}^2(n-3)\right) +$$
$$M_{\tilde{b}_1}^2\left((n-2)M_{\tilde{b}_2}^2 - M_{\tilde{t}_1}^2 - M_{\tilde{g}}^2(n-3)\right)\Big)\Big)\Big) \Big/$$
$$\left(\left(M_{\tilde{b}_1}^2 - M_{\tilde{g}}^2\right)^2\left(M_{\tilde{b}_2}^2 - M_{\tilde{g}}^2\right)^2\left(m_t^4 - 2\left(M_{\tilde{t}_1}^2 + M_{\tilde{g}}^2\right)m_t^2 + \left(M_{\tilde{t}_1}^2 - M_{\tilde{g}}^2\right)^2\right)\right)\Bigg] +$$

$$T_{134}(m_t, M_{\tilde{t}_2}, M_{\tilde{g}})\Bigg[-\Big(1024\Big(-\left(M_{\tilde{b}_1}^2 + M_{\tilde{b}_2}^2 - 2M_{\tilde{g}}^2\right)m_t^6 - \left(-nM_{\tilde{g}}^4 + 6M_{\tilde{g}}^4 +\right.$$
$$6M_{\tilde{t}_2}^2 M_{\tilde{g}}^2 + M_{\tilde{b}_2}^2\left(M_{\tilde{g}}^2(n-5) - 3M_{\tilde{t}_2}^2\right) + M_{\tilde{b}_1}^2\left(-(n-4)M_{\tilde{b}_2}^2 - 3M_{\tilde{t}_2}^2 + M_{\tilde{g}}^2(n-5)\right)\Big)$$
$$m_t^4 - \Big(-6M_{\tilde{g}}^2 M_{\tilde{t}_2}^4 + 2M_{\tilde{g}}^4 M_{\tilde{t}_2}^2 + M_{\tilde{b}_2}^2\left(3M_{\tilde{t}_2}^4 + M_{\tilde{g}}^4\right) +$$
$$M_{\tilde{b}_1}^2\left(3M_{\tilde{t}_2}^4 + M_{\tilde{g}}^4 - 2M_{\tilde{b}_2}^2\left(M_{\tilde{t}_2}^2 + M_{\tilde{g}}^2\right)\right)\Big)m_t^2 -$$
$$\left(M_{\tilde{t}_2}^2 - M_{\tilde{g}}^2\right)^2\Big(nM_{\tilde{g}}^4 - 4M_{\tilde{g}}^4 + 2M_{\tilde{t}_2}^2 M_{\tilde{g}}^2 - M_{\tilde{b}_2}^2\left(M_{\tilde{t}_2}^2 + M_{\tilde{g}}^2(n-3)\right) +$$
$$M_{\tilde{b}_1}^2\left((n-2)M_{\tilde{b}_2}^2 - M_{\tilde{t}_2}^2 - M_{\tilde{g}}^2(n-3)\right)\Big)\Big)\Big) \Big/$$
$$\left(\left(M_{\tilde{b}_1}^2 - M_{\tilde{g}}^2\right)^2\left(M_{\tilde{b}_2}^2 - M_{\tilde{g}}^2\right)^2\left(m_t^4 - 2\left(M_{\tilde{t}_2}^2 + M_{\tilde{g}}^2\right)m_t^2 + \left(M_{\tilde{t}_2}^2 - M_{\tilde{g}}^2\right)^2\right)\right)\Bigg]\Bigg\}$$

Bibliography

[1] A. Einstein. The foundation of the general theory of relativity. *Annalen Phys.*, 49:769–822, 1916.

[2] Paul A. M. Dirac. The Quantum theory of the Electron. *Proc. Roy. Soc. Lond.*, A117:610–624, 1928.

[3] R. P. Feynman. Space-time approach to quantum electrodynamics. *Phys. Rev.*, 76:769–789, 1949.

[4] R. P. Feynman. Mathematical formulation of the quantum theory of electromagnetic interaction. *Phys. Rev.*, 80:440–457, 1950.

[5] S. L. Glashow. Partial Symmetries of Weak Interactions. *Nucl. Phys.*, 22:579–588, 1961.

[6] M. Gell-Mann. A Schematic Model of Baryons and Mesons. *Phys. Lett.*, 8:214–215, 1964.

[7] G. Zweig. An SU(3) model for strong interaction symmetry and its breaking. 1964. CERN-TH-412.

[8] M. Y. Han and Y. Nambu. Three-triplet model with double SU(3) symmetry. *Phys. Rev.*, 139:B1006–B1010, 1965.

[9] S. Weinberg. A Model of Leptons. *Phys. Rev. Lett.*, 19:1264–1266, 1967.

[10] A. Salam. Weak and Electromagnetic Interactions. Elementary Particle Theory, Proceedings Of The Nobel Symposium Held 1968 At Lerum, Sweden, Stockholm 1968, 367-377.

[11] R. P. Feynman. Very high-energy collisions of hadrons. *Phys. Rev. Lett.*, 23:1415–1417, 1969.

[12] J. D. Bjorken and E. A. Paschos. Inelastic Electron Proton and gamma Proton Scattering, and the Structure of the Nucleon. *Phys. Rev.*, 185:1975–1982, 1969.

[13] D. Gross and F. Wilczek. Ultraviolet behavior of non-abelian gauge theories. *Phys. Rev. Lett.*, 30(26):1343–1346, 1973.

[14] D. J. Gross and F. Wilczek. Asymptotically Free Gauge Theories. 2. *Phys. Rev.*, D9:980–993, 1974.

[15] H. D. Politzer. Setting the scale for predictions of asymptotic freedom. *Phys. Rev.*, D9:2174–2175, 1974.

[16] Steven Weinberg. Conceptual Foundations of the Unified Theory of Weak and Electromagnetic Interactions. *Rev. Mod. Phys.*, 52:515–523, 1980.

[17] R. P. Feynman. QED. The Strange Theory of Light and Matter. 1985. Princeton, NJ: Princeton University Press.

[18] P. W. Higgs. Broken symmetries, massless particles and gauge fields. *Phys. Lett.*, 12:132–133, 1964.

[19] P. W. Higgs. Broken Symmetries and the Masses of Gauge Bosons. *Phys. Rev. Lett.*, 13:508–509, 1964.

[20] P. W. Higgs. Spontaneous Symmetry Breakdown Without Massless Bosons. *Phys. Rev.*, 145:1156–1163, 1966.

[21] LEP. A combination of preliminary electroweak measurements and constraints on the standard model. 2003. hep-ex/0312023.

[22] T. Hambye and K. Riesselmann. Matching conditions and Higgs boson mass upper bounds reexamined. *Phys. Rev. D*, 55:7255, 1997.

[23] Yu. A. Golfand and E. P. Likhtman. Extension of the Algebra of Poincare Group Generators and Violation of p Invariance. *JETP Lett.*, 13:323–326, 1971.

[24] J. Wess and B. Zumino. Supergauge Transformations in Four-Dimensions. *Nucl. Phys.*, B70:39–50, 1974.

[25] J. Wess and B. Zumino. A Lagrangian Model Invariant Under Supergauge Transformations. *Phys. Lett.*, B49:52, 1974.

[26] Edward Witten. Mass Hierarchies in Supersymmetric Theories. *Phys. Lett.*, B105:267, 1981.

[27] M. Carena and H. Haber. Higgs Boson Theory and Phenomenology. 2002. hep-ph/0208209.

[28] J. Guasch, P. Häfliger, and M. Spira. MSSM Higgs boson decays to bottom quark pairs reexamined. *Phys. Rev. D*, 68:115001, 2003.

[29] M. Spira. QCD Effects in Higgs Physics. *Fortschr. Phys.*, 46:203, 1998.

[30] ATLAS Collaboration. Technical Design Report. *CERN-LHCC*, 99-14, 1999.

[31] CMS Collaboration. Technical Proposal. *CERN-LHCC*, 94-38, 1994.

[32] Steven Weinberg. What is quantum field theory, and what did we think it was? 1996. hep-th/9702027.

[33] M. Peskin and D. Schroeder. An Introduction to Quantum Field Theory. *Westview Press*, 1995.

[34] A. Denner. Techniques for calculation of electroweak radiative corrections at the one loop level and results for W physics at LEP-200. *Fortschr. Phys.*, 41:307–420, 1993. hep-ph/0709.1075.

[35] Andrzej J. Buras. Weak Hamiltonian, CP violation and rare decays. 1998. hep-ph/9806471.

[36] J. Goldstone, A. Salam, and S. Weinberg. Broken Symmetries. *Phys. Rev.*, 127:965–970, 1962.

[37] G. 't Hooft. Renormalization of massless Yang-Mills fields. *Nucl. Phys. B*, 33:173, 1971.

[38] G. 't Hooft. Renormalizable Lagrangians for massive Yang-Mills fields. *Nucl. Phys. B*, 35:167, 1971.

[39] G. 't Hooft and M.J. Veltman. Combinatorics of gauge fields. *Nucl. Phys. B*, 50:318, 1972.

[40] Sidney R. Coleman and J. Mandula. All possible Symmetries of the S-Matrix. *Phys. Rev.*, 159:1251–1256, 1967.

[41] Rudolf Haag, Jan T. Lopuszanski, and Martin Sohnius. All Possible Generators of Supersymmetries of the S-Matrix. *Nucl. Phys.*, B88:257, 1975.

[42] P. Fayet and S. Ferrara. Supersymmetry. *Phys. Rept.*, 32:249–334, 1977.

[43] S. Martin. A Supersymmetry Primer. 2006. hep-ph/9709356.

[44] S. Dawson. SUSY and SUCH. 1997. hep-ph/9612229.

[45] H. Kalka and G. Soff. Supersymmetrie. *Teubner*, 2001. (in german).

[46] Makoto Kobayashi and Toshihide Maskawa. CP Violation in the Renormalizable Theory of Weak Interaction. *Prog. Theor. Phys.*, 49:652–657, 1973.

[47] M. C. Gonzalez-Garcia and Yosef Nir. Developments in neutrino physics. *Rev. Mod. Phys.*, 75:345–402, 2003.

[48] N. Cabibbo. Unitary Symmetry and Leptonic Decays. *Phys. Rev. Lett.*, 10:531–532, 1963.

[49] M. Spira, P. Zerwas, and H. Spiesberger. The Standard Model: Physical Basis and Scattering Experiments. 2000. hep-ph/0011255.

[50] J. Ellis, G. Ridolfi, and F. Zwirner. Radiative Corrections to the Masses of Supersymmetric Higgs bosons. *Phys. Lett. B*, 257:83–91, 1991. .

[51] H. Haber and R. Hempfling. Can the mass of the lightest Higgs boson of the minimal supersymmetric model be larger than m_Z? *Phys. Rev. Lett.*, 66:1815–1818, 1991. .

[52] M. Carena, J. Espinosa, M. Quiros, and C. Wagner. Analytical expressions for radiatively corrected Higgs masses and couplings in the MSSM. *Phys. Lett. B*, 355:209–221, 1995. .

[53] M. Carena, S. Heinemeyer, C. Wagner, and G. Weiglein. Suggestion for benchmark scenarios for MSSM Higgs boson searches at hadron colliders. *Eur. Phys. J.*, 26:601–607, 2003. hep-ph/0202167.

[54] M. Carena and H. Haber. Higgs boson theory and phenomenology. *Prog. Part. Nucl. Phys.*, 50:63–152, 2003. hep-ph/0208209.

[55] W. Yao et al. Review of Particle Physics. *J. Phys. G*, 33:1, 2006. Particle Data Group.

[56] G. Degrassi, S. Heinemeyer, W. Hollik, P. Slavich, and G. Weiglein. Towards High-Precision Predictions for the MSSM Higgs Sector. *Eur. Phys. J. C*, 28:133–143, 2003. hep-ph/0212020v2.

[57] ALEPH Collaboration, S. Schael, et al. Search for Neutral MSSM Higgs Bosons at LEP. *Eur. Phys. J.*, 47:547–587, 2006. hep-ex/0602042.

[58] ALEPH Collaboration, A. Heister, et al. Search for Charged Higgs bosons in e^+e^- Collisions at Energies up to $\sqrt{s} = 209$ GeV. *Phys. Lett. B*, 543:1–13, 2002. hep-ex/0207054.

[59] T. Scanlon. Search for supersymmetric neutral Higgs bosons at the Tevatron. hep-ph/0710.5049.

[60] H. Haber and Y. Nir. Multiscalar Models with a High-Energy Scale. *Nucl. Phys. B*, 335:363, 1990.

[61] M. Gomez-Bock, M. Mondragon, M. Mühlleitner, M. Spira, and P. Zerwas. Concepts of Electroweak Symmetry Breaking and Higgs Physics. *CERN-PH-TH*, 262, 2007. hep-ph/0712.2419v1.

[62] H. M. Georgi, S. L. Glashow, M. E. Machacek, and Dimitri V. Nanopoulos. Higgs Bosons from Two Gluon Annihilation in Proton Proton Collisions. *Phys. Rev. Lett.*, 40:692, 1978.

[63] M. Spira, A. Djouadi, D. Graudenz, and P. Zerwas. Higgs boson production at the LHC. *Nucl. Phys. B*, 453:17–82, 1995. hep-ph/9504378.

[64] A. Djouadi, M. Spira, and P. M. Zerwas. Production of Higgs bosons in proton colliders: QCD corrections. *Phys. Lett.*, B264:440–446, 1991.

[65] D. Graudenz, M. Spira, and P. M. Zerwas. QCD corrections to Higgs boson production at proton proton colliders. *Phys. Rev. Lett.*, 70:1372–1375, 1993.

[66] S. Dawson, A. Djouadi, and M. Spira. QCD corrections to SUSY Higgs production: The role of squark loops. *Phys. rev. Lett.*, 77:16–19, 1996. hep-ph/9603423.

[67] M. Mühlleitner and M. Spira. Higgs boson production via gluon fusion: Squark loops at NLO QCD. *Nucl. Phys. B*, 790:1–27, 2008. hep-ph/0612254.

[68] R. N. Cahn and Sally Dawson. Production of Very Massive Higgs Bosons. *Phys. Lett.*, B136:196, 1984.

[69] Guido Altarelli, B. Mele, and F. Pitolli. Heavy Higgs Production at Future Colliders. *Nucl. Phys.*, B287:205–224, 1987.

[70] Tao Han, G. Valencia, and S. Willenbrock. Structure function approach to vector boson scattering in p p collisions. *Phys. Rev. Lett.*, 69:3274–3277, 1992.

[71] S. L. Glashow, Dimitri V. Nanopoulos, and A. Yildiz. Associated Production of Higgs Bosons and Z Particles. *Phys. Rev.*, D18:1724–1727, 1978.

[72] Z. Kunszt, Z. Trocsanyi, and W. James Stirling. Clear signal of intermediate mass Higgs boson production at LHC and SSC. *Phys. Lett.*, B271:247–255, 1991.

[73] Tao Han and S. Willenbrock. QCD correction to the p p → W H and Z H total cross- sections. *Phys. Lett.*, B273:167–172, 1991.

[74] Z. Kunszt. Associated Production of Heavy Higgs Boson with Top Quarks. *Nucl. Phys.*, B247:339, 1984.

[75] Duane A. Dicus and Scott Willenbrock. Higgs Boson Production from Heavy Quark Fusion. *Phys. Rev.*, D39:751, 1989.

[76] William J. Marciano and Frank E. Paige. Associated production of Higgs bosons with t anti-t pairs. *Phys. Rev. Lett.*, 66:2433–2435, 1991.

[77] W. Beenakker et al. Higgs radiation off top quarks at the Tevatron and the LHC. *Phys. Rev. Lett.*, 87:201805, 2001. hep-ph/0107081.

[78] S. Dawson, L. Orr, L. Reina, and D. Wackeroth. Associated top quark Higgs boson production at the LHC. *Phys. Rev. D*, 67:071503, 2003. hep-ph/0211438.

[79] S. Dawson, C. Jackson, L. Reina, and D. Wackeroth. Exclusive Higgs boson production with bottom quarks at hadron colliders. *Phys. Rev D*, 69:074027, 2004. hep-ph/0311067.

[80] P. Häfliger. Associated MSSM Higgs Production with Heavy Quarks: SUSY-QCD Corrections. *Dissertation ETH*, 16970, 2006.

[81] M. Walser. NLO QCD and SUSY-QCD Corrections to Associated MSSM Higgs Production with Heavy Quarks at Hadron Colliders. *Dissertation ETH*, 17592, 2008.

[82] ATLAS Collaboration. Present results for the overall MSSM discovery potential. http://atlas.web.cern.ch/atlas/groups/physics/higgs/higgs-inputConfTalks/MSSMplots2001/MSSMplots2001.html.

[83] G. L. Bayatian et al. CMS technical design report, volume II: Physics performance. *J. Phys.*, G34:995–1579, 2007.

[84] V. Buescher and K. Jakobs. Higgs Boson Searches at Hadron Colliders. *Int. J. Mod. Phys. A*, 20:2523–2602, 2005. hep-ph/0504099v1.

[85] J. Ellis, M. Gaillard, and D. Nanopoulos. A Phenomenological Profile of the Higgs Boson. *Nucl. Phys. B*, 106:292, 1976.

[86] B. Kniehl and M. Spira. Low-energy theorems in Higgs physics. *Z. Phys. C*, 69:77–87, 1995.

[87] H. Georgi. Lie Algebras in Particle Physics. *Westview Press*, 1999.

[88] Vladimir A. Smirnov. Applied asymptotic expansions in momenta and masses. *Springer Tracts Mod. Phys.*, 177:1–262, 2002.

[89] Vladimir A. Smirnov. Asymptotic expansions in limits of large momenta and masses. *Commun. Math. Phys.*, 134:109–137, 1990.

[90] G. 't Hooft and M.J. Veltman. Regularization and renormalization of gauge fields. *Nucl. Phys. B*, 44:189, 1972.

[91] T. Appelquist and J. Carazzone. Infrared singularities and massive fields. *Phys. Rev. D*, 11(10):2856–2861, 1975.

[92] J.C. Collins, F. Wilczek, and A. Zee. Low-energy manifestations of heavy particles: Application to the neutral current. *Phys. Rev. D*, 18:242, 1978.

[93] P. Martin and M. T. Vaughn. Regularization dependence of running couplings in softly broken supersymmetry. *Phys. Lett. B*, 318:331–337, 1993. hep-ph/9308222.

[94] D. R. T. Jones. Two Loop Diagrams in Yang-Mills Theory. *Nucl. Phys.*, B75:531, 1974.

[95] William E. Caswell. Asymptotic Behavior of Nonabelian Gauge Theories to Two Loop Order. *Phys. Rev. Lett.*, 33:244, 1974.

[96] R. Tarrach. The Pole Mass in Perturbative QCD. *Nucl. Phys.*, B183:384, 1981.

[97] S. G. Gorishnii, A. L. Kataev, S. A. Larin, and L. R. Surguladze. Scheme dependence of the next to next-to-leading QCD corrections to Gamma(tot) (H0 $\rightarrow$ hadrons) and the spurious QCD infrared fixed point. *Phys. Rev.*, D43:1633–1640, 1991.

[98] K. G. Chetyrkin. Quark mass anomalous dimension to $\mathcal{O}\left(\alpha_s^4\right)$. *Phys. Lett.*, B404:161–165, 1997. hep-ph/9703278.

[99] J. A. M. Vermaseren, S. A. Larin, and T. van Ritbergen. The 4-loop quark mass anomalous dimension and the invariant quark mass. *Phys. Lett.*, B405:327–333, 1997. hep-ph/9703284.

[100] M. Carena, D. Garcia, U. Nierste, and C. Wagner. Effective Lagrangian for the $\bar{t}bH^+$ interaction in the MSSM and charged Higgs phenomenology. *Nucl. Phys. B*, 577:88–120, 2000.

[101] Lawrence J. Hall, Riccardo Rattazzi, and Uri Sarid. The Top quark mass in supersymmetric SO(10) unification. *Phys. Rev.*, D50:7048–7065, 1994. hep-ph/9306309.

[102] Marcela S. Carena, M. Olechowski, S. Pokorski, and C. E. M. Wagner. Electroweak symmetry breaking and bottom - top Yukawa unification. *Nucl. Phys.*, B426:269–300, 1994. hep-ph/9402253.

[103] T. Kinoshita. Mass Singularities of Feynman Amplitudes. *J. Math. Phys.*, 3:650, 1962.

[104] T.D. Lee and M. Nauenberg. Degenerate Systems and Mass Singularities. *Phys. Rev.*, 133:B1549, 1964.

[105] Andrei I. Davydychev and J. B. Tausk. Two loop selfenergy diagrams with different masses and the momentum expansion. *Nucl. Phys.*, B397:123–142, 1993.

[106] Frits A. Berends and J. B. Tausk. On the numerical evaluation of scalar two loop selfenergy diagrams. *Nucl. Phys.*, B421:456–470, 1994.

[107] E. Braaten and J. P. Leveille. Higgs Boson Decay and the Running Mass. *Phys. Rev.*, D22:715, 1980.

[108] N. Sakai. Perturbative QCD Corrections to the Hadronic Decay Width of the Higgs Boson. *Phys. Rev.*, D22:2220, 1980.

[109] Takeo Inami and Takahiro Kubota. Renormalisation Group Estimate of the Hadronic Decay Width of the Higgs Boson. *Nucl. Phys.*, B179:171, 1981.

[110] S. G. Gorishnii, A. L. Kataev, and S. A. Larin. The Width of Higgs Boson Decay into Hadrons: Three Loop Corrections of Strong Interactions. *Sov. J. Nucl. Phys.*, 40:329–334, 1984.

[111] Manuel Drees and Ken-ichi Hikasa. Heavy Quark Thresholds in Higgs Physics. *Phys. Rev.*, D41:1547, 1990.

[112] Andrei L. Kataev and Victor T. Kim. The Effects of the QCD corrections to $\Gamma(H_0 \to b\bar{b})$. *Mod. Phys. Lett.*, A9:1309–1326, 1994.

[113] Levan R. Surguladze. Quark mass effects in fermionic decays of the Higgs boson in $\mathcal{O}\left(\alpha_s^2\right)$ perturbative QCD. *Phys. Lett.*, B341:60–72, 1994. hep-ph/9405325.

[114] K. G. Chetyrkin. Correlator of the quark scalar currents and Gamma(tot)(H $\to$ hadrons) at $\mathcal{O}\left(\alpha_s^3\right)$ in pQCD. *Phys. Lett.*, B390:309–317, 1997. hep-ph/9608318.

[115] K. G. Chetyrkin and A. Kwiatkowski. Second order QCD corrections to scalar and pseudoscalar Higgs decays into massive bottom quarks. *Nucl. Phys.*, B461:3–18, 1996. hep-ph/9505358.

[116] S. A. Larin, T. van Ritbergen, and J. A. M. Vermaseren. The Large top quark mass expansion for Higgs boson decays into bottom quarks and into gluons. *Phys. Lett.*, B362:134–140, 1995. hep-ph/9506465.

[117] Marcela S. Carena et al. Reconciling the two-loop diagrammatic and effective field theory computations of the mass of the lightest CP-even Higgs boson in the MSSM. *Nucl. Phys.*, B580:29–57, 2000. hep-ph/0001002.

[118] A. Djouadi, J. Kalinowski, and M. Spira. HDECAY: A program for Higgs boson decays in the standard model and its supersymmetric extension. *Comput. Phys. Commun.*, 108:56–74, 1998. hep-ph/9704448.

[119] Wolfgang Kilian. Renormalized soft Higgs theorems. *Z. Phys.*, C69:89–98, 1995. hep-ph/9505309.

[120] David Noth and Michael Spira. Higgs Boson Couplings to Bottom Quarks: Two-Loop Supersymmetry-QCD Corrections. *Phys. Rev. Lett.*, 101:181801, 2008.

Danksagung

Ich möchte an dieser Stelle allen denen meinen Dank aussprechen, die zum Gelingen dieser Doktorarbeit beigetragen haben.
Zunächst möchte ich Professor Daniel Wyler dafür danken, dass er mich als Doktoranden aufgenommen hat und es mir somit ermöglichte, meine Doktorarbeit an einem interessanten und sympathischen Institut zu schreiben.
Sehr verbunden bin ich Michael Spira, der mich während der gesamten Zeit der gemeinsamen Arbeit exzellent betreut hat. Michael hatte immer ein offenes Ohr für meine Fragen, hat sich stets die nötige Zeit genommen, diese klar und fundiert zu beantworten und hat dabei immer eine außerordentliche Geduld und Fairness bewiesen.
Einen herzlichen Dank auch an die Kollegen vom Institut der Universität Zürich. Professor Thomas Gehrmann danke ich für unzählige, beantwortete Fragen und seine stete Bereitschaft zu helfen. Christian Kurz für seine Hilfe bei fachlichen Problemen und für die gute, gemeinsame Zeit. Lucia Hosekova für erfrischende Diskussionen über das Ende der Welt und die kaum abreißende Versorgung mit Süßigkeiten. Tobias Motz war so freundlich den Beweis anzutreten, dass es auch nette Bayern gibt. Beat Tödtli für lange Diskussionen, als eigentlich alle anderen schon zu Hause waren und seine Hilfe mit Mathematica. Pierpaolo Mastrolia, Gudrun Heinrich und Andrea Ferroglia waren stets bereit, Fragen kompetent zu beantworten. Stefan Bucherer für nette Gespräche auf dem Berg und anderswo. Nurhana Tajuddin für die ständige Zufuhr von richtigem Englisch. Nicht zu vergessen den ehemaligen Petra Häfliger, Manuel Walser und Christoph Meier einen Dank für Hilfe besonders in der Anfangsphase.
Den Kollegen vom Paul Scherrer Institut, Roland Rosenfelder, Ansgar Denner, Heidi Rzehak und besonders Bernd Jantzen für seine Hilfe mit meinen Integralen ein großes Dankeschön.
Einen ganz persönlichen Dank meinem guten Freund und Wegbegleiter Christian Heid für seinen Rat und seine Tat und seine unerschütterliche Loyalität. Ebenso Raphaëlle Dayer für ihren seelischen Beistand in der Endphase.
Schließlich meinen Eltern, Barbara und Volker Noth, für ihre Unterstützung und ihr Interesse und für die Sicherheit, die sie mir geben.